Managed aquifer recharge into a karst groundwater system at the Wala reservoir, Jordan

zur Erlangung des akademischen Grades eines

Doktors der Naturwissenschaften

von der Fakultät für Bauingenieur-, Geo- und Umweltwissenschaften
des Karlsruher Instituts für Technologie (KIT)

genehmigte

Dissertation

von

Dipl.-Geol. Julian Xanke

aus Leimen

Tag der mündlichen Prüfung:
20. Januar 2017

Referent: Prof. Dr. Nico Goldscheider
Korreferent: Prof. Dr. Hervé Jourde

Karlsruhe 2017

Abstract

Managed aquifer recharge (MAR) is a promising approach to augment groundwater availability in water scarce regions. Especially in semi-arid areas with a high seasonal variability in water availability the temporal storage of storm water in the underground helps to bridge dry periods and therefore represents a key technology in water management. However, a particular challenge for the technical implementation and operation of MAR is posed by karst aquifers since they usually reveal a strong hydraulic anisotropy and heterogeneity and are therefore highly vulnerable to contamination.

The main focus of this work is on the investigation of flood water storage at the Wala dam in Jordan and the managed recharge of the underlying karst aquifer. Of particular interest is the impact on the downstream Hidan wellfield, which contributes to the drinking water supply of the cities Amman, Madaba and small communities in the immediate surrounding. For this purpose a comprehensive hydrogeological conceptual model was developed, which in turn served as the basis for a numerical groundwater model. Based on the simulated water levels and scenarios the main impacts on groundwater levels trends were assessed on the long-term. Furthermore, a combined protection zone concept was developed for the karstic environment of the reservoir and the wellfield considering the interaction of surface water and groundwater.

Calculations showed that about 6.7 million cubic meters (MCM) of water infiltrated on annual average (2002-2012) from the reservoir into the underground, which accounts for about 60 % of the annual average groundwater abstraction of about 11.7 MCM in the same period. Tritium data proved the immediate impact of reservoir infiltration on the wellfield, whereas the mean residence time of natural groundwater flow was calculated using the ^{14}C-method to be of several thousand years. An impact on the groundwater chemistry by the low mineralized surface water on the highly mineralized groundwater was observed only in the first years with strong variations in salinity at the wellfield.

For the numerical model an "equivalent porous medium" (EPM) approach was used with special adaptation to account for the karst specific heterogeneity and anisotropy of the hydraulic properties. Therefore, the 3-dimensional aquifer geometry was projected onto a 2-dimensional profile along the wadi and further divided into hydraulic zones, which represent both zones of low flow and high flow velocities. Simulations matched the measured groundwater level very well and showed that its declining long-term trend is a result of the sedimentation and the associated decreasing infiltration rate in the reservoir. However, strong groundwater level fluctuations at the wellfield on the short-term are caused by changes in the average pumping depth.

Investigations on aquifer vulnerability and contamination revealed frequent bacteriological occurrence in groundwater as a result of surface runoff infiltration near the wellfield. Here, rain events and groundwater seepage into the wadi, as a result of high infiltration rates from the reservoir, were identified as the main triggering events. The findings were used to create a simplified vulnerability- and risk map, which in turn served as the basis for a combined protection zone concept that considers both the catchment areas of the Wala reservoir and the Hidan wellfield and the interaction of surface water and groundwater.

The results show that the Wadi Wala provides appropriate structural conditions for the application of MAR into the underlying karst aquifer since intensified karstification along the course of the wadi facilitates the infiltration of substantial amounts of flood water into the underground. Furthermore, the steep flanks and narrowed profile of the wadi form a suitable topographical setting to capture storm water with a dam. Additionally, the distance between the reservoir and the wellfield allows the underground storage of water until the summer, when the demand increases. However, the hydrogeological structures, which are beneficial for MAR, generate also problems and therefore the operation of the MAR facility must be improved. Hence, there is an urgent need of measures to reduce the sedimentation process and remove sediments from the Wala reservoir to mitigate a further dropping of the groundwater level and to preserve the infiltration rate of the reservoir on the long-term. Additionally, an improved concept for operating the Hidan wellfield is required in order to avoid strong groundwater level fluctuations in the short-term. A further increase in abstraction is not recommended. The implementation of protection zones and a better coordination of water injection into the recharge wells are urgently needed to reduce further groundwater pollution during precipitation events and to avoid groundwater seepage into the wadi. The methods presented in this study, in particular the numerical approach and the combined protection zones concept, are transferable to existing or planned MAR sites in comparable semi-arid karst areas.

Kurzfassung

Die kontrollierte Grundwasseranreicherung (engl.: managed aquifer recharge, MAR) ist ein vielversprechender Ansatz zur Erhöhung der Grundwasserverfügbarkeit in wasserarmen Regionen. Speziell in semi-ariden Gebieten, mit einer hohen Variabilität der Wasserverfügbarkeit, hilft die zeitliche Speicherung von Regenwasser im Untergrund Trockenperioden zu überbrücken und ist somit eine Schlüsseltechnologie in der Wasserwirtschaft. Eine besondere Herausforderung für die technische Umsetzung und den Betrieb von MAR stellen jedoch Karstgrundwasserleiter dar, da sie in der Regel eine starke hydraulische Anisotropie und Heterogenität aufweisen und daher sehr anfällig für Verunreinigungen sind.

Hauptfokus dieser Arbeit liegt auf der Untersuchung der Flutwasserspeicherung im Wala Stausee in Jordanien und der Anreicherung des darunter liegenden Karstgrundwasserleiters. Von besonderem Interesse ist hierbei die Auswirkung auf das stromabwärts liegende Hidan Brunnenfeld, welches zur Trinkwasserversorgung der Städte Amman, Madaba und kleinerer Gemeinden beiträgt. Dazu wurde ein umfassendes hydrogeologisches Konzeptmodell erstellt, das wiederum als Grundlage für ein numerisches Grundwassermodell diente. Anhand der simulierten Wasserstände und Szenarien konnten die Haupteinflüsse auf den Langzeittrend des Grundwasserspiegels abgeleitet werden. Für einen verbesserten Schutz des Stausees und des Brunnenfeldes wurde ein kombiniertes Schutzzonenkonzept für die Karstumgebung entwickelt, dass die Interaktion von Oberflächen- und Grundwasser berücksichtigt.

Berechnungen zeigten, dass etwa 6.7 Millionen m³ Wasser pro Jahr im Durchschnitt (2002-2012) vom Stausee in den Untergrund infiltrierten, was einem durchschnittlichen Grundwasserentnahmeanteil von ca. 60 % im gleichen Zeitraum entspricht. Tritiumdaten zeigen den unmittelbaren Einfluss der Stausee-Infiltration auf das Brunnenfeld, wobei die mittleren Verweilzeiten des natürlichen Grundwasserzustroms nach der ^{14}C-Methode auf mehrere tausend Jahren berechnet wurden. Eine Auswirkung auf die Grundwasserchemie durch das niedrig mineralisierte Oberflächenwasser auf das hochmineralisierte Grundwasser wurde nur in den ersten Jahren anhand starker Schwankungen der Salinität im Brunnenfeld beobachtet.

Für das numerische Modell wurde ein „äquivalent poröses Medium“ (engl: equivalent porous medium, EPM) Ansatz gewählt und eine spezielle Anpassung an die karstspezifischen heterogenen und anisotropen Eigenschaften vorgenommen. Dafür wurde die 3-dimensionale Aquifergeometrie auf ein 2-dimensionales Profil entlang des Wadis projiziert und weiter in hydraulische Zonen unterteilt, welche sowohl Zonen niedriger als auch hoher Fließgeschwindigkeit repräsentieren. Die Simulationen

zeigten, dass der absteigenden Langzeittrend des Grundwasserspiegels auf die Sedimentation bzw. auf die dadurch sinkende Infiltrationsrate im Stausee zurückzuführen ist. Kurzfristige starke Grundwasserspiegelschwankungen im Brunnenfeld gehen allerdings auf Änderungen der durchschnittlichen Entnahmetiefe zurück.

Untersuchungen zur Vulnerabilität des Grundwasserleiters und auftretender Kontamination haben gezeigt, dass regelmäßig auftretende bakteriologische Verunreinigungen des Grundwassers auf Infiltration von Oberflächenabfluss nahe dem Brunnenfeld zurückzuführen sind. Dieser wird sowohl durch Regenereignisse ausgelöst, als auch durch Grundwasseraustritte im Wadi aufgrund hoher Infiltrationsraten im Reservoir. Diese Erkenntnisse dienten zur Erstellung einer vereinfachten Vulnerabilitäts- und Risikokarte, die wiederum die Basis für ein kombiniertes Schutzzonenkonzept ist, dass sowohl das Einzugsgebiet des Wala Stausees als auch das des Hidan Brunnenfeldes berücksichtigt, sowie die Interaktion von Oberflächen- und Grundwassers.

Die Ergebnisse zeigen, dass das Wadi Wala geeignete strukturelle Voraussetzungen für die Anwendung von MAR in den darunter liegenden Karstgrundwasserleiter bieten, da die starke Verkarstung entlang des Wadis die Infiltration von erheblichen Mengen an Flutwässern in den Untergrund ermöglicht. Weiterhin bilden die steilen Flanken und der verengte Talquerschnitt geeignete topographische Voraussetzungen für die Flutwasserspeicherung mit Hilfe eines Staudammes. Darüber hinaus ermöglicht der Abstand zwischen dem Reservoir und dem Brunnenfeld die unterirdische Speicherung von Wasser bis zum Sommer, wenn die Nachfrage steigt. Allerdings stellen diese für MAR vorteilhaften Strukturen auch Probleme dar, weshalb der Betrieb der MAR-Anlagen einer Verbesserung bedarf. Folglich sind dringend Maßnahmen erforderlich, die den Sedimentationsprozess verringern und Sedimente aus dem Wala Reservoir entfernen, um langfristig die Infiltrationsraten des Stausees zu erhalten und somit auch die Grundwasserspiegelabsenkung abzuschwächen. Darüber hinaus ist ein verbessertes Konzept zur Betreibung des Hidan Brunnenfeldes erforderlich, um kurzfristige starke Grundwasserspiegel-schwankungen zu vermeiden. Eine weitere Erhöhung der Förderrate ist nicht empfohlen. Die Umsetzung der Schutzzonen und eine bessere Abstimmung der Anreicherungsbrunnen sind dringend erforderlich, um eine weitere Verschmutzung des Grundwassers während Niederschlagsereignissen zu vermindern und um Grundwasseraustritte in das Wadi zu vermeiden. Die angewandten Methoden, insbesondere der numerische Ansatz und das kombinierte Schutzzonenkonzept, sind übertragbar auf bestehende oder geplante MAR Standorte in vergleichbaren semi-ariden Karstgebieten.

Table of Contents

Abstract ..... **i**

Kurzfassung ..... **iii**

Table of Contents ..... **v**

List of Figures ..... **viii**

List of Tables ..... **xi**

1 Introduction **1**

1.1 General motivation 1

1.2 Managed aquifer recharge in karstic environments 3

1.2.1 Karst hydrogeology 3

1.2.2 Managed aquifer recharge 3

1.2.3 Specific challenges of managed aquifer recharge in karstic environments 9

1.3 Water resources and management in Jordan 10

1.3.1 Water resources and demand 10

1.3.2 Jordan's water strategy 12

1.3.3 Managed aquifer recharge 12

1.4 Objectives and approaches 14

1.5 Structure of the thesis 16

2 Impact of managed aquifer recharge on the chemical and isotopic composition of a karst aquifer, Wala reservoir, Jordan **17**

Abstract 17

2.1 Introduction 18

2.2 Site description 19

2.2.1 Geographical setting 19

2.2.2 Geology and Hydrogeology 22

2.3 Methodology 23

2.3.1 Available data and methods 23

2.3.2 Major Ions 24

2.3.3 Isotopes 24

2.3.4 Water balance 26

2.4 Results and Discussion 27

2.4.1 Water balance 27

2.4.2 General hydrogeochemistry 28

2.4.3 Isotopes 33

2.4.3.1 Deuterium and Oxygen-18 33
2.4.3.2 Tritium 34
2.4.3.3 Carbon-13 and carbon-14 35
2.4.4 Conceptual groundwater flow model 35
2.5 Conclusion 36
Acknowledgement 37
3 Numerical long-term assessment of managed aquifer recharge from a reservoir into a karst aquifer in Jordan 39
Abstract 39
3.1 Introduction 40
3.2 Site characterisation 42
3.2.1 Geographical setting 42
3.2.2 Hydrogeological setting and conceptual model 43
3.2.3 Problem setting 46
3.3 Database and Methods 47
3.3.1 Water level and abstraction data 47
3.3.2 Modeling background 48
3.3.3 Model setup and discretization 49
3.3.3.1 The recharge model (upper section) 50
3.3.3.2 The abstraction model (lower section) 50
3.3.4 Scenarios 51
3.4 Results and discussion 53
3.4.1 Model calibration and simulation 53
3.4.1.1 The recharge model (upper section) 53
3.4.1.2 The abstraction model (lower section) 55
3.4.2 Model performance criteria 56
3.4.2.1 Uncertainty analysis 56
3.4.2.2 Model sensitivity 56
3.4.3 Scenarios 57
3.5 Conclusions 60
Acknowledgement 61
4 Contamination risk and drinking water protection for a large-scale managed aquifer recharge site in a semi-arid karst region, Jordan 63
Abstract 63
4.1 Introduction 64

4.2 Site description 64
4.2.1 Geographical setting 66
4.2.2 Geology and hydrogeology 69
4.3 Methodology 70
4.3.1 Data acquisition 70
4.3.2 Methods for assessing groundwater contamination 70
4.3.2.1 Correlation of rainfall and microbial occurrence 71
4.3.2.2 Tracer test 71
4.3.2.3 Vulnerability and risk assessment 73
4.4 Results 73
4.4.1 Correlation of rainfall and microbial occurrence 74
4.4.2 Tracer test 78
4.4.3 Vulnerability and risk assessment 80
4.4.3.1 Groundwater vulnerability 80
4.4.3.2 Assessment of contamination risk 82
4.5 Conclusions 82
Acknowledgement 83
5 Synthesis 85
5.1 Conclusion 85
5.2 Perspective and Outlook 87
Acknowledgement 89
Declaration of Authorship 91
References 92
Curriculum Vitae 107
Supplementary Information 109
Supplementary Material - Chapter 2 109
Supplementary Material - Chapter 4 120

List of Figures

Fig. 1.2 Schematic illustrations of different MAR techniques (modified after Dillon 2005). 7
Fig. 1.3 View on the Wala dam, Jordan (Photo: Xanke 2012) 14
Fig. 2.1 a) Geographical setting of Jordan 21
Fig. 2.2 Stratigraphy of formations at the Wala reservoir test site 22
Fig. 2.3 Chart of the water balance of the Wala reservoir and the aquifer 26
Fig. 2.4 Infiltration from the aquifer and water level fluctuations in observation wells CD 1097 and CD 3133 of Hidan wellfield (Fig. 2.1c) 27
Fig. 2.5 Piper diagram displaying water samples from Wala reservoir, Wala wells 1 and 14, and Hidan wells 9 and 13. All samples are slightly dominated by calcium and bicarbonate; higher proportions of bicarbonate are present in the reservoir 29
Fig. 2.6 Binary diagrams from waters of Wala reservoir, Wala wells and Hidan wells a) Ca2++Mg2+ vs. SO42−+HCO3−, b) Na+ vs. Cl-, c) Cl− vs. SO42− and d) Ca2+ vs. Mg2+ 31
Fig. 2.7 a) Electrical conductivity changes at Hidan and Wala wells, and b) water levels in individual wells. During the first flushing of the aquifer the salinity increased in all wells (between 2003 and 2005). The infiltration from the Wala reservoir water decreased from 2007 and the reservoir dried up in 2008, which caused a decrease in the EC of water in the Hidan wells. Long-term increase of average EC is observed from 1980 to 2011 32
Fig. 2.8 Distribution of the δ2H (δ D) and δ18O for samples of a) rainfall, the reservoir, the recharge well and Wala groundwater, and b) Hidan groundwater. Samples of Wala, recharge and Hidan wells are clustered along the MMWL and the GMWL, whereas data from precipitation and the reservoir are more scattered 33
Fig. 2.9 Tritium (3H) content of precipitation and Wala reservoir shows the decrease over time as a consequence of natural decay. The concentration in groundwater increases after 2002, caused by the mixing with recent water from Wala reservoir infiltration 34
Fig. 2.10 Schematic profile along the wadi, showing mixture of young and old groundwater as a consequence of different flow regimes in the fracture and conduit network of the karst aquifer. Drawdown cones are seen at Wala and Hidan wells and infiltration mounds at the recharge well. Water balance values are displayed in million cubic meters as annual average (2002–2012) 36
Table 3.1 Stratigraphic description of the test site (Humphreys 1991; Xanke et al. 2015). 43
Fig. 3.1 a) Location of the study area, b) Dead Sea groundwater basin, Mujib drainage basin and Wala Surface catchment. c) Mean annual rainfall of the Wala surface catchment. d) Trend

of groundwater level in observation well CD 1075 and CD 1212 in the Wala catchment. e) General location of Wadi Wala, Wala reservoir, recharge and abstraction wells and geological setup. f) Overview about Hidan wellfield and the NW-SE trending flexure and the SW-NE trending syncline axis. g) The schematic cross sections of the dam axis. (h) Schematic cross section of Wadi Wala / Wadi Hidan with the distribution of different mean groundwater ages. The values of the water balance are displayed in average annual million cubic meters (MCM) from 2002 to 2012 (modified after Xanke et al. (2015)). 45

Fig. 3.2 a) Water level fluctuations at recharge well 1 and 8, b) water level fluctuations at observation well CD 1097 and CD 3133 at Hidan wellfield and c) the abstraction rates of Hidan wells. 47

Fig. 3.3 Superelevated presentation of a) the distribution of hydraulic zones of the recharge model and b) the hydraulic head distribution during low groundwater level and c) high water level in the recharge model. d) Distribution of hydraulic zones of the abstraction model and e) hydraulic head during low groundwater level and f) high groundwater level in the abstraction model. 52

Fig. 3.4 a) Reservoir infiltration increases exponentially when the water level in the reservoir increases. b) Increased sedimentation and thicker sediment layer reduce the infiltration rate. c) The manually adapted in-transfer rate and its decrease over time in dependency of the water level in the reservoir. 55

Fig. 3.5 a) Reservoir water level and in-transfer rate, b) measured and simulated hydraulic head at recharge well RW 1 and RW 8 and c) groundwater level simulations at CD 3133 and results of sensitivity analysis performed with the abstraction model when the high permeable zone 2X or the aquifer section 2B were removed and replaced by the hydraulic parameters from section 2C. The correlation between measurement and observation at d) RW 1, e) RW 8, f) CD 3133 with abstraction depth no 1 and g) changing abstraction depth. f) Sketch of the different abstraction depths no 1-3. Scenario period (2013-2022) of h) water level of Wala reservoir and in-transfer rate, i) water level at RW 1 and RW 8 and j) the impact of the four scenarios on water level at observation well CD 3133. 59

Fig. 4.1 a) View of the Wala Dam and b) a recharge well. c) Sheep herd at Hidan wellfield between unprotected wells and d) well with destroyed fence. 67

Fig. 4.2 a) Location of Wala surface catchment relative to Jordan's major aquifer systems. b) Mean annual rainfall distribution in the Wala catchment and its wadi channel network, c) topography and d) outcropping aquifer systems and geological structures. e–f) Geological map and location of Wala reservoir, recharge and production well. 68

Fig. 4.3 a) Goat herd at a pool, which is continuously filled with water. b) Location of tracer injection between the abstraction wells of Hidan wellfield. The selected dry pool is only filled with water after rainfall or flood events. Pools north of the wellfield receive continuous wadi flow. c) Schematic cross section of Hidan wellfield with the selected pool between well CD 3475 and CD 3243 and the assumed infiltration path of the NaCl solution. 72

Fig. 4.4 a) Mean monthly rainfall at different stations within the Wala catchment (Fig. 1b) and b) the resulting mean monthly surface runoff of Wadi Wala. 74

Fig. 4.5 Comparison of daily reservoir infiltration, rainfall and total coliforms at Wala and Hidan wells a) from 2002 to 2006 and b) from 2007 to 2012. C) Comparison of E. coli with rainfall and injection into recharge wells from January to July 2012 and with rainfall and E. coli in February 2012. The lag time between rainfall and E. coli is less than 24 h. d) Water level of Wala reservoir and E. coli occurrence in the reservoir from January to July 2012. 77

Table 4.1 Results from the NaCl tracer test. 79

Fig. 4.8 a) Hazard map based on land use, b the resulting risk map and c proposed protection zones I and II and the risk areas. 81

Fig. 5.1 Humidity index of semi-arid, arid and hyper arid zones of the Mediterranean region and Middle East in relation to outcrops of carbonate rocks (carbonate map by Chen et al. (2017); humidity data from University of Auckland, New Zealand: http://web.env.auckland.ac.nz/our_research/karst/; humidity data from UNEP (2016)). 88

List of Tables

1.3.2 Table 1.1 Historical development of population number, water demand and water supply (compiled from: MWI 2013; DOS 2016; Hadadin 2010; MWI 2013). 11

Table 1.2 Water supply in Jordan in 2014 and the proportion of water sources and consumers (MWI 2016). 11

Table 1.3 List of dams in Jordan used for MAR (modified after Steinel 2012; Hadadin 2015; Xanke et al. 2015). 13

Table 2.1 Physico–chemical parameters of 51 Wala reservoir and groundwater samples from 2001 to 2011 30

Table 2.2 Calculated mean residence times of groundwater after Fontes and Garnier (1979); Plummer and Glynn (2013) and Evans (1979). 35

Table 3.1 Stratigraphic description of the test site (Humphreys 1991; Xanke et al. 2015). 43

Table 4.1 Results from the NaCl tracer test. 79

Chapter 1

Introduction

1.1 General motivation

In many regions on earth, fresh water reserves are increasingly threatened by various aspects that come along with the growing population and the impact of climate change, especially in semi-arid and arid regions (WWAP 2015). Thus, water demand for industrial, agricultural and domestic purposes is rising and often exceeds water availability. As a consequence, strong withdrawal of groundwater causes a decline of water levels, more rapidly than they can be renewed by natural recharge (Foley 2005). Concurrently, water quality is progressively deteriorated by human activities, which consequently challenges the access to safe drinking water (WHO 2004). In addition to the unequal distribution of freshwater resources on earth, semi-arid regions are exposed to varying climate conditions discernible in droughts in summer and heavy rainfall in winter. This presents challenges on water management since resources are depleted in dry periods and high rainfall intensities often produce floods and hence a surplus in water availability during wet periods. This surface runoff is commonly stored in surface ponds or reservoirs (Sowers et al. 2011), but in many cases it remains unused and flows into the receiving water bodies.

A promising alternative to surface storage in semi-arid and arid regions is managed aquifer recharge (MAR) since it poses significant advantages (Dillon 2005). Thus, it is apparent that the recharged water is protected from direct surface contamination and evaporation as well as it prevents declining groundwater levels and promotes the natural treatment during the infiltration process and residence time in the underground. Depending on the hydrogeological setting, the surplus water can be stored during the winter season, for short-term or long-term, and recovered when demand increases in summer. However, besides rainwater also other water sources can be used for MAR, such as treated wastewater, lake water or groundwater from other aquifers (Dillon 2009). Different aquifers types are suitable for managed underground storage, such as unconsolidated porous aquifers, fractured rocks and karst aquifers, but their suitability for MAR depend on different aspects concerning the storage properties and permeability. The most challenging geological setup is posed by carbonate rocks since they reveal strong heterogeneity and anisotropy and are vulnerable to contamination, which makes them difficult to assess (Daher et al 2011). However, in many countries of the Mediterranean region and of the Middle East carbonate rocks are present and serve as an important fresh water supplier (Bakalowicz et al. 2008) and also bear the potential for the application of MAR.

Generally, the management of karst aquifers, and therefore also the successful application and sustainable operation of MAR, need a comprehensive knowledge about the site specific hydraulic characteristics (Bakalowicz 2005; Einsiedl 2005). Thus, it requires a detailed investigation of the local hydrogeology to define the input and output of the system and to evaluate the resources and reserves (Bakalowicz 2011; van Beynen 2011). Here, hydrochemical and isotopic data are needed to document the spatial impact of surface water on groundwater since hydraulic tests, geophysical measurements and water level observations only give local information. Additionally, groundwater models are helpful to close the gap between local hydraulic information and the properties of the entire drainage system. Here, modeling approaches have to be developed which address not only the local groundwater flow pattern but also the operation of the MAR site. Furthermore, scenarios need to be developed and simulated with numerical models to predict the long-term impact of technical measures and climate change on groundwater level trends. A further important aspect in terms of karst aquifer management, and hence the application of MAR, is the vulnerability of the groundwater system to contamination. Therefore, adapted protection concepts are essential that address the protection of the surface water and groundwater.

Since only a few examples of MAR into carbonate rocks exist worldwide (Daher et al. 2011) there is a lack of comprehensive studies that propose convenient investigation methods and management options which are transferable to existing or planned MAR sites in karstic environments in semi-arid regions. Here, Jordan is one of the countries which established MAR as a key element in the national water strategy and applied it also to karst aquifers. It ranks among the world's driest regions and highly depends on its groundwater resources which mainly comprise carbonate aquifers. Here, the largest MAR site in Jordan is the Wala reservoir where flood water is recharged since 2002 to the underlying karst aquifer and increases water availability at the downstream Hidan wellfield. However, its long-term operation is not well investigated and a sophisticated management strategy is missing since problems with sedimentation and bacterial contamination occurred. The main motivation of this thesis is a detailed hydrogeological investigation of the Wala reservoir, the understanding of the karst aquifer system and its response on artificial recharge and abstraction, and the development of management options to improve the operation of the MAR site. Nevertheless, prior to a detailed local investigation, it presupposes an understanding of the general hydraulic characteristics of karst aquifers, the functional principle of the different MAR techniques and their advantages and disadvantages when applied in karst.

1.2 Managed aquifer recharge in karstic environments

1.2.1 Karst hydrogeology

Karst aquifers are very unique compared to uniformly porous (Darcian) aquifers, since the process of carbonate rock dissolution (karstification) generates a distinct heterogeneity and anisotropy, observable in the characteristic duality of discharge patterns (Bakalowicz 2005; Goldscheider and Drew 2007; Ford and Williams 2007). Most of the conspicuous landscapes on earth are formed by karstification, where sinkholes (dolines), swallow holes, poljes and karren are present (Fig. 1.1) on the surface (exokarst) and a discrete network of conduits and caves are developed subterraneanly (endokarst; Kresic 2013). The upper few meters of the rock layers are usually more affected by karstification and weathering (epikarst) and often reveal a higher degree in permeability as the aquifer below. Since permeability decreases with depth and fine sediments partly clog the vertical infiltration paths, in many karst environments this zone is regarded as a transition zone where infiltrating water is often stored temporally (perched aquifer), sometimes for several years. In the epikarst, water is drained laterally towards discrete vertical fissures and shafts, from where it percolates towards the phreatic zone (Jones 2013). However, in arid regions, the epikarst may be developed to a much lesser extent than in humid regions (Jones 2013) since carbonate dissolution depends on the presence of water (H_2O) and dissolved carbon-dioxide (CO_2; Bakalowicz 2005; van Beynen 2011). Therefore, karst features are mostly independent from the geographic and climatic setting, but may vary in their degree of karstification and morphological shape (Kresic 2013).

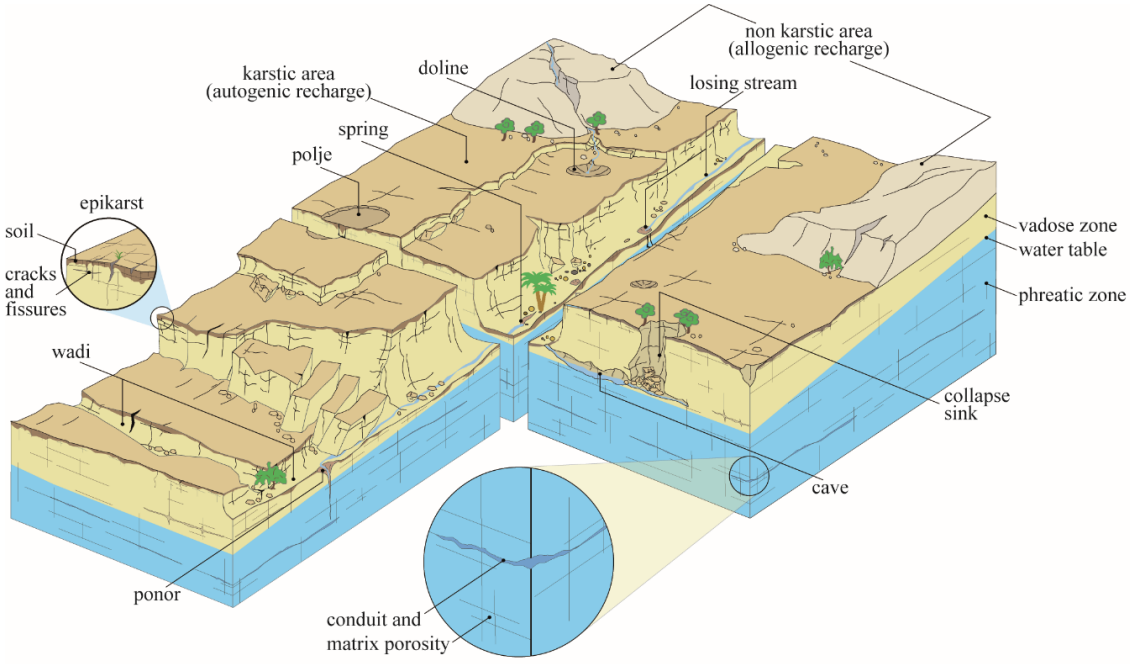

Fig. 1.1 Conceptual block diagram of a karst groundwater system in a semi-arid setting (inspired by Mangin 1975; Bakalowicz et al. 1999; Goldscheider and Drew 2007; Schmidt 2014).

The distinctive duality of discharge pattern is attributed to the triple porosity character of karst aquifers, where intergranular porosity (primary porosity), fracture porosity (secondary porosity) and conduit porosity (tertiary porosity) coexist (Ford and Williams 2007; Hartmann et al. 2014). The governing processes for the primary porosity development take place during rock genesis, but the hereby generated permeability is often insignificant. The secondary porosity is the result of tectonic stress that causes a variety of fractures and fissures with different orientation, length and aperture width. Primary and secondary porosity are often declared as the matrix porosity (Goldscheider and Andreo 2007). Depending on the hydraulic interconnectivity of the fracture network, water progressively dissolves the rock and enlarges the fractures to channels, conduits or caves. Since this combined process of water flow, rock dissolution and widening of the fractures is self-reinforcing, it often develops directions of preferential flow within the bedrock (Goldscheider and Drew 2007; Kresic 2013). For instance, Green et al. (2011) propose an intensified karstification along dry river beds (wadis) in semi-arid regions as a result of increased water flow and infiltration along the wadi course. Generally, the carbonate rock solubility increases with increasing CO_2 partial pressure and decreasing water temperature and can also be reinforced by the mixing of different mineralized water (mixing corrosion). Thus, conduit networks usually develop more rapidly in the shallow phreatic zone and this much stronger in the horizontal than in the vertical direction. Due to different base levels in former times, conduit networks may have developed on different elevations within the aquifers (Ford and Williams 1989; Bakalowicz 2007), as it is e.g. attributed to carbonate aquifers around the Mediterranean Sea (Bakalowicz 2015).

Hydraulic conductivity in karst aquifers can span many orders of magnitude as a result of the different types of porosities. Diffuse groundwater flow through the matrix porosity may reveal flow velocities of a few centimeters a day, whereas concentrated flow through channels and conduits can reach velocities of several hundred meters per hour (Teutsch and Sauter 1991; Kresic et al. 1992; Ford and Williams 2007; Goldscheider and Drew 2007). This wide range in flow velocities is also reflected in the mean residence times of groundwater (Worthington 2007), which depend on the degree of karstification and the extent of the catchment (Bakalowicz et al. 2007). The hydraulic anisotropy and heterogeneity also affects hydraulic conductivity values which are obtained by e.g. pumping tests. They may be valid for local hydraulic conditions, but are not transferable to the whole aquifer (Goldscheider and Drew 2007). Here, results may differ strongly between wells that are placed close to each other, since well-developed fractures and conduit networks are difficult to locate. Thus, production wells may also reveal strong differences in their productivity (Bakalowicz 2011).

The mechanism of groundwater recharge in karstic environments is driven by two different types of infiltration: diffuse infiltration and point infiltration (Goldscheider and Drew 2007). Diffuse infiltration

generally results from precipitation at karstic formations (autogenic recharge), where water directly infiltrates through cracks and fissures. In the contrary, point infiltration is facilitated by sinkholes or swallow holes, where water from rainfall or losing streams is drained from adjacent non-karstic areas towards there receiving points (allogenic recharge). Here, water quickly percolates via vertical shafts and fractures towards the phreatic zone by passing the epikarst zone. This duality in recharge pattern is also reflected in spring discharge, where the fast response to rainfall events is mainly a result of allogenic recharge processes, whereas autogenic recharge is responsible for the base flow during the year. The hydrodynamic variability in spring discharge is therefore always a function of the degree of karstification, of the conduit network in the vadose and phreatic zone, the dominating fast or slow infiltration conditions as well as of the storage properties of the phreatic zone (El Hakim 2007).

The unique character in terms of storage and drainage pattern poses a particular challenge for the management of karst aquifers (Worthingthon 2013). Spring discharge usually responds rapidly to rainfall events with a high discharge and is also often associated with water quality deterioration through turbidity or bacteriological contamination (Goldscheider and Drew 2007), whereas discharge rates during dry periods are often not sufficient to cover the increasing water demand. Even groundwater tables are often subject to strong fluctuations during the year since abstraction increases in dry periods when groundwater recharge takes place less frequently. These seasonal differences are much stronger when semi-arid climate is prevailing and high seasonal variability in rainfall, surface runoff and groundwater recharge exacerbate a continuous water supply. Investigation methods and technical measures must therefore consider different hydraulic conditions (summer and winter), which presuppose improved monitoring tools (Gundmundson 2011) to gain a sufficient knowledge about the recharge and discharge behavior of the system and changes in water quality. Therefore, an active management of karst aquifers requires a “case-by-case” plan (Bakalowicz 2011) including different methods and methodological adaptions (Hartmann et al. 2014) such as a qualitative monitoring, determination of input and output, evaluation of the resource and reserve, the application of tracers, modelling approaches, vulnerability and risk assessments and technical measures addressing groundwater and spring capturing and managed aquifer recharge (Kresic et al. 1992; Goldscheider and Drew 2007; Bakalowicz 2011).

Various field studies are available to characterize karst aquifers, both hydraulically and hydrochemically (Goldscheider 2015), and provide the basis information for further evaluation with physical or mathematical models (Wang and Anderson 1995). Therefore, a comprehensive investigation should always be carried out to obtain the most accurate hydrogeological description of the system. Here, hydraulic tests, geophysical measurements, and water level monitoring can provide valuable local information, whereas physical and chemical data allow identifying changes in water

quality or the mixing of different waters on intermediate or catchment scale. Isotopic data can be used to reveal the origin of the groundwater, its mean residence time in the underground or also the mixing of different water types (Gonfiantini et al. 1998; Etcheverry and Vennemann 2009). Next to isotopes as natural tracers artificial tracers are also very useful to identify flow path and time of groundwater and are successfully applied in many examples (Seiler et al. 1996; Geyer et al. 2007; Goeppert and Goldscheider 2007; Rappl et al. 2010; Margane 2011). However, a general problem of using the hydraulic data obtained by field experiments is their transferability to another locality or at a larger scale. Here, numerical models can help to close the gap between local information and the entire hydraulic system and therefore represent an important management tool for karstic environments despite their use is of different complexity, depending on whether a simple transformation of the input into the output signal (lumped models) or a spatial discretization of the model domain (distributed models) is required. To evaluate the characteristic vulnerability and contamination risk of karst aquifers, different methods are available, which consider the protective function of the soil cover, the epikarst, the unsaturated zone, and the two different types of infiltration patterns (Zwahlen 2004). The results obtained by the vulnerability and risk assessments are often used for a resource (entire aquifer) and source protection (well or spring) concept.

1.2.2 Managed aquifer recharge

In addition to natural recharge processes (section 1.2.1), human activities also often contribute in different ways to aquifer recharge, e.g. by unintentional irrigation return flow or leakage from water- and sewer networks or unmanaged from storm water tanks, leach fields etc. (Dillon et al. 2009). Here, Managed Aquifer Recharge (MAR) poses the third case of man-made intervention into aquifers with intentional underground storage of water for later recovery, to counteract falling groundwater tables, to improve water quality, prevent sea water intrusions or for a general environmental benefit (Bouwer 2000; Dillon et al. 2009). However, depending on the source water e.g. recycled water, rainwater or treated drinking water, a potential contamination risk is given (Page et al. 2010; Page and Levett 2010).

Key factors for the suitability of locations for MAR are the availability of water used for infiltration and a sufficient storage space in the aquifer. Both criteria can be evaluated with reasonable effort on a large scale, but never replace a substantial assessment on a local scale since more detailed investigations are required to address the hydrogeological setting. Moreover, socio-economic and political aspects play an important role in the planning and implementation phase (Gale et al. 2006). Generally, the source water must be of suitable quality and quantity and should not be needed elsewhere. The hydraulic aquifer properties must reveal an adequate permeability and storativity to ensure the recharge of a sufficient amount of water and its recovery when needed. Hence, it is essential

to set up a conceptual model of the site to reveal the water balance of the system, its hydraulic function, the best recharge and abstraction method, the environmental and socio-economic benefit, and also the knowledge gaps (Gale et al. 2006).

Generally, it can be distinguished between two recharge methods the direct injection of water into the vadose or phreatic aquifer zone through wells or galleries and the infiltration from the ground surface through natural or artificial surface water bodies. Fig. 1.2 shows the general function of different MAR techniques and their combination after Dillon (2009), where it is obviously that surface infiltration is only valid for unconfined settings. In most cases, the major objective of MAR is the recovering of the recharged water. This can be done at the same well where it was injected, as aquifer storage and recovery (ASR), or by transferring it to another well, known as aquifer storage transfer and recovery (ASTR). Infiltration from the surface comprises the method of bank infiltration from rivers or lakes where the water is filtered by passing the underground towards an abstraction well. The same cleaning effect can be achieved by water percolation from one pond to another or to an abstraction well which is located at a lower level. Furthermore, infiltration from surface pools through the unsaturated zone can be done via channeled water into ponds (off-stream) or via percolation tanks that are located in

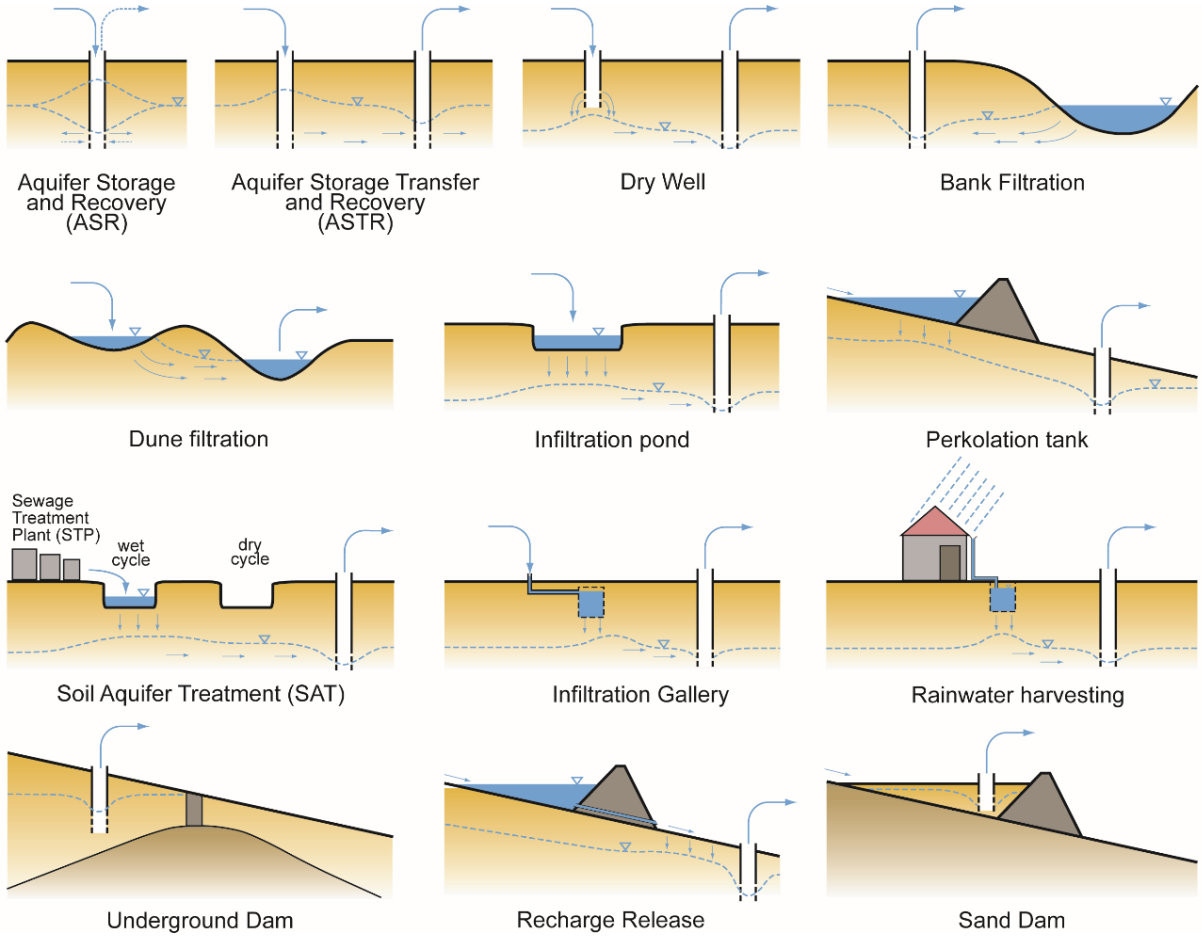

Fig. 1.2 Schematic illustrations of different MAR techniques (modified after Dillon 2005).

ephemeral wadis (on-stream). Treated wastewater can be used further on by soil aquifer treatment (SAT) where remaining nutrients or pathogens are removed during the soil passage. Underground facilities, such as galleries or caissons, allow infiltration protected from the sunlight or the impact of dust, which can facilitate further algae growing or turbidity. Different types of dam constructions onthe surface or underground are valuable to store large amounts of water to increase groundwater availability (Dillon 2009). Groundwater recovery is usually done via abstraction wells, but recharge facilities upstream of a spring, to increase their discharge, are also possible.

In addition to the described positive impacts of MAR on groundwater level and groundwater quality, also other economic and ecological benefits can be achieved. Hence, an important reason for MAR is to improve water supply for drinking or agricultural use, especially when demand increases during dry periods in water scarce regions. Therefore, it affects indirectly the quality of life by an improved water supply and also life standard by e.g. an increased crop yield due to an improved irrigation. A further benefit is the avoidance of evaporation losses from surface water bodies, the reduction of treatment costs or the control of flood events. However, MAR is not a substitution for a water demand management (Gale et al. 2006) but plays an important role in this context.

Despite the positive effects of MAR as described above, the life span of the recharge facilities can be reduced by clogging as a result of different chemical, physical, mechanical or biological processes (Martin 2013). Hence, the sedimentation, the growing of algae and biofilms as well as the precipitation of minerals are common processes which lead to clogging of the infiltration path at recharge basins or injection wells. The occurring processes depend on the source of the water (e.g. from rivers, lakes, canals, treatment plants or captured storm water), but also on the environmental conditions. The chemical reactions of mineral precipitation, ion exchange or adsorption and oxygen reduction are often caused by changes in temperature or pH, whereas physical clogging occurs through the accumulation of suspended solids or clay swelling. Furthermore, mechanical clogging can be the result of trapped air or gas in the soil, produced by bacteria (e.g. sulfate reduction; Bouwer 2002; Martin 2013) or of hydraulic failure of the underground. Biological processes also play a common role in clogging since eutrophication in surface water bodies lead to algae growing or microorganism and bacteria produce biofilms that physically adsorb to the rock matrix. As a consequence, the source water for MAR should always be of sufficient quality or must be treated before the infiltration. Furthermore, an adequate strategy to avoid or reverse clogging processes must be developed. Here, surface infiltration schemes allow an easier maintenance, e.g. by removing sediments or ploughing the clogging layer, than wells that are clogged by suspended material or by precipitation of iron or manganese since these processes are far more difficult to be reversed. This can partly be avoided by chemical treatment or backwashing (Martin 2013).

1.2.3 Specific challenges of managed aquifer recharge in karstic environments

The number of examples for MAR in karstic environments is small compared to those in porous media (Daher et al. 2011) since the highly dynamic discharge behavior of karst aquifers (as described in section 1.2.1) challenges its application. The degree of development of matrix porosity and conduit network plays a determining role for the general suitability of MAR and the possible recharge methods that can be applied. Hence, a strongly karstified aquifer, dominated by cave and conduit flow, may be less suitable for certain methods (section 1.2.2) than if applied in moderately karstified aquifers with a matrix dominated flow. A decisive difference between the two dominant flow velocities is the possible storage time which can be achieved. Thus, the local injection and recovery (ASR) of a water bubble into a brackish, moderate karstified aquifer with a low hydraulic gradient and under confined settings was successful e.g. applied in Australia over a period of a few years (Pavelic et al. 2006). The same hydrogeological setting is also declared to be suitable for ASTR (Page et al. 2010). However, a high groundwater flow velocity would aggravate the application. Generally, the installation of wells in karst aquifers for abstraction or injection is difficult since the location of the conduit network is not easy to explore, but may have the highest probability to be tapped close to springs (Bakalowicz 2011). Due to the fast flow of water in the conduit network, and thus also the fast transport of potential contaminants, direct recharge into the phreatic zone via injection wells should be conducted with particular caution or, if infiltration from the surface is possible, be completely avoided. However, when applied, the quality of the source water must be adequate, especially for the application of ASR. Here, a pre-treatment would be extremely important. In the case of ASTR, the distance between the injection well and the abstraction well should be long enough to avoid direct contamination and promote degradation processes. A further problem for both recharge and abstraction wells are zones of low permeability, since the volume of injection (or abstraction) may be of insufficient quantity (Daher et al. 2011) and makes the application of ASR or ASTR obsolete. The construction of underground dams is a very effective technique for highly karstified aquifers with large conduit and cave systems, where discrete conduits or caves are blocked and water is stored for the extraction by wells. Examples for underground dams can be found e.g. in China (Kresic 2009; Bakalowicz 2011).

Since the epikarst zone often acts as a buffer for diffuse water infiltration (section 1.2.1), surface recharge techniques can be favorably applied in karstic settings (Daher et al. 2011). The diffuse infiltration of water, its temporary storage in the epikarst zone, and the dispersed transfer to the phreatic zone favors the degradation of pollutants and thus reduces the risk of contamination at springs or abstraction wells downstream the MAR facility. However, caution is advised since the direct percolation of surface water into the phreatic zone through sinkholes or vertical shafts may promote the impact of contaminants. This can be an option for recharge and release dams upstream of sinks, where

flood water is temporally stored and released after turbidity has been settled down (Kresic 2009). Direct recharge from surface reservoirs is successfully applied large-scale e.g. at the karstified Edwards aquifer in Florida, USA (Hammond 1993; Kresic 2009).

One of the key processes in the application of MAR in karst aquifers is the extent of carbonate dissolution on the long-term by mixing different types of water (Herzeq et al. 2012). The further rock dissolution intensifies the enlargement of fractures and conduits, which increases the storage capacity and groundwater flow. However, it may also affect water quality in terms of changes in its chemical composition and in some cases also causes changes in salinity. For MAR from the surface, such as storage dams, carbonate dissolution can counteract clogging by widening the infiltration paths. However, this can also negatively affect the stability of dam constructions (Hiller et al. 2011). Beside the carbonate dissolution, Herzeq et al. (2012) also describes other chemical reactions observed during numerous cycles of ASR. Hence, sulfide mineral oxidation was detected, but tapered off after a few cycles since only a few amounts of oxidizable sulfide minerals were present. However, sulfate reduction plays a more important role, but in both cases, water quality was not negatively affected. Further chemical reactions described by Herzeq et al. (2012) were the increase in acidity and consequently the dissolution of carbonate by organic matter oxidation via O_2 or Fe(III), as well as the change in chemical composition as a result of cation exchange.

1.3 Water resources and management in Jordan

1.3.1 Water resources and demand

Karst aquifers play a vital role in Jordan's water supply management since large parts of the country are covered by carbonate rocks. However, most of the groundwater basins have been overexploited in the past decades as a consequence of the fast demographic and economic growth and an associated increase in water demand (Table 1.1; MWI, 2004). The situation has been exacerbated since the population number increased from about 3.1 million in 1990 to about 6.1 million in 2010 and further to about 9.5 million people in 2015 (Table 1.1) as a result of Iraq war in 2003 and the ongoing Syrian civil war and the associated increase in refugees (MWI 2016). Consequently water demand increased to about 1,401 MCM in 2014, but water supply remained at a constant level of about 972 MCM. This is composed of 589 MCM of groundwater, 259 MCM of surface water, and 125 MCM of treated wastewater. However, the safe yield of groundwater is of about 275 MCM. The water demand side is dominated by the agricultural sector, which represents the biggest water consumer with 505 MCM, followed by the domestic sector with 429 MCM and the industry with 39 MCM. Still, there is an annual water deficit of about 429 MCM (MWI 2016).

Considerable amounts of fresh water that are used for drinking are contributed by the predominant carbonate aquifers (60 %), and to a lesser extent by sandstone aquifers (19 %), basalt aquifers (13 %) and alluvial aquifers (7 %). The specified percentages are derived from the abstraction data of the groundwater basins and the estimation of the proportion of the individual aquifer systems.The former proportion of carbonate rock of about 70 % in 1993 (Margane 2002) has decreased while the abstraction of non-renewable groundwater from the Disi sandstone aquifer increased in the past years.

1.3.2 Table 1.1 Historical development of population number, water demand and water supply (compiled from: MWI 2013; DOS 2016; Hadadin 2010; MWI 2013).

Items	1990	1998	2010	2014
Population (millions)	3.17	4.63	6.11	*9.5
Water demand (MCM)	975	1,242	1,383	1,401
Water supply (MCM)	754	843	893	972
Deficit (MCM)	221	399	490	429

* Population number in 2015

The surface water resources in Jordan are mainly composed of base flow, provided by spring discharge, and seasonal flood water. Here, the most vital surface water resources are the Yarmouk River in the north and flood water, captured in numerous storage reservoirs along the escarpment of the Jordan Valley.

Table 1.2 Water supply in Jordan in 2014 and the proportion of water sources and consumers (MWI 2016).

Uses in 2014	Surface Water (MCM)	Groundwater (MCM)	Treated wastewater (MCM)	Total Volume (MCM)
Domestic	103.8	325	0	429
Irrigation	150	231	123.3	504
Industry	4.8	32.2	1.7	39
Total	258.6	588.2	125	972

Non-conventional water resources are generally very important to enhance water supply in water scarce regions (Qadir et al. 2007). Therefore, also in Jordan water resources development focuses more and more on brackish- and seawater desalination, rainfall-runoff capturing, reuse of treated wastewater and managed aquifer recharge. Currently, about 91 % of treated wastewater is reused for agricultural purposes with a total volume of about 125 MCM in 2014, which helped considerably to reallocate fresh water for drinking water purposes (MWI 2016). Desalination of seawater is planned to be conducted in the eastern and central parts (Badia and Aghwar) and in the southern parts (Aqaba) of Jordan. Since 1967 surface runoff is stored into several reservoirs along the hill slope of the Jordan Valley and also in the desert with a total storage capacity of about 350 MCM, whereof the Jordan

Valley dams account for about 317 MCM and the desert dams for about 31.8 MCM. About 2 MCM are stored in small harvesting ponds. The stored water is mainly used for irrigation, electricity generation, desalination and managed aquifer recharge (Hadadin 2015).

1.3.3 Jordan's water strategy

Jordan's water strategy generally aims to augment water supply concurrently with a sustainable use of the available water resources. Since these are very limited and influenced by climate change and a steadily growing population number, the water strategy was first summarized in 1997 proclaiming the sustainable management of the regional surface- and groundwater (Riepl 2013; MWI 2016) in term of policies, water utilities and wastewater reuse. However, geopolitical circumstances changed in the following years and the water strategy was continuously adapted and updated by a new one in 2008 and in 2016. A further complementation was the national water master plan (NWMP), implemented in 2004, and several investment programs and action plans (e.g. Disi-Amman Conveyor and the Red Sea-Dead Sea Project). Over the time, Jordan's water strategy developed more and more to an integrated water resource management (IWRM) approach and was also adopted on the millennium development goals (MDGs) and the sustainable development goals (SDGs) of the United Nations (MWI 2016).

Generally, water planning in Jordan shifted "from a supply-side management to a more integrated and demand –driven water management" (Hussein et al. 2005). Hence, Jordan's water strategy does not only includes a sustainable use of groundwater and surface water, but also addresses water economics, financing, food and energy relations, decentralized wastewater management, reuse of treated wastewater and the application of new technologies and techniques. In this context, the application of managed aquifer recharge has become more and more an important concept, among others (MWI 2016), since it represents a key tool for water management in semi-arid and arid regions. A few examples have been implemented in Jordan in the past (Steinel 2012; Xanke et al. 2015) and further research studies are commissioned by the Ministry of Water and Irrigation including the identification of the overall potential of MAR and possible locations on porous aquifers (Steinel 2012, 2016).

1.3.4 Managed aquifer recharge

The tradition of flood water harvesting in Jordan by building check dams can be dated back to the Bronze Age (Agnew et al. 1995) and still plays an important role in water supply management today. Since 1967, ten dams were constructed in the side wadis of the eastern escarpment of the Jordan Valley with storage capacities ranging from 1.4 MCM (Shueib dam) to 110 MCM (Al-Wehda dam). Additionally, numerous smaller dams are located in the desert (MWI 2013; Hadadin 2015).

Some of the reservoirs showed high infiltration rates despite being constructed for surface storage (e.g. Shueib dam, Kafrein dam) and others have been constructed with the purpose of managed aquifer recharge, such as the Wala dam, Madoneh dams, Butum dams and some smaller desert dams (Steinel 2012). The performance of managed aquifer recharge is mainly conducted by using percolation reservoirs and recharge and release dams. Only in the case of the Wala reservoir, recharge wells are applied too (Table 1.3; Xanke et al. 2015). In addition to the use of surface runoff for MAR, the use of treated wastewater is also proposed by the Government to augment groundwater availability, but not in aquifers that are used for drinking water purposes. The standard regulations and legislations quote maximum concentrations of diverse parameters that must be met when reclaimed water is used for MAR. Furthermore, the targeted aquifers must only be used for irrigation. However, considerations are made to achieve a more flexible adaptation of these standards, e.g. to allow the recharge of less treated wastewater to aquifers of poor quality that are still suitable for irrigation purposes (MWI 2001).

Table 1.3 List of dams in Jordan used for MAR (modified after Steinel 2012; Hadadin 2015; Xanke et al. 2015).

Location	Period of operation	Mean annual infiltration (MCM)	Initial and actual storage capacity (MCM)	Geological formation (labeling)	MAR techniques/ Comment
Wala dam	2002 - today	*6.7	9.3/7.7	Limestone (A7)	percolation reservoir, injection wells
Shueib dam	1968 - today	**0.7	2.5/1.43	Alluvial deposits	percolation reservoir
Kafrein dam	1968 - today	n.a.	8.5/6.0	Alluvial deposits	percolation reservoir
Wadi Madoneh	2003 - today	n.a.	0.09	Limestone (A7)	4 recharge and release dams
Wadi Butum	2011 - today	n.a.	0.47	Limestone (B4)	3 percolation reservoirs
Sultani dam	1962 - n.a.	n.a.	1.2	Limestone (B2/A7)	percolation reservoir/clogged
Qatrana dam	1964 - n.a.	n.a.	4	Limestone (B2/A7)	percolation reservoir/clogged
Rajil dam	1992 - n.a.	n.a.	3.5	Limestone (B4/B5)	percolation reservoir/clogged
Siwaqa dam	1993 - n.a.	n.a.	2.5	Limestone (B2/A7)	percolation reservoir/clogged

* 2002-2012; ** 2001-2009

In most cases, the MAR sites in Jordan are not well investigated, and a comprehensive understanding of the hydraulic system is missing due to the absence of a proper monitoring of the relevant hydrogeological data. However, when data are available they are often inadequately evaluated and not set into the overall context of the hydraulic system in terms of surface runoff storage, groundwater recharge and recovery both quantitatively and qualitatively. The main problem in the application of MAR in Jordan is posed by the high sediment loads that reduce the storage capacity and infiltration rates, as it has occurred for some conventional desert dams, the Sueib dam and the Kafrein dam and the Wala dam (Table 1.3; Steinel 2012). Hence, detailed hydrogeological investigations and appropriate management strategies are required to preserve the MAR sites on the long-term.

1.4 Objectives and approaches

The main objective of this thesis is to better understand the impact of managed recharge of flood water on the karst groundwater system at the Wala reservoir in Jordan (Fig. 1.3). This includes the evaluation of the reservoir infiltration and its proportion on the abstracted groundwater, the impact of sedimentation on the infiltration rate as well as the general impact of the surface water infiltration on groundwater salinity and rock dissolution. Furthermore, it is aimed to characterize the hydraulic behavior of the karst aquifer in dependency of the reservoir infiltration and groundwater abstraction and to identify the driving factors of strong groundwater level fluctuations. Additionally, it is intended to assess the impact of increasing water demand and climate change on groundwater level trend. A further important aspect is to reveal the natural vulnerability of the aquifer to contamination with regard to the reservoir infiltration. Overall, it is aimed to improve the management of the MAR site to ensure a constant water supply of suitable quality to the downstream Hidan wellfield. Additionally, the results and conclusions shall contribute to the general understanding of the hydrogeological processes, which are relevant for MAR into karst. In addition, an important purpose of this thesis is to apply transferable methods that can be used for other existing or planned MAR facilities in similar karst environments of semi-arid or arid regions.

Fig. 1.3 View on the Wala dam, Jordan (Photo: Xanke 2012)

In a first step, a comprehensive spatial characterization of the study site was conducted, which included the collection and evaluation of historical data in terms of geological, hydrogeological and hydrochemical information. This comprises the calculation of the water balance of the MAR system and its individual components of the input (natural groundwater flow and reservoir infiltration) and output (reservoir losses by evaporation and pumping from the wellfield), but also the determination of the proportion of reservoir infiltration on the abstracted groundwater. The impact of reservoir water on groundwater was proven by the consultation of isotopic data and a water chemistry assessment. Hence, the major ions and electrical

conductivity were used to reveal the impact of the low-mineralized surface water on the highly mineralized groundwater and to quantify the extent of rock dissolution.

The hydrogeological conceptual model formed the basis for a numerical groundwater model of the study area, which was implemented to facilitate the investigation of the hydraulic behavior of the aquifer and to expose the impact of reservoir infiltration on the groundwater level. Here of main interest was to predict the long-term impact of sedimentation on reservoir infiltration and hence on the groundwater level trend in the immediate surrounding of the reservoir. Furthermore, it was aimed to assess the impact of increasing water demand (pumping from the aquifer) and climate change (periods of draughts) on the long-term groundwater level trend in the wellfield. A further aspect was to identify the driving factors for large water level fluctuations in the wellfield.

Since karst aquifers are prone to contamination, the site-specific vulnerability and contamination risk was assessed on the basis of the occurrence of coliform bacteria in the reservoir and the groundwater. The variability of contamination was investigated by correlating this bacteria occurrence to rainfall events and reservoir infiltration, whereby the results of a tracer test were used to identify the major impact pathways of the contaminants from the surface into the aquifer. The results from the field investigations were used to further develop and adapt an existing vulnerability and risk assessment onto the site-specific geology and land use characteristics. Based on the vulnerability assessment, a protection approach was developed under consideration of the surface-groundwater interaction and the catchment separation by the Wala reservoir.

1.5 Structure of the thesis

The presented thesis has a cumulative structure and consists of three studies (chapter 2, 3 and 4) and a synthesis (chapter 5) which focus the different aspects of managed aquifer recharge into a karstic environment at the example of the Wala reservoir in Jordan. Chapter 2 documents the general impact of the Wala reservoir on groundwater at the Hidan wellfield by evaluating historical data concerning hydrochemistry, isotopic signature and water level fluctuations. Furthermore, it provides a hydrogeological conceptual model of the test site. Chapter 3 presents the numerical model of the Wala reservoir and the Hidan wellfield. The study aims to identify the major impacts on groundwater level fluctuations and to assess the long-term impact of sedimentation in the reservoir on groundwater level trend at the Hidan wellfield under climate change and increasing water demand. Chapter 4 introduces a combined protection approach for the Wala reservoir and the Hidan wellfield by considering the interaction of surface water and groundwater. It documents the contamination risk at the Hidan wellfield and Wala reservoir by identifying the triggering events for the occurrence of coliform bacteria. Additionally, a protection zone concept is presented for the reservoir and the wellfield based on the results of the vulnerability and risk assessment. Chapter 5 summarizes and evaluates the major results and highlights the important aspects to understand the successful operation of the MAR site at the Wadi Wala. Furthermore, the site-specific conclusions of managed aquifer recharge into karst are set into a regional and global context and future research questions are outlined. Chapter 2 and 3 have been published in peer-reviewed journals, whereas chapter 4 is in the revisions phase.

Chapter 2

Impact of managed aquifer recharge on the chemical and isotopic composition of a karst aquifer, Wala reservoir, Jordan

Reproduced from: Xanke J, Goeppert N, Sawarieh A, Liesch T, Kinger J, Ali W, Hötzl H, Hadidi K, Goldscheider N (2015) Impact of managed aquifer recharge on the chemical and isotopic composition of a karst aquifer, Wala reservoir, Jordan. Hydrogeol. J. 1–14. http://dx.doi.org/10.1007/s10040-015-1233-6.

Abstract

Storm-water harvesting and storage via managed aquifer recharge (MAR) is a promising approach to combat water scarcity in semi-arid regions, but poses a challenge for karst aquifers and regions with highly variable water availability. The infiltration of low-mineralized surface water and its impact on highly mineralized groundwater of a karst aquifer was investigated at Wala reservoir in Jordan over a period of approximately 10 years. The results show significant groundwater-level rise in a wellfield, in response to the yearly average infiltration of about 6.7 million m^3. This corresponds to about 60 % of the yearly average abstraction of about 11.7 million m^3, confirmed by mixing calculations with tritium. A decreasing trend in infiltration due to sedimentation is observed. Mean groundwater residence times of several thousand years, derived from carbon-14 dating, indicate a large storage capacity of the aquifer. The heterogeneous distribution of the residence times is caused by strong groundwater withdrawals and artificial recharge along with karst-specific aquifer characteristics. Temporal groundwater salinity fluctuations in the wellfield are observed after the first MAR infiltration. Enhanced groundwater flow along the wadi course was demonstrated, which is an important aspect with regards to future MAR projects in similar wadis of the region.

2.1 Introduction

Access to safe drinking water is a major challenge in many regions of the world (WHO 2004), especially in countries with a fast-growing population and a natural deficit of water that is prone to high seasonal variability. In Jordan, these factors come together and limit the availability of freshwater resources and their management, hence, limiting the supply of domestic water. Furthermore, overexploitation of Jordan's groundwater resources has led to a lowering of the water tables in the last few decades (El-Naqa and Al-Shayeb 2009). Besides pumping from alluvial aquifers and deep sandstone aquifers, the major water sources are the prevailing carbonate formations found in large parts of the country (MWI 2004).

Managed aquifer recharge (MAR) is an important approach to provide people with water, especially in semi-arid and arid regions (Dillon 2005) and to counteract falling water tables (Bouwer 2000; Mays 2009). Furthermore, Wolf et al. (2007) and Daher et al. (2011) refer to its important role in integrated water resources management (IWRM). Common MAR techniques for underground storage of water are described by Dillon (2005), Dillon et al. (2009) and Bouwer (2002). However, the global number of MAR examples in karst aquifers is small compared to those in porous media (Daher et al. 2011) because MAR implementation in karst poses a particular challenge due to strong hydraulic heterogeneity of the underground (Bakalowicz 2005; Einsiedl 2005). This is characterized by the occurrence of variable storage and flow conditions, which are attributed to the varied porosities of the rock matrix, fractures and conduits (Goldscheider and Drew 2007). An intensified karstification along riverbeds is proposed by Green et al. (2014) for carbonate aquifers in semi-arid regions.

For the purpose of MAR in karst terrains, especially along wadis, high recharge infiltration rates, fast hydraulic response of the aquifers and carbonate dissolution are expected and often come with challenges. Thus, the reduction of reservoir infiltration due to sediment accumulation often causes significant problems (Bouwer 2002). Furthermore, Vanderzalm et al. (2010) describe the dominant influence of calcite dissolution on the change of the water chemistry, which can be intensified below dam sites and reservoirs (Dreybrodt et al. 2002; Hiller et al. 2011; Romanov et al. 2007). The contamination of abstraction wells can be minimized by keeping a sufficient distance from the zone of infiltration (Masciopinto et al. 2012) while being aware that karst aquifers reveal a wide range of groundwater flow velocities.

In order to make use of the limited knowledge about the local hydraulic characteristics of karst aquifers, derived from hydraulic tests, geophysical measurements and water-level observations (Daher et al. 2011), additional hydrochemical data need to be obtained, for example, to identify possible interactions of different water sources. Major ions in the water can indicate chemical processes

(Lakshmanan et al. 2003), whereas the comprehension of the geochemical history and the hydrological conditions of the water can be obtained from isotopic data. Oxygen-18 ($\delta^{18}O$) and deuterium ($\delta^{2}H$) create a relationship between groundwater and its place of origin, whereas tritium ($\delta^{3}H$) and carbon-14 allow for determination of the mean residence time of young groundwater (<60 years; Gonfiantini et al. 1998) and old groundwater, respectively (Plummer 2005). This information is suitable, for example, to identify and avoid the exploitation of fossil groundwater. Additionally, both applications are useful for documenting the mixing of different waters (Etcheverry and Vennemann 2009).

The Wala reservoir is one of the larger MAR test sites in carbonate aquifers, with a mean annual recharge of around 6.7 million cubic meters (MCM; 2002–2012). Water is recharged mainly by natural seepage from the reservoir and small amounts via recharge wells (since 2011) and then recovered at Hidan wellfield. The wellfield serves as an important drinking-water supplier of the cities of Amman, Madaba and nearby communities.

This study presents the evaluation and interpretation of hydrochemical and isotopic data, recharge rates from the reservoir, abstraction rates and water level records from the aquifer, which have been obtained from the database of the Ministry of Water and Irrigation (MWI), Jordan. It is intended to understand and assess the dynamic system of natural recharge and groundwater flow as well as the spatiotemporal impact of artificial recharge and abstraction on the karst aquifer. The central research questions are concerned with (1) the proportion of reservoir infiltration in the abstracted groundwater and the associated groundwater level fluctuations, (2) the influence of sedimentation on the reservoir infiltration, (3) the impact of recharge on the groundwater salinity, and (4) an understanding of the extent of rock dissolution. The results of this study serve as the basis for a conceptual groundwater flow model of the Wala area and as a reference example for future MAR operations in karst aquifers in semiarid regions.

2.2 Site description

2.2.1 Geographical setting

Jordan's landscape is mainly characterized by the Jordan Valley, the adjacent mountain range and the mountain plateau extending to the east of it. The Wala reservoir is located in the mountain range around 40 km south of Jordan's capital, Amman, at an elevation of 485 m above sea level (asl) (Fig. 2.1a). Its surface catchment is a part of the Mujib drainage basin and the Dead Sea groundwater basin (Al-Assa'd and Abdulla 2010) and extends east of the reservoir (Fig. 2.1b) with a total area of around 1,770 km^2 and an elevation of around 1,000 m asl in the northeast to around 960 m asl in the southeast.

The climate in Jordan is semiarid with rainfall mainly during winter. Rainfall data in Wala catchment reveal an increasing trend from north to south with mean annual values of 500 mm (north) and 100 mm (south), whereas the rainfall maximum can reach 800 mm (north) and 250 mm (south). Dry years supply less than 200 mm (north) to 50 mm (south). It can be inferred that most of the runoff is generated in the northern part of the catchment. Mean annual potential evaporation ranges from 2,300 mm (north) to 3,000 mm (south; Margane et al. 2009). The evaporation rate of the Mujib basin ranges from 85 to 93 % and the infiltration rate from 3 to 11 % of the total precipitation (El-Naqa 1993). The remaining rainfall generates surface runoff, which ranges from 0.5 to 10 % of the total rainfall, and flows via numerous tributaries into Wadi Wala. On its way downwards, water passes into Wadi Hidan (variant spelling: Haidan, Heidan, Heedan) and finally discharges into the Dead Sea. Groundwater flow generally follows the topographic gradient from east to west (Fig. 2.1b).

The Hidan wellfield is located around 7 km west of Wala dam at an elevation of around 350 m asl and comprises 16 active abstraction wells with depths between 100 and 200 m. Wala abstraction wells are spread along the wadi and in the valley between the adjacent hills, between the Hidan wellfield and the dam, with depths between 100 and 400 m (Fig. 2.1c).

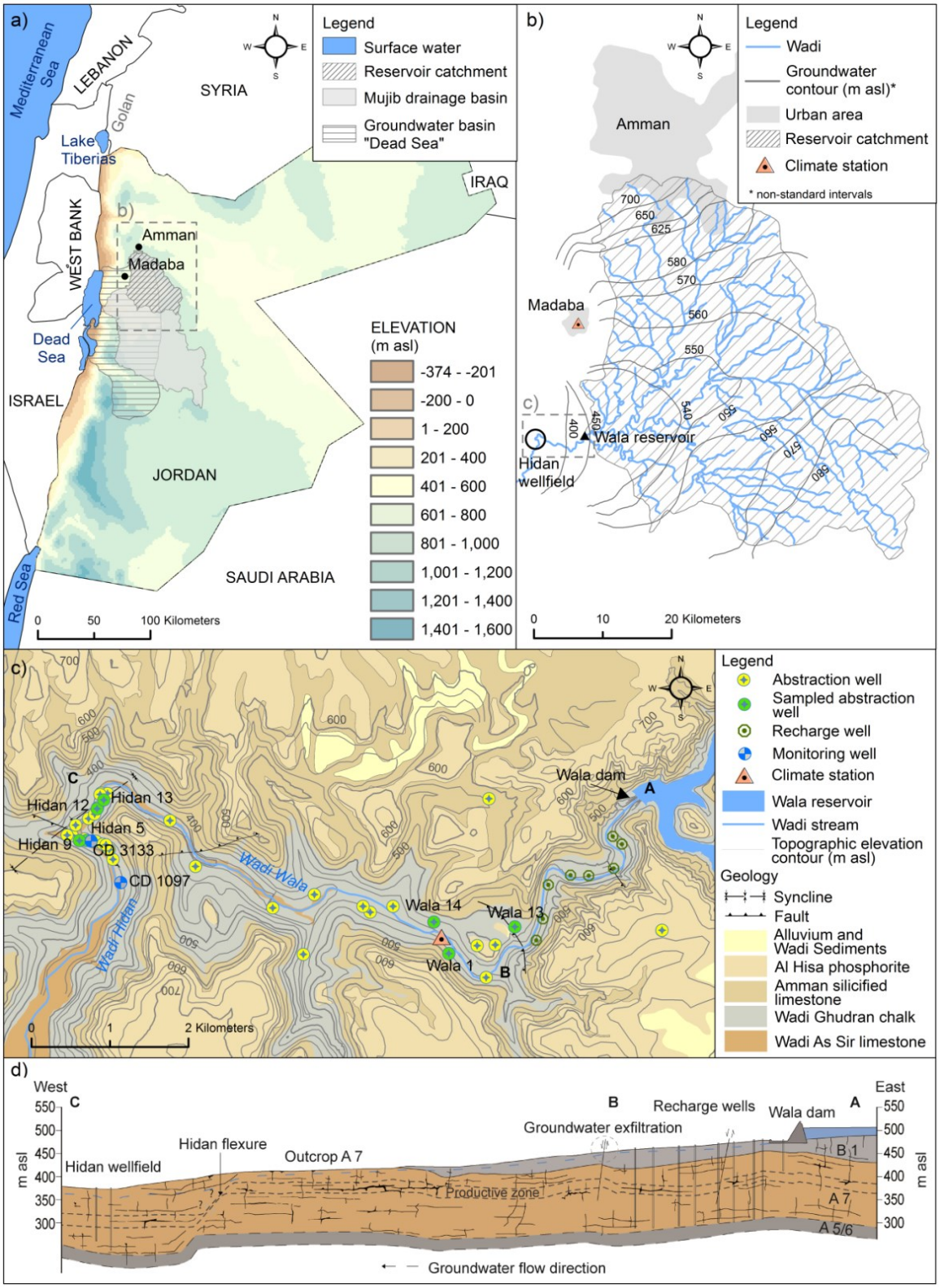

Fig. 2.1 a) Geographical setting of Jordan and location of the Dead Sea groundwater basin, the Mujib drainage basin and the surface catchment of Wala reservoir. b) The Wala reservoir catchment with groundwater flow direction and the location of the reservoir and Hidan wellfield. c) The geology of the Wadi Wala area, recharge, abstraction and observation wells (modified after Al Hunjul 1993). d) Schematic geological profile along Wadi Wala with the location of the recharge wells and abstraction wells (modified after Humphreys 1991, stratigraphy as Fig. 3.2)

2.2.2 Geology and Hydrogeology

The Wala reservoir and its catchment are embedded into a sequence of Upper Cretaceous to Eocene sedimentary rocks (Fig. 2.2), predominantly limestone, dolomite and chalk, and partly covered with Quaternary deposits. The structural setup of the area is within the tectonic framework of the Jordan Rift Valley, which has been tectonically active mainly in the past 12 million years (Bayer et al. 1988).

Period	Epoch	Group	Formation: rock type			Symbol	Inferred thickness (m)	Aquifer type	
Tertiary	Paleocene	Belqa	Umm Rijam: limestone, chalk, chert			B4	120-150	Aquitard	Reservoir
	Maastrichtian/ Paleocene		Muw aqqar: chalk, marl, limestone, chert			B3	~100	Aquitard	
Upper Cretaceous	Maastrichtian		Al Hisa: phosphatic limestone, chert			B2b	40-65	Aquifer	
	Campanian		Amman: limestone, chert			B2a	75	Aquifer	
	Santonian		Wadi Ghudran: chalk	Member	Dhiban	B1c	12-15	Aquitard	
					Tafilah	B1b	~ 50	Poor aquifer	
					Mujib	B1a	12-15	Aquitard	
	Turonian	Ajlun	Wadi As Sir: limestone			A7c	~120-150	Aquifer	Recharge wells
						A7b		Aquifer	
						A7a		Aquifer	
	Cenomanian		Shueib: marl, limestone			A5/6	100-165	Aquitard	

Fig. 2.2 Stratigraphy of formations at the Wala reservoir test site (after Humphreys 1991; Margane et al. 2002)

Marl and limestone sequences of the A5/6 formation (Fig. 2.1d) underlie the regional aquifer system of the Wadi As Sir (A7) formation. This consists of a well-bedded hard and dense limestone, where, in some studies, thin beds of evaporates such as gypsum, anhydrite and halite are observed (Powell and Moh'd 2011; El-Naqa 2004). The limestone outcrops along Wadi Wala around 3 km east of Hidan wellfield, constituting the main regional aquifer system, and can be subdivided into three hydraulic zones with less permeable parts on the top and the bottom and a productive zone in between. Groundwater flow takes place primarily horizontally along the bedding planes, which are enlarged due to rock dissolution. Vertical flow takes place mainly along joints and fractures (Humphreys 1991). Numerous swallow holes are present along the wadi, filled and traversed by the surface water, which is discharged into the wadi from temporal springs around 2 km downstream of the Wala reservoir (Fig. 1d). Higher karstification along the wadi course and thus higher permeability values for the A7 outcrops along the wadi can be assumed.

The Ghudran formation builds the basement of Wala reservoir and is divided into three members: Dhiban (B1c), Tafilah (B1b) and Mujib (B1a). The first and third members consist mainly of chalk and act as aquitards. The second consists of chalk and limestone beds and is considered to be a poor aquifer. The basement of the limestone and chert sequences of the Amman (B2) formation starts at the

top of Wala dam construction and reveals subhorizontal bedding with several minor fold structures and faults. Outcrops of the B3 and B4 formation are found in the Wala catchment and along the wadi and consist of chalk, limestone and chert with thin beds of gypsum and halite (B3) and of limestone, chalk and chert (B4; Humphreys 1991; Bender 1968; Margane et al. 2002).

Around 5 km west of the dam, a flexure crosses the wadi from E to WSW with a dipping of around 40–60° to the north. There, the Ghudran formation is constrained and thinned out between the A7 and B2 formation and might act as a hydraulic barrier for horizontal groundwater flow but promotes the vertical flow along numerous fractures. The axis of a syncline follows the direction of the wadi (NE–SW) at Hidan wellfield and crosses another small flexure (SE–NW) orthogonally (Fig. 2.1c).

2.3 Methodology

2.3.1 Available data and methods

Hydrological, hydrogeological and hydrochemical data were obtained from the database of the Ministry of Water and Irrigation (MWI). The available data and the applied methods for analyzing the chemical constituents and physical parameters are listed in the following:

- Electrical conductivity (EC) and pH were analyzed in situ with field equipment.
- Bicarbonate was determined by titration in the laboratory, 2–4 h after sampling.
- Major anions and cations were measured using an ion chromatography method.
- Oxygen-18 was analyzed with the CO_2 equilibrium/Delta Plus XP isotope ratio mass spectrometer (hydrogen deuterium oxygen, HDO), using a platinum catalyst method. Precision is ±0.15 ‰, according to Bajjali and Abu-Jaber (2001) and Bajjali (2006).
- Deuterium was analyzed using the Delta Plus XP isotope ratio mass spectrometer (hydrogen deuterium oxygen, HDO), using the platinum catalyst method. Precision is ±1 ‰, according to Bajjali and Abu-Jaber (2001) and Bajjali (2006).
- Tritium was determined using the electrolytic tritium enrichment method. Precision is ±1 TU, according to Bajjali and Abu-Jaber (2001) and Bajjali (2006).
- ^{14}C was measured with a benzene synthesis line and liquid scintillation counter.
- ^{13}C was measured by mass spectrometry.

Time series of hydrogeological data:

- Monthly water level from observation wells CD 3133 and CD 1097.
- Daily water level from Wala reservoir. Geometric data of Wala reservoir include the water surface area and reservoir volume for each centimeter of water level.

- Daily precipitation (rainfall collector) and evaporation (measured with a class A pan) from Wadi Wala station.
- Monthly abstraction rates from Hidan and Wala wells.

Isotope data exist from 1994 to 2010, whereas major ions, temperature and EC are available from 2001 to 2011. Data from 1994–2010 for major ions are not available, but additional EC data exist from 1982 to 2000 from 342 samples. Groundwater level data are available from 1994 to 2012. Data gaps in the time series exist due to irregular operation of the wells. Most of the abstraction wells are equipped with taps for manual control, which allow permanent or individual sampling at any time. All data are listed in the electronic supplementary material (ESM).

2.3.2 Major Ions

Data from 51 water samples are taken from the Wala reservoir (2003–2006), two Hidan wells (2001–2011) and two Wala wells (2003–2009). Their locations are displayed in Fig. 1c. Wells with only one sample were not considered. The differentiation of the water types was done on the basis of the major ions Na^+, K+, Mg^{2+}, Ca^{2+}, Cl^-, SO_4^{2-} and HCO_3^-. To check the reliability of the results, the error of the charge balance of the ions was calculated to be less than 5 %, which excluded around 20 % of the available data. Total dissolved solid (TDS) values were deduced from the EC ($TDS \approx 0.65 \times EC$). In order to calculate the saturation index (SI), samples with missing temperature measurements were complemented by the average temperature from other samples of the same well.

2.3.3 Isotopes

Existing tritium (^3H), deuterium (δ^2H) and oxygen-18 ($\delta^{18}O$) data are evaluated for 3 Wala wells, 14 Hidan wells, 6 recharge wells, precipitation from Madaba climate station (Fig. 1b) and the Wala reservoir. The timeframes of the 133 tritium and 163 deuterium and oxygen-18 samples differs greatly, and for several wells only one record exists. A few data are available from 1990 at Hidan wellfield; all other data are from 2002 to 2010. Rainfall data already exist from 1987 until 2000, while data for the reservoir exist from 2002 to 2010.

The δ^2H and $\delta^{18}O$ data have been evaluated to determine the origin of groundwater and to identify possible mixing of water with different isotopic signatures. Therefore, the values are put in relation to the global meteoric water line (GMWL) (Craig 1961). The rainfall of regional origin is represented by the Mediterranean meteoric water line (MMWL; Gat et al. 1969).

Additional information about mixing ratios has been obtained from tritium data. Here, mean residence time of groundwater can be determined for timeframes of less than 60 years, due to its half-life of

around 12.43 years (Etcheverry and Vennemann 2009). Values of 0.8–4 tritium units (TU) in groundwater point to the mixing of old and recent water, whereas values between 5 to 10 TU come from recent recharge (after Clark and Fritz 1997, in Ofterdinger et al. 2004).

Carbon-14 and carbon-13 data of one Hidan and two Wala wells are available from 2002 to 2006, to determine the groundwater age of 8 samples. The method is based on the fact that ^{14}C cuts off from atmospheric exchange when it infiltrates underground. From that point, it can be used for age dating of groundwater bodies, due to its radioactive decay and half-life of around 5,730 years (Gonfiantini and Zuppi 2003; Etcheverry and Vennemann 2009). The formula for age dating is (Plummer and Glynn 2013):

$$T = \frac{5730}{\ln 2} \ln \left(\frac{\delta^{14}C_{\text{Initial}}}{\delta^{14}C_{\text{Measured}}} \right) \quad (1)$$

where T is the time and 5730 is the modern half-life of ^{14}C.

In order to solve the formula for T, the initial ^{14}C activity is required, which is always reported in percent modern carbon (pmc). For calibration, the oxalic acid standard is used, where 95 % of the standard corresponds to 100 % pmc (Gonfiantini and Zuppi 2003; Meredith 2009). It is known from previous studies that dissolution and precipitation of $CaCO_3$ influences the ^{14}C content in groundwater. Therefore, to estimate the source of the different carbon quantities, the ^{13}C content of the total dissolved inorganic carbon (DIC) can be consulted (Kattan 1995). The ^{13}C enrichment and ^{14}C depletion in DIC is caused by the isotope exchange between DIC and carbonate rock (Pearson and Hanshaw 1970; Geyh 1970). ^{13}C activities are related to the Vienna Pee Dee Belemnite (VPDB) standard. Several models have been developed in the past decades to estimate the initial ^{14}C activity (Vogel 1968; Tamers 1967; Eichinger 1983; Salem et al. 1980; Evans et al. 1979; Pearson and White 1967; Fontes and Garnier 1979).

The Fontes and Garnier (1979) equation has been chosen for this study, because it considers most of the chemical processes in carbonate aquifers such as the carbonate, gypsum and soil gas CO_2 dissolution, and the exchange of CO_2 in the gas and aqueous phase, as well as the calcite-bicarbonate exchange (Plummer and Glynn 2013). For comparison, the differing results from the IAEA model (Plummer and Glynn 2013) and Evans model (1979) are also applied. The IAEA model is a further development of the Pearson model, which is based on the isotopic mass balance relation of ^{13}C and ^{14}C, and considers the equilibrium of bicarbonate with the gas phase and the subsequent dissolution of solid carbonate. The Evans (1979) model considers the isotopic fractionation, due to the dissolution and precipitation process of calcium carbonate in groundwater, when equilibrium between calcite and

dissolved bicarbonate is supposed (Plummer and Glynn 2013). For the calculations, the following basic assumptions are made according to studies from Kattan (1995) and Kattan (2001) in Syria: initial ^{14}C activities in the rock are 0 and 1 ‰ for ^{13}C. Activities in soil CO_2 are 100 ‰ for ^{14}C and −21 ‰ for ^{13}C.

2.3.4 Water balance

The amount of input and output from the reservoir is reflected in the daily water level changes and calculated with the related reservoir volume increase (input) or decrease (output). The surface water inflow (Q_{Rin}) is calculated by subtracting the amount of precipitated water (P_R) on the lake surface from the total water volume increase (input). The aquifer recharge (R_R) is calculated by subtracting the daily amount of evaporated (ET_R) water from the total water volume decrease (output). The height of precipitation and evaporation is calculated by multiplying the daily values with the water surface area from the corresponding day (see Fig. 2.3).

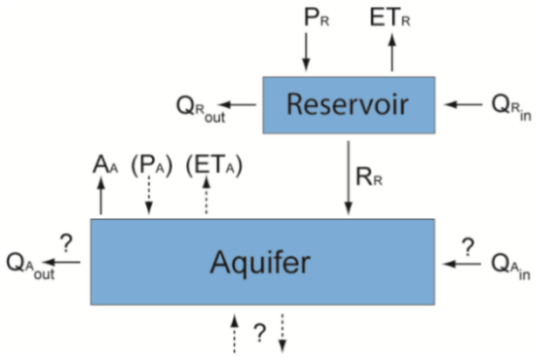

Fig. 2.3 Chart of the water balance of the Wala reservoir and the aquifer

A simultaneous determination of Q_{Rin} and R_R cannot be made because both factors depend on water level increase and water level decrease respectively. Therefore, calculation errors occur on days with inflow into the reservoir. The amount of surface outflow (Q_{Rout}) is measured and calculated by the Ministry of Water and Irrigation (MWI 2012). The aquifer output is determined using the monthly abstraction rates from the wells (A_A). The provided amount from natural groundwater flow is unknown (Q_{Ain} and Q_{Aout}). Direct recharge along the wadi between the reservoir and wellfield by precipitation (P_A), and by loss through evapotranspiration (ET_A) are neglected, as well as possible water exchange with a deeper aquifer.

2.4 Results and Discussion

2.4.1 Water balance

From 2002 to 2012, the reservoir received around 136 MCM of floodwater during the winter seasons, while around 52 MCM were lost via the spillway and around 84 MCM were stored. Approximately 74.1 MCM of the stored water infiltrated into the ground naturally and around 7.8 MCM were lost by evaporation. The difference of 2.1 MCM is composed of the roughly 1.5 MCM of remaining water in the reservoir and a loss that is not covered by the calculations.

The annual amount of infiltration ranges from around 1 MCM in 2008 to around 13 MCM in 2003 with an average of around 6.7 MCM. A clear decrease in infiltration can be observed (Fig. 2.4) with time, due to ongoing sedimentation in the reservoir. Thus, the initial storage capacity of around 9.3 MCM is reduced to approximately 7.7 MCM in 2012, which was caused from the increasing sediment in the reservoir. The total infiltration from 2002 to 2012 facing complete abstraction of around 129 MCM from Hidan and Wala wells, meaning roughly 57 % of the abstracted water is provided by the reservoir. The proportion of infiltrated water on the abstracted water was about 71 % in the period from 2002 to 2007 and decreased to around 42 % from 2008 to 2012. Yearly abstraction rates range from around 10 MCM in 2002 to more than 13.7 MCM in 2008 with an average of 11.7 MCM, where around 96 % is used for drinking-water supply and around 4 % for irrigation. Overexploitation, accompanied by the decreasing infiltration rate from the reservoir, causes water level drop in Hidan wellfield, as observed in 2008/2009 and 2011/2012 (Fig. 2.4). The yearly amount of groundwater flow to the Hidan wellfield is difficult to determine due to variations in natural recharge and withdrawals in the catchment. Assuming the mean annual abstraction rate of around 11.7 MCM and artificial recharge of around 7.3 MCM keep the water level constant, the natural groundwater flow provides a minimum of 4.4 MCM on average per year to Hidan wellfield.

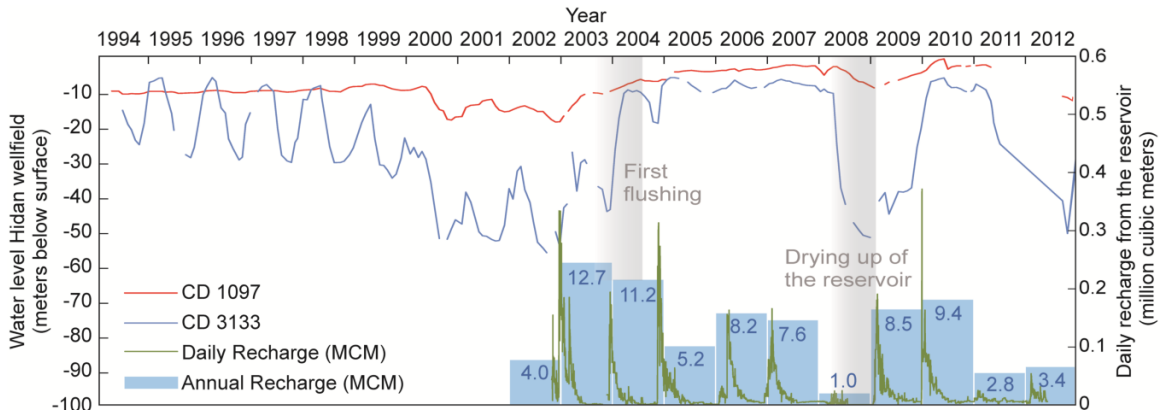

Fig. 2.4 Infiltration from the aquifer and water level fluctuations in observation wells CD 1097 and CD 3133 of Hidan wellfield (Fig. 2.1c)

2.4.2 General hydrogeochemistry

Table 1 presents a summary and statistical analysis of the available data from 2001 to 2011. The mean pH of the reservoir is 7.9, and for the groundwater samples is between 6.9 and 7.7. Temperature data are rarely documented and range between 23.5 and 30.5 °C in the groundwater and 23.0 °C in the reservoir. Water temperature in the reservoir is taken from the surface and does not represent the entire lake. Electrical conductivity (EC) data show higher values in Wala wells than in Hidan wells and indicate a better connection of Hidan wells to the conduit and fracture network, where flow velocities are generally higher and rock–water interaction is less. The significant differences in the average ion concentration concern mainly sulfate, chloride and bicarbonate. However, differences occur also among Hidan wells. Here, the impact of less-mineralized surface water from wadi infiltration at the outcrops of A7 aquifer (Fig. 2.1d) might be marginal. EC values of reservoir water are generally lower and vary due to occasional filling with low-mineralized floodwater or evaporation processes during summer. The average EC of around 470 µS/cm reveals that surface water has already dissolved rock during its flow through the soil and epikarst of the catchment..

The Piper diagram (Fig. 2.5) reveals a dominance of calcium and bicarbonate in groundwater and surface water, as is expected from limestone and dolomite. The anion triangle shows that the percentage of bicarbonate in surface water is much higher than in groundwater, whereas cations are much more clustered. The order of the abundance of the ions in both waters is $Ca^{2+} > Na^{+} > Mg^{2+} > K^{+}$ and $HCO_3^{-} > Cl^{-} > SO_4^{2-}$.

Mean nitrate values of 4.2 mg/L for the reservoir are lower than expected from the influence of agricultural and farming activities in the catchment as well as the sewage from nearby communities. The low values can be explained by nitrate consumption by cyanobacteria and algae at the water surface. Mean concentrations in Wala and Hidan wells range from 11.2 to 27.5 mg/L and indicate return flow from irrigation areas around the wells carrying ammonia (NH3), which is turned into nitrate by nitrification (Schmoll 2006). Potassium in reservoir water samples ranges between 7 and 15.6 mg/L, whereas groundwater values range from around 3 to 12 mg/L. Here, the influence of fertilizers is likely.

The excess of Cl^{-} over Na^{+} (Fig. 2.6b) in the groundwater points to additional sources of chloride, e.g. $CaCl_2$, $MgCl_2$ or KCl, which explains the slight excess of Ca^{2+} and Mg^{2+} over SO_4^{2+} and HCO_3^{-} in some groundwater samples. Higher Na^{+} values in the reservoir water might come from cation exchange, where Ca^{2+} is replacing the Na^{+} on clay minerals. However, Na^{+} and K^{+} are also the result of silicate dissolution (Bakalowicz 1994), whereas high Cl^{-} and SO_4^{2-} content is often associated with wastewater.

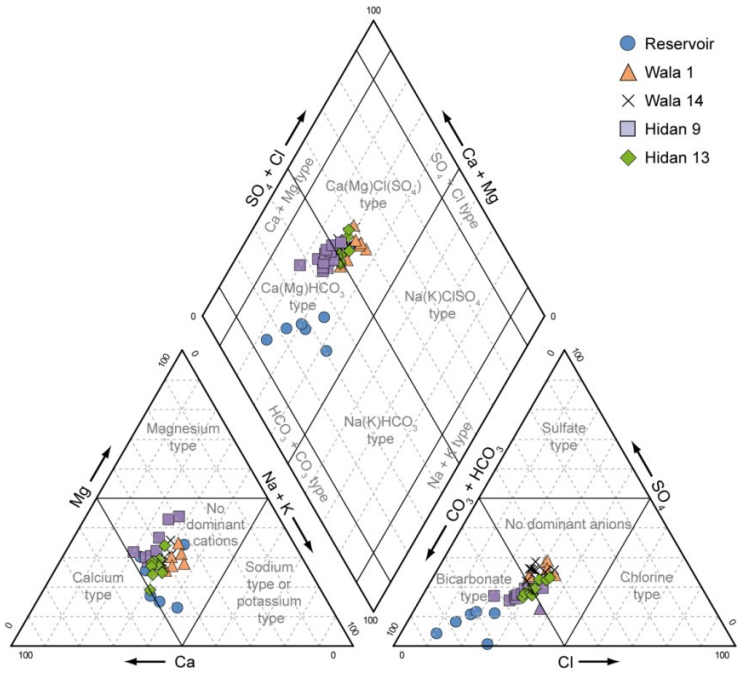

Fig. 2.5 Piper diagram displaying water samples from Wala reservoir, Wala wells 1 and 14, and Hidan wells 9 and 13. All samples are slightly dominated by calcium and bicarbonate; higher proportions of bicarbonate are present in the reservoir

Furthermore, the groundwater samples reveal that Cl^- is contributing more to the salinity than SO_4^{2-} (Fig. 2.6c). The same applies for Ca^{2+} over Mg^{2+}, which is explained by the presence of Ca^{2+} in more minerals than Mg^{2+}. Only a few samples contain the same amount of Mg^{2+} and Ca^{2+} (Fig. 2.6d).

Almost all water samples show slight supersaturation with respect to calcite, dolomite and aragonite. The fact that $SI_{Calcite}$ values over 0.5 are always associated with a CO_2 partial pressure of less than 1 % of the atmospheric pressure indicates degassing of CO_2 from almost half of the water samples. Consequently, SI values are computed to be too high and only a slight supersaturation can be assumed. Only one sample reveals a CO_2 partial pressure above 10 %. Such high values are typical for active tectonic areas (Bakalowicz 1994) and point to CO_2 originating from a deeper aquifer. Saturation of gypsum, anhydrite and sodium chloride is not reached due to their high solubility.

The difference of the average ion concentration in the surface (reservoir) and groundwater (Hidan well 9 + 13) and the total amount of infiltrated water from 2002 to 2012 (74 MCM) is taken for a rough calculation of the total volume of dissolved rock (only calcite, gypsum and halite are considered), which resulted in a value of around 6,500 m^3. Around 1,550 m^3 of it is attributed to calcite, 2,400 m^3 to halite and 2,550 m^3 to gypsum. The total volume of dissolved rock is less than 0.004 % of the volume of the productive aquifer section along the wadi corridor (≈1 km). However, the hydraulic impact of this dissolution cannot be evaluated by simple means, as it strongly depends on the spatial distribution pattern of the dissolution phenomena.

Table 2.1 Physico–chemical parameters of 51 Wala reservoir and groundwater samples from 2001 to 2011

SampleID	Statistic	pH	Temp (°C)	EC (μS/cm)	TDS (mg/L)	Na (mg/L)	K (mg/L)	Mg (mg/L)	Ca (mg/L)	Cl (mg/L)	SO_4 (mg/L)	HCO_3 (mg/L)	NO_3 (mg/L)	SI Calcite	SI Aragonite	SI Dolomite	SI Gypsum	SI Anhydrite	pCO2 in vol % of [atm]
Reservoir	Min	7.5	23.3	231	192	18.2	5.9	4.1	23.7	16.0	13.0	99.4	0.8	0.1	−0.1	−0.3	−2.7	−2.9	0.1
(No. =7)	Max	8.3	23.3	633	876	95.2	15.6	53.4	84.0	147.7	146.9	372.1	9.5	1.2	1.1	2.5	−1.3	−1.5	1.1
	Ave	8.0	23.3	462	438	37.2	9.6	19.8	51.1	47.3	39.0	230.1	4.2	0.6	0.4	0.9	−2.2	−2.4	0.3
	SD	0.2	0.0	151	218	24.7	3.1	15.8	19.9	42.7	48.5	96.7	2.6	0.4	0.4	0.9	0.4	0.4	0.3
Wala 1	Min	7.2	27.5	1092	710	75.7	3.1	34.1	95.2	104.0	74.9	309.3	13.9	0.2	0.1	0.4	−1.5	−1.7	1.1
(No. = 8)	Max	7.5	27.5	1501	1046	123.9	12.1	61.4	109.8	182.8	186.2	410.5	42.2	0.6	0.5	1.3	−1.1	−1.3	2.5
	Ave	7.3	27.5	1341	916	98.0	8.7	46.9	104.5	154.7	153.8	357.4	27.5	0.4	0.3	0.8	−1.2	−1.4	1.8
	SD	0.1	0.0	139	121	13.7	2.9	8.4	4.4	22.8	35.7	29.6	9.1	0.1	0.1	0.3	0.1	0.1	0.4
Wala 14	Min	6.6	30.2	1278	831	84.0	3.9	45.5	100.2	131.0	138.7	343.4	6.8	−0.2	−0.3	−0.3	−1.2	−1.4	0.6
(No. = 10)	Max	7.9	32.2	1430	1024	97.8	7.0	63.4	123.9	170.4	191.5	425.2	15.6	1.1	1.0	2.4	−1.0	−1.2	12.3
	Ave	7.4	31.0	1327	942	88.9	5.4	50.1	110.5	143.8	169.5	386.9	11.2	0.6	0.4	1.2	−1.1	−1.3	2.6
	SD	0.3	0.9	45	63	4.1	1.0	4.9	8.1	11.2	15.3	22.2	2.8	0.3	0.3	0.7	0.0	0.0	3.3
Hidan 9	Min	7.1	23.5	767	546	36.8	3.1	27.2	78.8	59.3	65.3	265.4	17.8	0.1	−0.1	0.1	−1.6	−1.8	0.2
(No. = 13)	Max	8.2	28.2	1240	772	70.4	5.9	47.1	91.8	127.8	101.7	323.9	33.7	1.1	1.0	2.1	−1.4	−1.6	2.9
	Ave	7.8	26.2	931	641	56.2	4.4	35.0	85.4	93.7	79.1	300.1	23.3	0.7	0.6	1.4	−1.5	−1.7	0.7
	SD	0.3	2.0	105	68	7.5	1.0	5.9	3.8	15.0	9.5	18.6	3.8	0.3	0.3	0.5	0.0	0.0	0.7
Hidan 13	Min	7.0	25.5	928	603	62.8	3.1	32.7	88.0	106.5	80.2	305.0	17.3	0.1	0.0	0.2	−1.5	−1.7	0.3
(No. = 13)	Max	8.1	29.3	1271	830	80.5	6.7	48.0	110.0	147.3	135.4	361.7	28.3	1.1	0.9	2.1	−1.2	−1.5	3.5
	Ave	7.6	27.2	1090	758	73.1	5.2	38.0	98.3	123.0	102.5	337.4	21.9	0.6	0.5	1.2	−1.4	−1.6	1.1
	SD	0.3	1.6	86	70	5.9	0.9	4.0	5.5	9.2	13.5	15.8	3.2	0.3	0.3	0.6	0.1	0.1	0.8

Min minimum, Max maximum, Ave average, SDstandard deviation, Nnumber of samples. Temperature data are rarely measured and are completed by adding the average value of the sampling point

Investigations of Goode et al. (2013) on salinity trends in Jordan ascribe its increase mainly to the lower parts of basins and areas of discharge and withdrawals, influenced by the natural recharge and the geological setting. However, water-table declines do not necessarily correlate to salinity increases. The EC values of 342 samples, taken from 18 Hidan and 12 Wala wells, indicate a significant increase of the salinity from 1980 to 2011 (Mann Kendall trend test, p-value for Hidan wells 3.3E-3; for Wala wells <1E-4), visualized in Fig. 2.7a with average values of all wells and samples from the 1980s, 1990s and 2000s. Similar observations for salinity increase were done by Schmidt et al. (2013) in a comparable aquifer system at the western margin of the Lower Jordan Valley and attributed to progressive impact of wastewater. A final conclusion about the reason for long-term salinity increase in the study area is not possible due to missing a detailed survey of groundwater chemistry and water level. Otherwise, changes could be attributed to a specific water constituent, or temporal EC variations could be identified and correlated with groundwater levels and abstraction rates. Therefore, the impact of wastewater, along with declining water tables in the entire catchment, is probable. Substantial amounts of additional rock dissolution can be excluded.

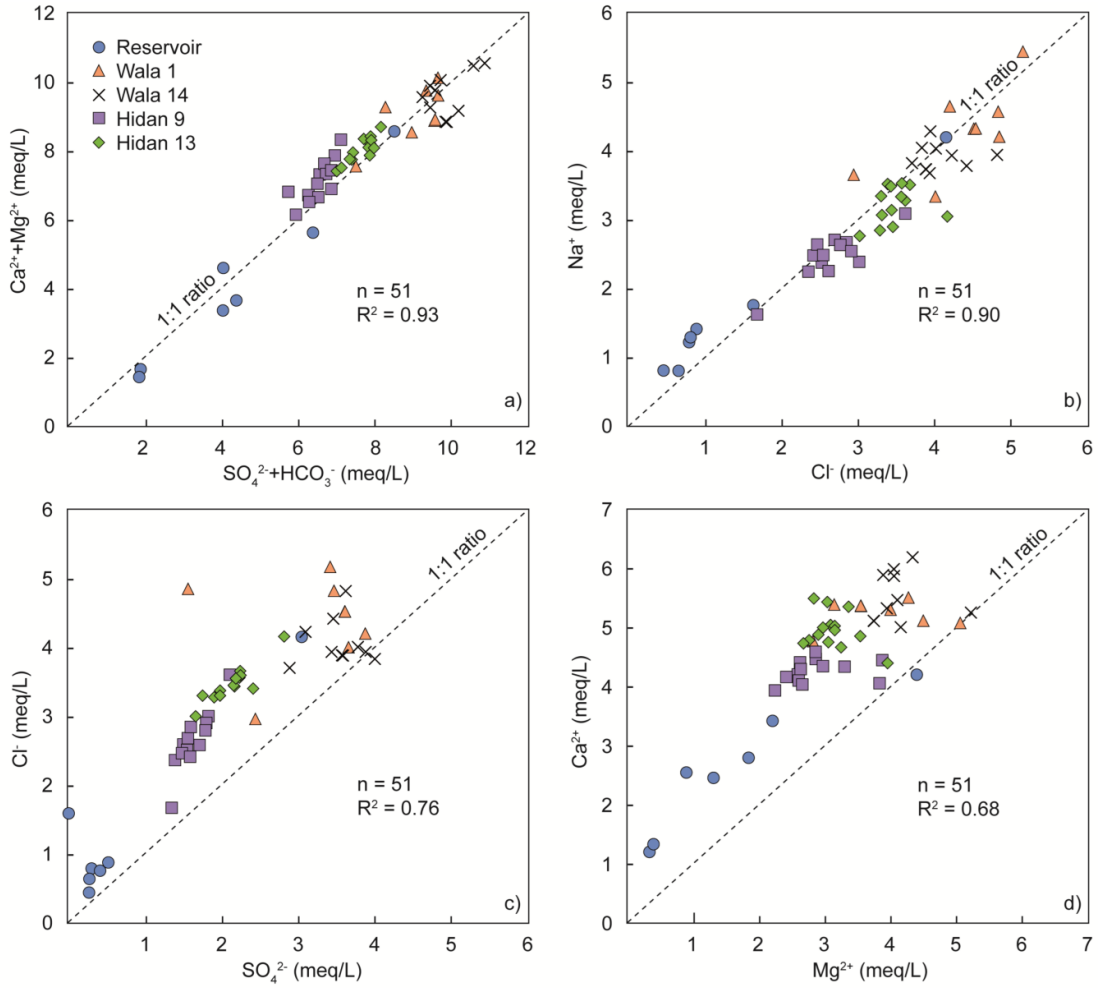

Fig. 2.6 Binary diagrams from waters of Wala reservoir, Wala wells and Hidan wells a) Ca^{2+}+Mg^{2+} vs. SO_4^{2-}+HCO_3^-, b) Na^+ vs. Cl^-, c) Cl^- vs. SO_4^{2-} and d) Ca^{2+} vs. Mg^{2+}

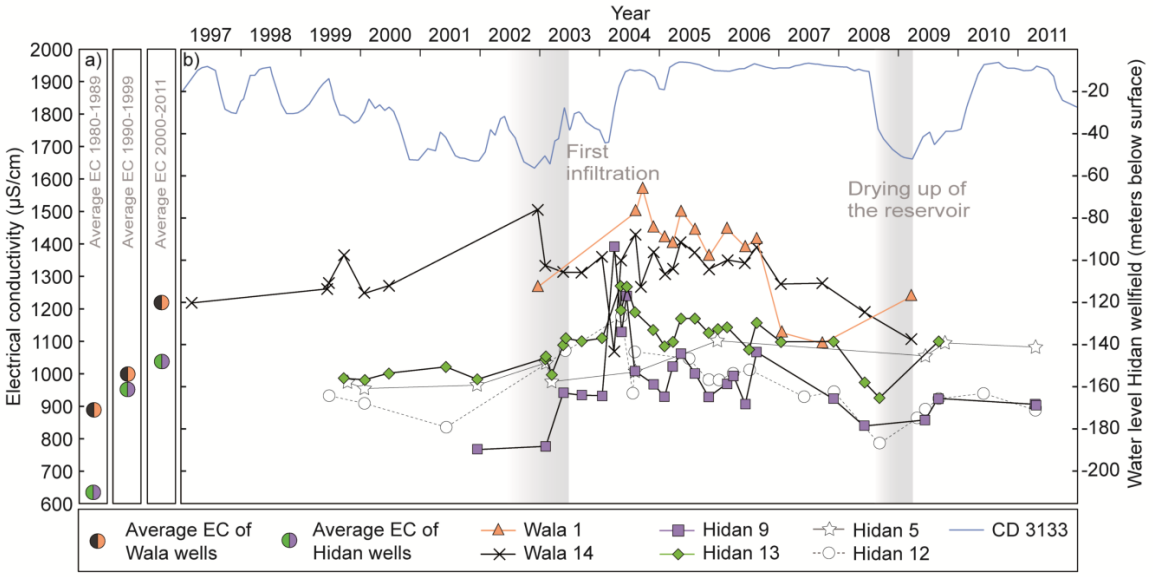

Fig. 2.7 a) Electrical conductivity changes at Hidan and Wala wells, and b) water levels in individual wells. During the first flushing of the aquifer the salinity increased in all wells (between 2003 and 2005). The infiltration from the Wala reservoir water decreased from 2007 and the reservoir dried up in 2008, which caused a decrease in the EC of water in the Hidan wells. Long-term increase of average EC is observed from 1980 to 2011

EC data for four Hidan wells are taken as an example for the wellfield from 1999 to 2011 and compared to water level records of well CD 3133 (Fig. 2.7b). Water level correlations with the two Wala wells are not possible. Hidan wells show almost constant EC values from 1999 to 2002, but temporal fluctuations cannot be excluded, partly because only one annual record exists. The EC peak in 2003/2004 is interpreted as a reaction to the hydraulic impulses from reservoir infiltration. It is assumed that (1) higher-mineralized groundwater from the rock matrix is pushed into the fracture and conduit network, (2) there is mobilization of fine material, e.g. the leaching of precipitated salt from irrigation return flow in the unsaturated zone, (3) the impact of wastewater from the adjacent area is too minor to raise salinity constantly, and (4) rock dissolution is excluded because this process would not cause a single peak but a general long-term increase of salinity. EC increase in Hidan wells can be attributed mainly to chloride and sulfate, which supports the assumption of mixing with water from areas of higher salinity (Wala wells). It is doubtful, however, whether the amount of salt from irrigation return flow is sufficient to constantly increase the salinity, but it is plausible that it could cause a temporal effect. Salt residues associated with the approximately 1–2 MCM of annual irrigation applied to the unsaturated zone are certainly some tens of tons. The sharp decrease of the EC in Hidan wells in 2007 and 2008 can be related to the drying up of the reservoir in 2008, when infiltration had almost stopped and the groundwater level dropped. At the same time, EC values decreased almost to corresponding values before 2001, and natural hydraulic conditions appeared again. The results show that the system strongly reacts to combined changes of groundwater level, abstraction rates and infiltration.

2.4.3 Isotopes

2.4.3.1 Deuterium and Oxygen-18

The $\delta^{18}O$ values of rainfall range from −8.33 to −0.05 ‰ with corresponding $\delta^{2}H$ values of −42.5 to −0.9 ‰. These are mainly scattered along the MMWL, meaning Mediterranean origin, and a few samples are close to the GMWL (Fig. 2.8). The wide range of values for reservoir water can be attributed to the large catchment area, where precipitation with different isotopic signatures occurs and is influenced by the condensation process. Additionally, evaporation processes in the open reservoir lead to a high variation. The input signals of reservoir water are scattered along the MMWL and the GMWL and show $\delta^{18}O$ values ranging from −8.46 to −0.4 ‰ and $\delta^{2}H$ values from −40.7 to −21.6 ‰.

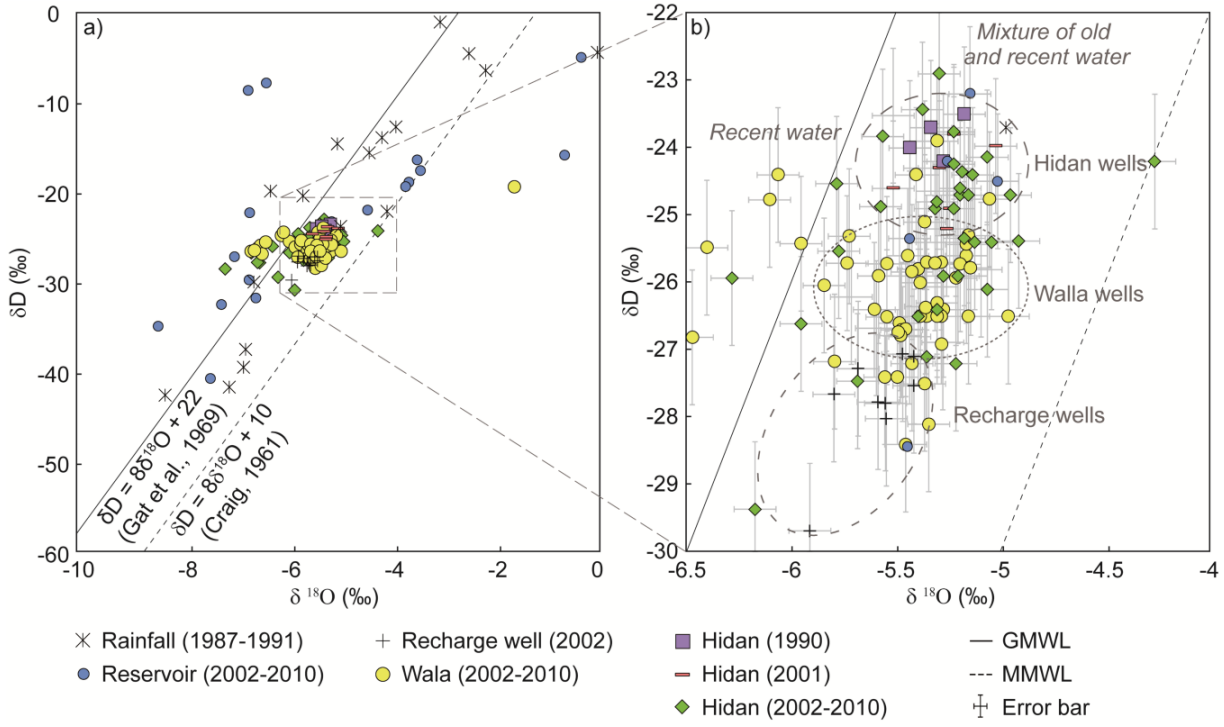

Fig. 2.8 Distribution of the $\delta^{2}H$ (δ D) and $\delta^{18}O$ for samples of a) rainfall, the reservoir, the recharge well and Wala groundwater, and b) Hidan groundwater. Samples of Wala, recharge and Hidan wells are clustered along the MMWL and the GMWL, whereas data from precipitation and the reservoir are more scattered

Samples of Wala, recharge and Hidan wells are more clustered and reveal values in the range of −7.2 to −1.6 ‰ for $\delta^{18}O$ and from −30.8 to −19.3 ‰ for $\delta^{2}H$. Most of the samples are located between the MMWL and the GMWL. Samples above the MMWL were collected after 2002. Missing annual time series of single wells does not allow the detection of seasonal cycles or variations attributed to, for example, the impact of the reservoir.

Water samples from Wala wells and recharge wells are generally more depleted in $\delta^{2}H$ as compared to Hidan wells (Fig. 2.8), but have only a slight difference in $\delta^{18}O$. This also applies to the time before the

first infiltration, because some samples were collected before November 2002. Given the fact that evaporation creates a flatter line, it is obvious that water with a different isotopic signature rises towards Hidan wellfield, pointing to the mixing of water of different ages.

2.4.3.2 Tritium

The tritium values of rainfall, reservoir and groundwater samples are displayed in Fig. 2.9. Values for the rainfall samples in the Wala catchment confirm the decrease through natural radioactive decay from 1987 to 2000. Initial values range between around 11–30 TU and drop down to less than 10 TU.

Tritium values of reservoir water are similar to those of local rainfall and range between 3.1 and 8.7 TU with an average of 5.2 TU. It is obvious that ^{3}H values from rainfall and, hence, from the reservoir water vary strongly due to evaporation and condensation in the atmosphere. Initial values at Hidan and Wala wells in 2001–2002 of around 0.8 TU rise to a mean value of 2.3 TU in the years 2008–2010. This confirms the increasing contribution of reservoir water to the abstraction at Hidan wellfield. The ^{3}H values before 2002, of less than 1 TU in Hidan and Wala wells, indicate that the groundwater originates from a mixture of submodern (recharge before 1952) and recent water and it is evident that natural groundwater has a mean residence time of more than 60 years.

Mixing calculations of the median concentrations of ^{3}H in the reservoir and groundwater, recently and before the construction of the dam, show the proportion of the reservoir water in the groundwater is approximately 66% (until 2007). This almost corresponds to the calculated 71 % (2002–2007) and 57 % (2002–2012) from the water balance.

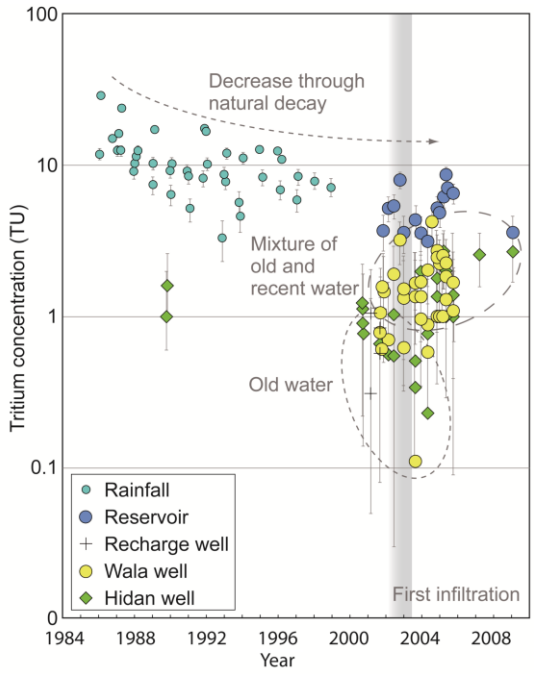

Fig. 2.9 Tritium (^{3}H) content of precipitation and Wala reservoir shows the decrease over time as a consequence of natural decay. The concentration in groundwater increases after 2002, caused by the mixing with recent water from Wala reservoir infiltration

2.4.3.3 Carbon-13 and carbon-14

The mean value of $\delta^{14}C$ activity of all wells is 13 ± 1.09 pmc with a maximum of 29.11 ± 1.44 pmc and a minimum of 4.97 ± 0.60 pmc. Corresponding $\delta^{13}C$ values range from −10.60 to −13.41 ‰ with an average of −12.32 ‰. Table 2.2 shows the results of the calculated mean residence times of the groundwater for Fontes and Garnier (1979), the IAEA model (Plummer and Glynn 2013) and Evans model (1979).

Values of Wala well 13 and 14 range between 9,700 and 24,900 years and of the Hidan well 9 between 4,000 and 13,000 years. It is expected that there will be similar values along the flow path or at least a slight increase. The fact that water becomes younger along the flow path points either to mixing with surface water, which is excluded by the tritium results, or mixing with groundwater of different ages, which agrees with the $\delta^{2}H$ and $\delta^{18}O$ results. The decrease of mean groundwater residence time between 2002 and 2006 is related to the increasing proportion of reservoir water infiltration. It can be derived from the calculated ages that water samples from 2002 originate from the late Pleistocene (older than 11,700 years) and some originate from the early to middle Holocene (11,700 to recent).

Table 2.2 Calculated mean residence times of groundwater after Fontes and Garnier (1979); Plummer and Glynn (2013) and Evans (1979).

Sampling point	Date	14C (pmc)	d13C (‰)	F and G (years)	IAEA (years)	Evans (years)
Wala 14[a]	14.10.2002	8.60±1.11	-11.76	24,741	19,174	19,174
Wala 14	17.03.2003	11.63±0.70	-13.39	19,344	17,643	17,643
Wala 14	09.07.2003	7.14±1.27	-12.6	26,835	21,227	21,227
Wala 14	05.04.2006	18.56±1.44	-13.1	14,781	13,628	13,628
Wala 13[a]	14.10.2002	5.50±0.76	-13.1	28,517	23,695	23,695
Wala 13	17.03.2003	4.97±0.60	-13.41	27,654	24,880	24,880
Wala 13	09.07.2003	13.62±0.90	-12.99	21,872	16,235	16,235
Hidan 9	02.12.2002	19.44±1.13	-11.24	17,136	12,090	12,090
Hidan 9	10.07.2003	17.13±1.55	-11.02	16,250	13,091	13,091
Hidan 9	05.04.2006	29.11±1.44	-10.6	8,711	8,306	8,306

[a] Before first reservoir infiltration (31.10.2002)

2.4.4 Conceptual groundwater flow model

The Hidan and Wala wells are fed by natural groundwater with mean residence times of several thousand years, originating from local precipitation. Generally, a higher productivity is attributed to the middle part of the Wadi As Sir aquifer between the Wala reservoir and Hidan wellfield. Likewise, an enhanced groundwater flow takes place along the wadi corridor, approved by the high recovery of infiltrated water at Hidan wellfield and the significant water-level increase after the first infiltration. This confirms the assumption made by Green et al. (2014) about increased karstification along wadis in

karst terraines of semi-arid areas. Karst-specific flow patterns through fine matrix pores, fractures and conduits are confirmed by the occurrence of different EC values in the wells. Furthermore, isotope data indicate mixing of water from zones with different degrees of karstification and fracturing at the Wala and Hidan wells caused by the different drawdowns from pumping activities and the associated vertical flow components (Fig. 2.10). Such differences in mean groundwater residence times in production wells are often associated with the interaction of the aquifer and the well (Jurgens et al. 2014; Eberts et al. 2012; Zinn and Konikow 2007; Małoszewski and Zuber 1982). Upwelling of substantial amounts of water from a deeper aquifer can be neglected because of the underlying B5/6 aquitard. Also, lateral groundwater flow to the Hidan and Wala wells from the north and south, which could provide younger water, is unlikely because of the <8 km aquifer extension in these directions and the >300 m thickness of the unsaturated zone that receives only little rainfall.

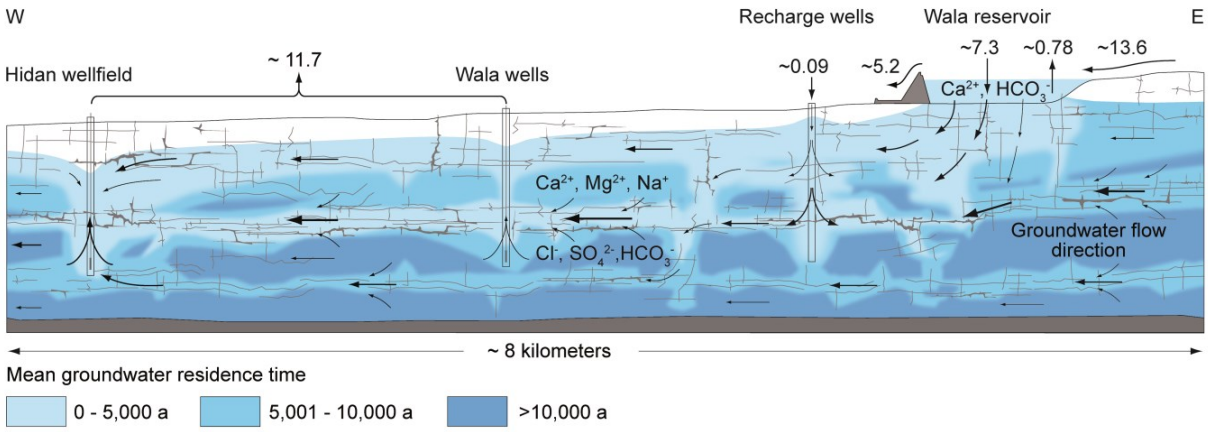

Fig. 2.10 Schematic profile along the wadi, showing mixture of young and old groundwater as a consequence of different flow regimes in the fracture and conduit network of the karst aquifer. Drawdown cones are seen at Wala and Hidan wells and infiltration mounds at the recharge well. Water balance values are displayed in million cubic meters as annual average (2002–2012)

2.5 Conclusion

The Wala reservoir is an example of a successfully managed aquifer recharge into a karst aquifer in a semi-arid region and demonstrates the promising potential that comes along with this technique regarding water management in Jordan.

Dry soil cover in the catchment leads to high sedimentation in the reservoir, which continuously decreases the infiltration rate and, thus, the proportion of artificially recharged water in the abstracted groundwater. The result will be a progressively dropping water level in the aquifer, when abstraction rates remain constant. Dry years will magnify this effect. Natural groundwater flow to Hidan wellfield is strongly dependent on the abstraction taking place in Wala catchment, upstream of the reservoir. Additional abstraction wells along Wadi Wala will directly affect Hidan wellfield as the water levels

drop. Furthermore, lower abstraction yields are expected due to smaller degrees in fracturation and karstification compared to Hidan wellfield. Salinity fluctuations in the wellfield are expected to be on the same order of magnitude as from 2002 to 2012 of around 200 μS/cm.

Acknowledgement

The authors thank the Ministry of Water (MWI), the Jordan Valley Authority (JVA) and the Water Authority of Jordan (WAJ) for their support and provision of the data. Furthermore, the German Federal Ministry of Education and Research (BMBF) are acknowledged for funding the SMART Project (Sustainable Management of Available Water Resources with Innovative Technologies) (FKZ 02WM1079-1086 and FKZ02WM1211-1212). Special thanks go out to Prof. Michel Bakalowicz for fruitful discussion, Marian Bechtel for language editing of the manuscript, and the editor Dr. Vincent Post and an anonymous reviewer for their helpful suggestions

.

Chapter 3

Numerical long-term assessment of managed aquifer recharge from a reservoir into a karst aquifer in Jordan

Reproduced from: Xanke J, Jourde H, Liesch T, Goldscheider N (2016) Numerical long-term assessment of managed aquifer recharge from a reservoir into a karst aquifer in Jordan. Journal of Hydrology, 540, 603-614 .http://dx.doi.org/10.1016/j.jhydrol.2016.06.058

Abstract

In semi-arid regions with high seasonal variability of water availability, adaptive management strategies and technical measures are required to ensure the sustainable use of water resources. In this study, managed recharge of storm water into a karst aquifer and the water level fluctuations related to pumping in a nearby wellfield were simulated at Wadi Wala, Jordan. We used a numerical equivalent porous medium (EPM) approach with specific adaptations to account for the heterogeneity and anisotropy of the karst aquifer. The model domain was vertically projected along the wadi course, resulting in a 2-dimensional model, and subdivided into hydraulic zones representing the karst-specific flow pattern of fast flow and slow depletion. Results show satisfying agreement of measured and simulated groundwater tables from 2002 to 2012 and predict a lowering of the average groundwater table until 2022 of around 2.7 m in the immediate surroundings of the reservoir and an increased depletion towards the wellfield, mainly caused by sedimentation in the reservoir and an associated decrease in infiltration. Abstraction at the wellfield changed considerably over the regarded time period and strongly influences the groundwater fluctuations, which shows the need of improved pumping management and monitoring. The results can serve as a basis for decision makers regarding an optimization of water management at the reservoir and wellfield. Furthermore, the presented numerical approach can be transferred to karst regions with similar physio-geographical conditions to assess managed aquifer recharge.

3.1 Introduction

The growth of the global population and economy along with the increasing demand of freshwater has led to a pressure on most of the natural freshwater reserves, exacerbated by their natural unequal distribution and climate change (UNEP 2012; WWAP 2015). Especially in arid and semi-arid regions, natural water scarcity and its variable availability challenge its sustainable use (Schwabe et al. 2013; Issar 2010) and therefore requires improved management strategies (Llamas and Custodio 2002). In many countries, the integrated water resources management (IWRM) approach has become an integral part of regional water strategies (Jønch-Clausen 2004; UNEP 2012), also in Jordan (MWI 2004; Wolf and Hötzl 2011). This approach comprises a variety of measures and regulations that encompasses governmental, educational, scientific and technical issues (Carr et al. 2012; Cosgrove and Loucks 2015) concerning regional surface and groundwater resources. Here, karst aquifer management poses a particular challenge, which generally requires a "case to case" adapted plan (Bakalowicz 2011) including monitoring of input and output of the system, evaluation of the resources and reserves, modeling approaches and technical interventions such as groundwater capturing, underground dams and managed aquifer recharge (MAR) (Ford and Williams 2007; Bakalowicz 2011; van Beynen 2011). The latter has become increasingly important within the framework of IWRM implementation, also in Jordan (Wolf et al. 2007; Daher et al. 2011).

The various fields of applications and techniques of MAR for underground storage of surface water are described by Dillon et al. (2009), with the main intention of a later recovery of the stored water, but also to counteract falling water levels. Hereby, the improvement of groundwater availability and its quality for drinking is of main interest (Bouwer 2002). Both aspects are also major challenges in the semi-arid Jordan region aggravated by the variability in availability and demand of water, which mostly behave reverse to each other, since water demand is higher in dry than in wet seasons (Jaber and Mohsen 2001). Here, MAR not only helps bridging the water supply gap during dry seasons by underground storage but also counteracts the long-term overexploitation of aquifers.

However, the characteristic duality of discharge pattern of karst aquifers aggravates the knowledge of temporal and spatial water availability, because the rock solubility in combination with well-developed fractures generates a wide range of variation in flow velocity and rock porosity. Intergranular porosity and fissure and fracture porosity, which are often seen together as matrix porosity, may differ strongly from conduits and caves porosity and therefore generate flow velocity variations from several centimetres per day (matrix porosity) to tens or hundreds of meters per hour (conduits and caves porosity) (Teutsch and Sauter 1991; Kresic et al. 1992; Ford and Williams 2007; Goldscheider and Drew 2007). This is reflected in strong groundwater level fluctuations or large variations in spring

discharge within short time as a consequence of a hydraulic impact. Furthermore, the anisotropic development of the karst and fracture network often produces directions of preferential flow.

Numerical models are essential tools to investigate and understand flow behavior (Wang and Anderson 1995) but their application in karst aquifers is challenging. Different approaches are discussed in detail by Scanlon et al. (2003), Sauter et al. (2006), Hinkelmann (2006) and Hartmann et al. (2014) and can be grouped into lumped parameter and distributed models. The choice of a model mainly depends on the research question, but also on data availability, system comprehension and investigation effort (Sauter et al. 2006). Lumped parameter models assess the aquifer as a unit and transform input signals into output signals where spatial information is not always considered. In contrast, the distributed modeling approach requires a spatial discretization of the model domain (Sauter et al. 2006; Birk et al. 2008; Ghasemizadeh et al. 2012; Hartmann et al. 2014) and is generally subdivided into equivalent porous medium models (EPM), double continuum models (DC), combined discrete-continuum approaches (CDC), discrete fracture network approach (DFN) and discrete conduit network approach (DCN). EPM models are usually applied for porous media (Birk et al. 2008) but appear also appropriate for aquifers with moderate heterogeneity such as poorly karstified carbonate aquifers (Scanlon et al. 2003). When applied to karst aquifers, suitable results for water level simulations at regional scale are possible (Abusaada and Sauter 2013), while flow directions, aquifer dynamics and contamination are often not adequately predicted (Scanlon et al. 2003; Worthington 2009). Since the model domain can be described by the representative elementary volume (REV) (Diersch 2014), EPM models often require a lower investigation and simulation effort than other modeling approaches (Birk et al. 2008), such as DC, CDC, DFN or DCN models. These approaches are better suited in simulating fracture and karst aquifers but require sufficient knowledge of hydraulic properties and therefore a higher number of calibration parameters (Barrett and Charbeneau 1997; Hartmann et al. 2014). However, numerous software tools are available for the different modeling approaches that allow an efficient and easy use.

In this study, groundwater level fluctuations in a moderately karstified aquifer as a result of freshwater infiltration from Wala reservoir and abstraction at a 7 km downstream wellfield were simulated. Since the construction, calibration and validation of three-dimensional (3D) models are often laborious, especially when applied to karst aquifers, Anderson et al. (2015) recommend an “appropriate simplification” of natural processes. Therefore, the complex 3D aquifer geometry is not addressed as the main flow components can be captured in a two-dimensional (2D) vertical cross-section of the aquifer along the winding course of the dry riverbed (wadi). This is shown by Xanke et al. (2015), which promote enhanced groundwater flow along the wadi course. The aquifer thickness and relevant variations of hydraulic properties with depth are incorporated in the 2D profile approach. To address a

volumetric equivalent simulation of reservoir infiltration and aquifer abstraction the 2D profile model can be extended to a 3D model in a follow-up study. The EPM approach was chosen, but with special adaptations to account for the heterogeneity and anisotropy of karst aquifers. The modeling approach was implemented with FEFLOW software (DHI®). The objectives of the groundwater model are (i) to characterize the hydraulic properties of the underground (ii) to correctly reproduce water level fluctuations in the aquifer depending on reservoir infiltration and groundwater withdrawal, (iii) to quantify the impact of predicted infiltration decrease caused by reservoir sedimentation, (iv) to identify the driving factors of the observed water level fluctuations at the wellfield and (v) to provide a defensible quantitative basis for optimized water resources management under conditions of climate change and increasing freshwater demand.

3.2 Site characterisation

3.2.1 Geographical setting

The Wadi Wala is located on the eastern mountain range of the Dead Sea (Fig. 3.1a). Its tributaries originate from elevations of more than 1000 m above sea level (m asl) in the north and south of the catchment and run together at an elevation of around 485 m asl at Wala reservoir. From there, the wadi runs down to Wadi Hidan (470 m asl), which finally passes into the Dead Sea (−420 m asl) (Fig. 3.1b and e). The Wala reservoir surface catchment extends to the east and covers an area of around 1770 km2. It belongs to the Mujib drainage basin and covers partly the Dead Sea groundwater drainage basin (Fig. 3.1b) (Al-Assa'd and Abdulla 2010; Xanke et al. 2015).

Rainfall mainly occurs only a few days a year during winter with high intensity, whereby mean values of the cumulative annual precipitation (Fig. 3.1c) decreases from north (500 mm) to south (100 mm) suggesting a higher surface runoff in the northern part of the catchment, ranging from 0.5% to 10% of total precipitation (Xanke et al. 2015). Due to the semi-arid climate, high evapotranspiration rates are prevailing, which cause a loss of 85–93% of the precipitation. Thus, only between 3% and 11% of the precipitation contributes to groundwater recharge (El-Naqa 1993). A falling trend of around 2.5 m per year (2001–2012) in groundwater levels is observed in the Wala catchment (Fig. 3.1d), which may affect also Hidan wellfield.

The Wala dam was constructed from 1999 to 2002 to serve as a water barrier to Wadi Wala (Fig. 3.1e) with the main purpose of flood-water storage in winter seasons for the recharge of the underlying karstic limestone aquifer. An additional artificial recharge is possible by using eight recharge wells, located downstream of the dam along the wadi Wala (Fig. 3.1e). They are rarely used and therefore considered as observation wells in this study. With a width of around 320 m and a height of 42 m, the

dam creates a storage volume of around 9.3 million cubic meter (MCM), which decreased to 7.7 MCM in 2012 due to sedimentation (Xanke et al. 2015).

Hidan wellfield comprises 16 active pumping wells (Fig. 3.1f) with depths ranging between 100 and 200 m (Xanke et al. 2015). Most of the wells were drilled and tested between 1989 and 1992, and some wells were added between 1999 and 2005. Pumping rates vary between 80 and 325 m^3/h. Derived from the yield and the assumed depth of the pumps, it can be considered that around 50% of the pumping occurs at a depth lower than 100 m below ground level (m bgl) and 50% at a greater depth, respectively.

3.2.2 Hydrogeological setting and conceptual model

Formations from Upper Cretaceous to Eocene characterize the study area and are partly covered by Quaternary deposits, described in detail by Humphreys (1991), Margane et al. (2009) and Xanke et al. (2015). The hydraulic system below the reservoir contains the Wadi Ghudran (B1) and Wadi As Sir (A7) formations (Table 3.1 and Fig. 3.1g). The A7 formation reveals and average thickness of about 150 m at the dam site and constitutes the regional aquifer. It consists of a hard dense limestone and the porosity is mainly formed by small vertical fractures and fissures as well as by enlarged fractures, horizontal bedding planes and karst conduits. Larger geological structures that may affect the hydraulic are a flexure around 2 km east of the wellfield, and another one at the wellfield (Xanke et al. 2015). The aquifer is divided by Humphreys (1991) into three hydraulic zones, with a very productive zone of extensive karstification in the middle and two less permeable zones above and below. The B1 formation is around 70 m thick at the dam site, it starts 40 m below the dam toe and reaches up to the dam crest (425 m asl), where the limestone-chert sequences of the B2 formation start (2b). The formation can be divided into three parts, with low permeable chalk members on the top and bottom and a more permeable layer in between.

Table 3.1 Stratigraphic description of the test site (Humphreys 1991; Xanke et al. 2015).

Formation	Member	Rock type	Symbol	Inferred thickness (meter)	Aquifer type	Average hydraulic conductivity K (m/s)	Horizontal hydraulic conductivity Kh (m/s)	Vertical hydraulic conductivity Kv (m/s)
Wadi Ghudran	Dhiban	Chalk	B1c	12 - 15	Aquitard	1×10^{-5}		
	Tafila	Chert, chalk, limestone	B1b	~ 50	Poor aquifer	5×10^{-5}	5×10^{-4}	5×10^{-6}
	Mujib	Chalk	B1a	12 - 15	Aquitard	1×10^{-7}	1×10^{-6}	1×10^{-8}
Wadi As Sir		Limestone	A7c	120 - 150	Aquifer	1×10^{-6}		
			A7b		Aquifer, productive zone	1×10^{-4}		
			A7a		Aquifer			

Hydraulic conductivity values of karst aquifers vary over a wide range due to the presence of fractures, fissures and karst conduits. Therefore, horizontal *K* values cover a wide range from 1 m/s to 1×10^{-8} m/s (Heath 1983; Domenico and Schwartz 1998) and their ratio to the vertical conductivity can reach from 1:50 up to 1:1,000,000 (Ford and William 2007). Derived from a small number of pumping tests, average *K* values of the A7 aquifer range from 1×10^{-4} to 1×10^{-6} m/s and average storage coefficients from 2×10^{-2} to 3×10^{-5} (Humphreys 1991; Margane et al. 2009). In reality, these values can differ much stronger depending on the degree of fracturing and karstification of the rock. Generally, the aquifer is considered to be unconfined and covered by the low permeable Ghudran formation and infiltration from the reservoir is taking place along faults, fractures and bedding planes. The model relevant formations are the B1b and B1a member with an average K of 5×10^{-5} to 1×10^{-7} m/s. Especially B1b may contain geological layers with higher *K* values.

Xanke et al. (2015) proposed an intensified groundwater flow along Wadi Wala, similar to findings from Green et al. (2014) for karst areas in semi-arid climate, that assume intensified karstification along river beds. The spatial heterogeneity of the hydraulic parameters along with varied hydraulic gradients and pumping activities cause uneven heterogeneous distribution of groundwater ages (Fig. 3.1h) (Xanke et al. 2015). Thus, highly fractured and karstified zones are carrying water with lower mean residence times, while the rock matrix and fine fractures include older water (Fig. 3.1h). The major groundwater flow direction is from east to west along a hydraulic gradient of around 1.5% between the reservoir and the wellfield.

At the Wala reservoir around 136 million cubic meters (MCM) of surface runoff were stored from 2002 to 2012 of which 74.1 MCM were recharged to the underlying aquifer mainly by natural infiltration (Xanke et al. 2015). Artificial injection through wells is additionally conducted since 2011, but represents only a small part of the total infiltration. This recharge covered around 57% of the total abstraction from Hidan wellfield of around 129 MCM until 2012. While the abstraction rates remained largely unchanged over the past years, the infiltration rate decreased continuously due to sedimentation in the reservoir and consequently lowered the proportion among the abstracted groundwater (Xanke et al. 2015). The reservoir infiltration takes place mainly laterally along the steep flanks of the reservoir.

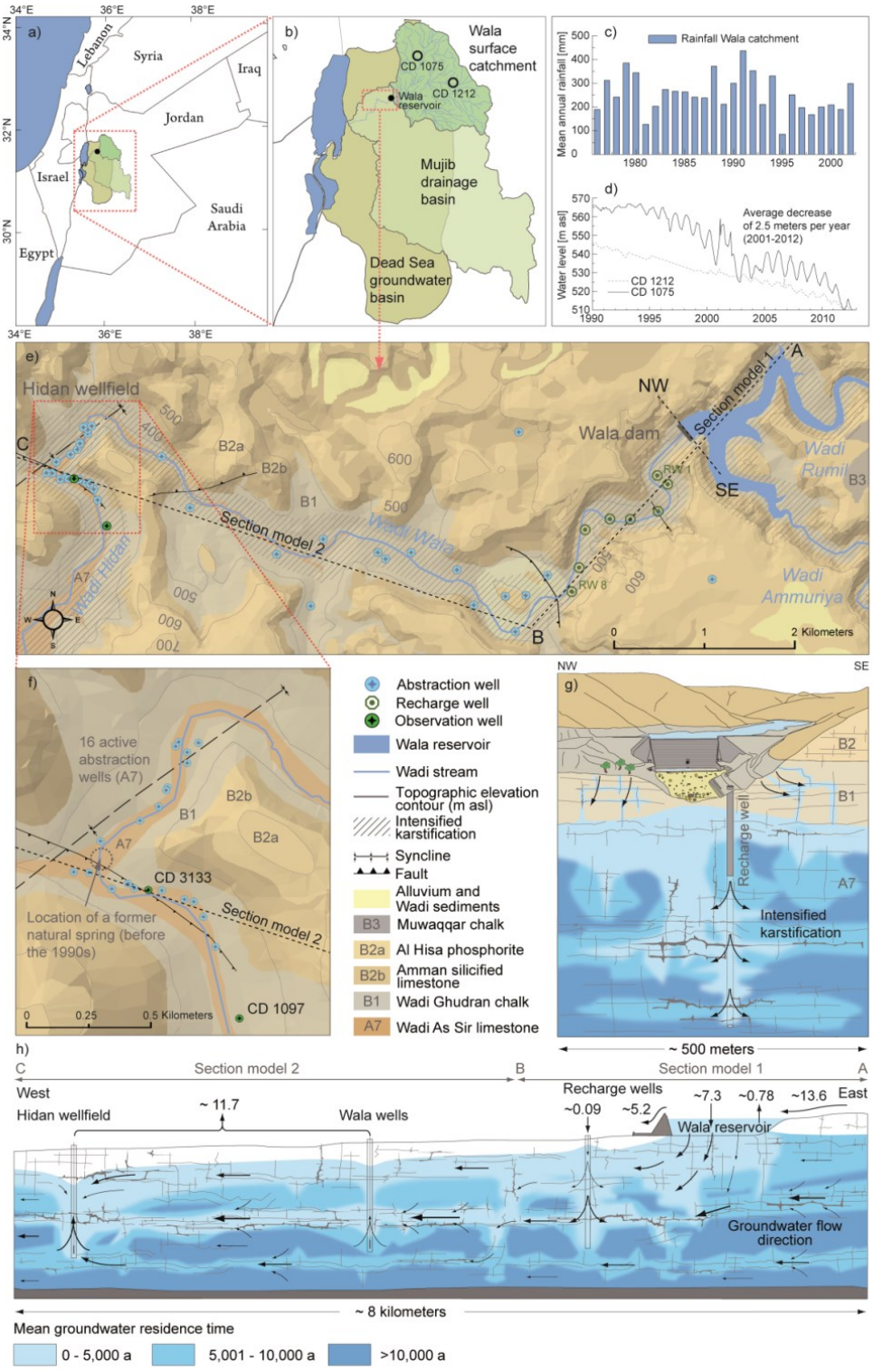

Fig. 3.1 a) Location of the study area, b) Dead Sea groundwater basin, Mujib drainage basin and Wala Surface catchment. c) Mean annual rainfall of the Wala surface catchment. d) Trend of groundwater level in observation well CD 1075 and CD 1212 in the Wala catchment. e) General location of Wadi Wala, Wala reservoir, recharge and abstraction wells and geological setup. f) Overview about Hidan wellfield and the NW-SE trending flexure and the SW-NE trending syncline axis. g) The schematic cross sections of the dam axis. (h) Schematic cross section of Wadi Wala / Wadi Hidan with the distribution of different mean groundwater ages. The values of the water balance are displayed in average annual million cubic meters (MCM) from 2002 to 2012 (modified after Xanke et al. (2015)).

3.2.3 Problem setting

A pre-sensitivity analysis allowed drawing conclusions on the hydraulic behavior of the aquifer system and a rough estimation of the magnitude of influence of the aquifer input signals on the groundwater fluctuations and can be found in the supplementary information (SI1). Thus, clear stated expectations on the model and their feasibility and potential model limitations could be defined in advance. Generally, numerical simulations of karst terrains at local scale may not be as much precise since local heterogeneity can only be averaged out over larger areas (Pankow et al. 1986; Scanlon et al. 2003; Abusaada and Sauter 2013). Therefore, the distance between the input signal and the measuring point is crucial for the implementability in the model. It is assumed that groundwater fluctuations at the recharge wells (RW 1 and RW 8) and at Hidan wellfield (CD 3133) result from the superposition of three different signals originating from (i) local, (ii) intermediate and (iii) catchment scales:

Local scale (i): The injection into the recharge wells is considered to be a local scale signal since the input signal (injection) and measuring point coincide at RW 1 and RW 8. However, the injection rates are not considered within the model because they are quantitatively unimportant.

Intermediate scale (ii): the hydraulic signal from reservoir infiltration on water level fluctuations at the wellfield is regarded as an intermediate signal due to its extensive impact and distance of around 7.000 m to the wellfield. Groundwater abstraction at the wellfield causes an immediate reaction in the observation well CD 3133 without much time delay. However, the abstraction signal seems to be dampened at CD 3133 since the large quantity of abstraction at Hidan wellfield (11.7 MCM/a), compared to the recharge from the reservoir (7.3 MCM/a), indicate an impact radius on intermediate scale. This is supported by the fact that abstraction takes place in multiple wells across a certain area and do not coincide in one point. Nevertheless, it is likely that local scale effects occur in the wellfield, which cannot be sufficiently simulated with the model. Changing abstraction rates (Fig. 2c) and the number of active wells at Hidan wellfield strongly affect the short-term increases or decreases in the water level of CD 3133 (Fig. 3.2b). However, the long-term trend is regulated by natural groundwater flow and recharge from Wala reservoir, respectively.

Catchment scale (iii): natural recharge of the entire aquifer system by rainfall infiltration takes place catchment-wide and causes a constant signal at Hidan wellfield. Derived from water-level fluctuations of observation well CD 3133 (Fig. 3.2b) it can be assumed that the water level drop from 2000 to 2003 is either caused by decreasing groundwater recharge in the catchment or a change in the abstraction depth took place.

Geological structures, such as flexures, synclines or anticlines, can have a great effect on groundwater flow as well as the presence of karst conduits. Thus, the overlapping syncline and flexure at the

wellfield (Fig. 3.1f) may cause local anisotropic hydraulic conditions that strongly effect groundwater fluctuations (Fig. 2b).

It is expected that signals on intermediate and catchment scale can be simulated at the recharge wells and Hidan wellfield. However, strong local impacts may occur, which cannot be precisely simulated. This concerns mainly strong and fast groundwater level fluctuations caused by variable abstraction at the wellfield and injection at the recharge wells.

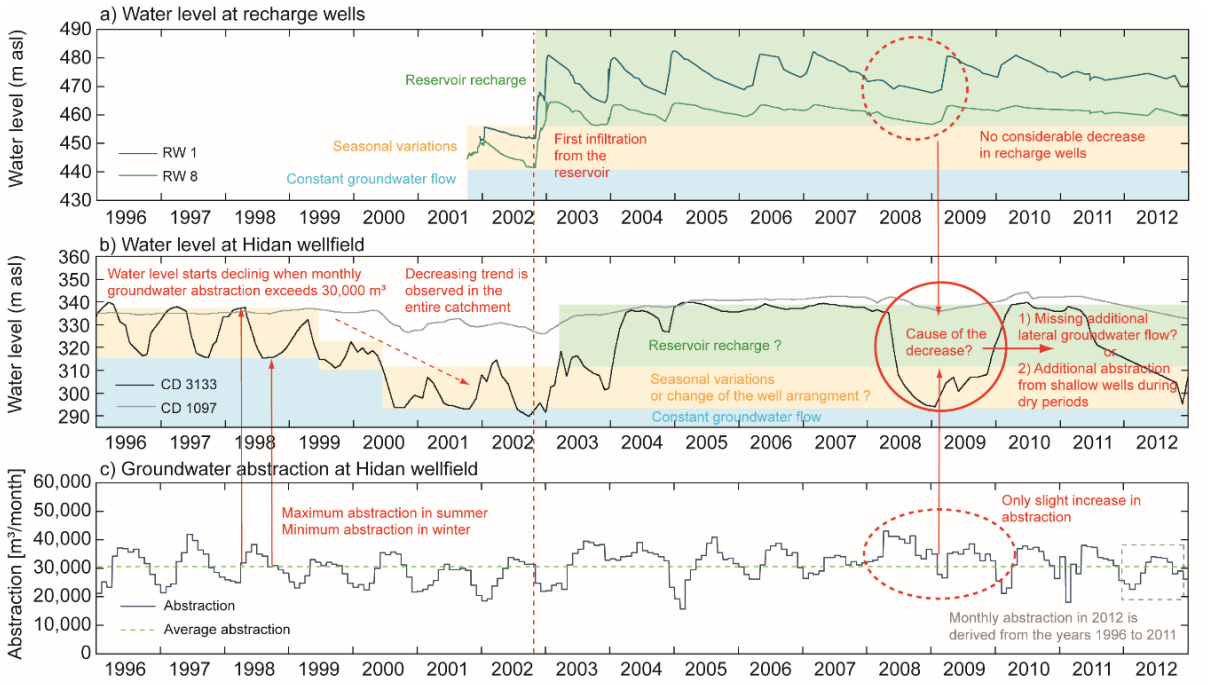

Fig. 3.2 a) Water level fluctuations at recharge well 1 and 8, b) water level fluctuations at observation well CD 1097 and CD 3133 at Hidan wellfield and c) the abstraction rates of Hidan wells.

3.3 Database and Methods

3.3.1 Water level and abstraction data

Water level data and abstraction rates were obtained from a data base of the Jordanian Ministry of Water and Irrigation (MWI, 2012). The records include water level fluctuations of the Wala reservoir (2002–2012), two recharge wells (2001–2012) and two observation wells at Hidan wellfield (1996–2012). Additionally, the infiltration rates from the reservoir and the abstraction rates from Hidan wellfield are available (1996–2012). The time series of the Wala reservoir are on a daily base. Water level measurements from the aquifer are irregular and are homogenized by linear interpolation onto a daily basis. The abstraction rates are given in million cubic meters per month (MCM/month) and represent the total amount of all abstraction wells. For 2012, only the total yearly amount is available. Therefore, the monthly abstraction is estimated with the monthly percentage derived from the years

1996 to 2011. Artificial injection of water into recharge wells started in June 2011 and is not considered. Data quality assurance was done by testing the data recording in situ.

3.3.2 Modeling background

The model implementation was realized using the finite element subsurface flow simulation software FEFLOW, which solves the flow equation in porous and fractured media. In this study, the applied equation is addressed to water flow in a single porosity medium under Darcy's law (Anderson et al. 2015), where the porous medium can be described by the representative elementary volume (REV) (Diersch 2014). The software provides the build-up of complex geometric and parametric structures in 2D and 3D projections. Furthermore, it offers the application of confined and unconfined settings and solves the groundwater flow equation numerically for saturated and unsaturated conditions (Nastev et al. 2005; Trefry and Muffels 2007; Diersch, 2014).

The 3rd type BC plays a particular role in this study and is therefore described more in detail. Because it uses a defined reference head in combination with an in-transfer rate (infiltration from surface water into the aquifer) or an out-transfer rate (exfiltration from the aquifer) this 3rd type BC can be used to incorporate clogging layers of infiltrating surface water bodies. This allowed considering the influence of sedimentation on reservoir infiltration. The resulting flow rate Q is dependent on the cross-sectional flow area, the properties of the clogging layer and the water level:

$$Q = A \times \Phi \times (h_{ref} - h) \quad (1)$$

where Q is the inflow or outflow to/from the model, A the relevant cross-sectional flow area, h_{ref} the reference water level, h the current hydraulic head in groundwater and Φ the transfer rate, which is defined as:

$$\Phi = \frac{K}{d} \quad (2)$$

K is the hydraulic conductivity of the clogging layer and d the thickness of the clogging layer.

Applied material properties in the model setup, according to the hydrogeological conditions, are the horizontal conductivity K_h, anisotropy of conductivity A_c, angle of anisotropy A_{angle} and the specific storage S_s. The anisotropy of conductivity is defined as (Diersch 2002):

$$A_c = \frac{K_{vertical}}{K_{horizontal}} \quad (3)$$

Since small inclinations of the geological layers throughout the study area are neglectable, the angle between horizontal and vertical conductivity is set to be 0°.

3.3.3 Model setup and discretization

The model was setup according to the conceptual model presented in Section 3.2.2. It is assumed that the recharge process between the reservoir and the underlying karst aquifer are dominated by vertical flux so that they can be captured in a 2D cross-section (Fig. 3.1e and h). Accordingly, the model takes into account the corridor along the wadi in a 2D vertical geometry, which in addition is well suited to consider the water level data in the calibration process, which were only available from wells close to the wadi course. Due to the geometry of the wadi course, which changes its main flow direction from southwest to northwest near recharge well 8 (Fig. 3.1e), two cross-sectional models (Fig. 3.1e) were used to simulate the whole flow process in the study area. The intersection point between these cross-sections was set up to separate the system into a "recharge model" (reservoir and recharge wells) and an "abstraction model" (Hidan wellfield), which made the calibration process easier. Since the main groundwater flow is assumed to occur along the wadi course, the intersection point was set at the bend of the wadi (Fig. 3.1e). The recharge model simulates the infiltration from the reservoir and the associated water level fluctuations in recharge well RW 1 and RW 8 (Fig. 3.2a). The abstraction model simulates the water level fluctuations at Hidan wellfield (Fig. 3.2b).

For both models, the simulation was performed for a fully saturated aquifer, which requires confined setting in cross-sectional models as stated by Anderson and Woessner (1992). Saturated conditions are in agreement with continuous percolation processes from the reservoir toward the underlying karst aquifer (for the recharge model) and for saturated aquifer layers where most of the flow occurs (for the abstraction model). Therefore, delays in groundwater table response on reservoir infiltration are not expected, which can be caused by the unsaturated zone as noted by Sumner et al. (1999). Furthermore, simulated drawdown at the wellfield might be slightly overestimated since the aquifer is considered to be unconfined and the model runs under confined and fully saturated conditions. More detailed explanations for this issue are given by Kruseman and De Ridder (1994) and Delleur (2006).

A high mesh resolution was chosen to ensure a precise water flux calculation along sensitive areas, e.g. the injection/abstraction wells, the wellfield and the reservoir bottom. An additional mesh quality improvement was achieved by minimizing the interior angles of the triangles as well as by a fine mesh discretization to avoid numerical instabilities. During steady state and transient state simulation water budget imbalance did not exceed 6.0 m^3/d for the recharge model and 210 m^3/d for the abstraction model, which is less than 2% of the maximum daily flux between both models. The results show for both models a stable and reliable setup.

3.3.3.1 The recharge model (upper section)

The area covered by the recharge model ranges from around 2 km upstream of the reservoir (Fig. 3.1e) to a horizontal length of 6.000 m (x-axis) and vertical extension of 200 m (y-axis). The y-axis is the width of the model and accounts for one unit (1.0 m). The generated mesh comprises about 200,000 elements (triangles) with an average size of 6.0 m^2 and 100,000 nodes.

For steady- and transient state calibration of the recharge model, the 1st type BC (Dirichlet type) at the eastern and western border were set up (Fig. 3.3a) to match average water level of RW 1 (450.5 m asl) and RW 8 (445.0 m asl) from October 2001 to January 2002 when groundwater flow is representative for natural flow conditions. Since rainfall in the wadi is scarce and the zone where the karst aquifer is exposed along the wadi is very small in relation to the entire aquifer, natural recharge along the profile was considered to be negligible. Water level data from RW 1 and RW 8 from October 2002 to December 2012 and the recharge from the reservoir in the same period were used to adapt hydraulic parameters.

The recharge from the reservoir was implemented by using the fluid-transfer boundary condition (3rd type BC) (Fig. 3.3a), which was connected to the water level records of the reservoir (Fig. 3.4c).

3.3.3.2 The abstraction model (lower section)

The abstraction model directly adjoins the western boundary of the recharge model (Fig. 3.1e) and runs around 7.0 km along the wadi until around 1.0 km west of Hidan wellfield. Its horizontal (x-axis) and vertical (y-axis) extents are 7.000 m and 200 m, respectively. The y-axis is 1.0 m. The model comprises about 152,000 mesh elements with an average size of 9.2 m^2 and 77,000 nodes, which are almost homogenously distributed. The abstraction wells were located at a depth between 40 and 100 m below the ground level.

In order to achieve a volumetric consistent water balance, steady- and transient state calibration was conducted using the downstream outflow from the recharge model (see supplementary Fig. SF2) as upstream inflow into the abstraction model, implemented with the 2nd type BC. The 1st type BC was applied at the western boundary (Fig. 3.3d) and also manually adjusted during transient state calibration to match the average groundwater level at CD 3133 (around 298 m asl) between 2000 and 2012. In 2D vertical section models, groundwater abstraction cannot be implemented by means of the 4th type BC, due to its radial symmetric flux (Anderson and Woessner 1992). Therefore, the 2nd type BC (Fig. 3.3d) was used as an internal boundary to account for the wellfield in the model, as recommended by Anderson et al. (2015). As a result, real pumping rates cannot be used directly but must be converted to the model specific setup by an empirical conversion factor, which is obtained

during calibration. This adds an additional calibration parameter to the model which affects the accuracy of the storage coefficient and hydraulic conductivity in terms of uniqueness. This problem consequently limits the ability of the model in predicting exact groundwater level fluctuations as a function of varied abstraction rates. However, since the principle correlation of drawdown and abstraction is still correct, as it can be shown by the ability of the model to simulate the correct groundwater levels in the validation period (see Section 3.4.1), we think this approach is still feasible. Furthermore, the primary aim of this study is the identification of the driving factors for groundwater level fluctuations at the wellfield and it can be shown, that the drawdown is dominated by infiltration rates of the reservoir, as well as abstraction depths and relatively insensitive to varied pumping rates (see Sections 3.4.1.2 and 3.4.3).

3.3.4 Scenarios

To predict possible future effects of sedimentation on reservoir infiltration and the possibility of an increased groundwater abstraction, two scenarios for the recharge model were simulated with (#1) a wet and (#2) a dry period of 10 years each, with the same annually repeating reservoir inflow and groundwater abstraction. Main point of interest was the effect on groundwater level trend over the regarded period from 2013 to 2022 in dependency of a growing sedimentation.

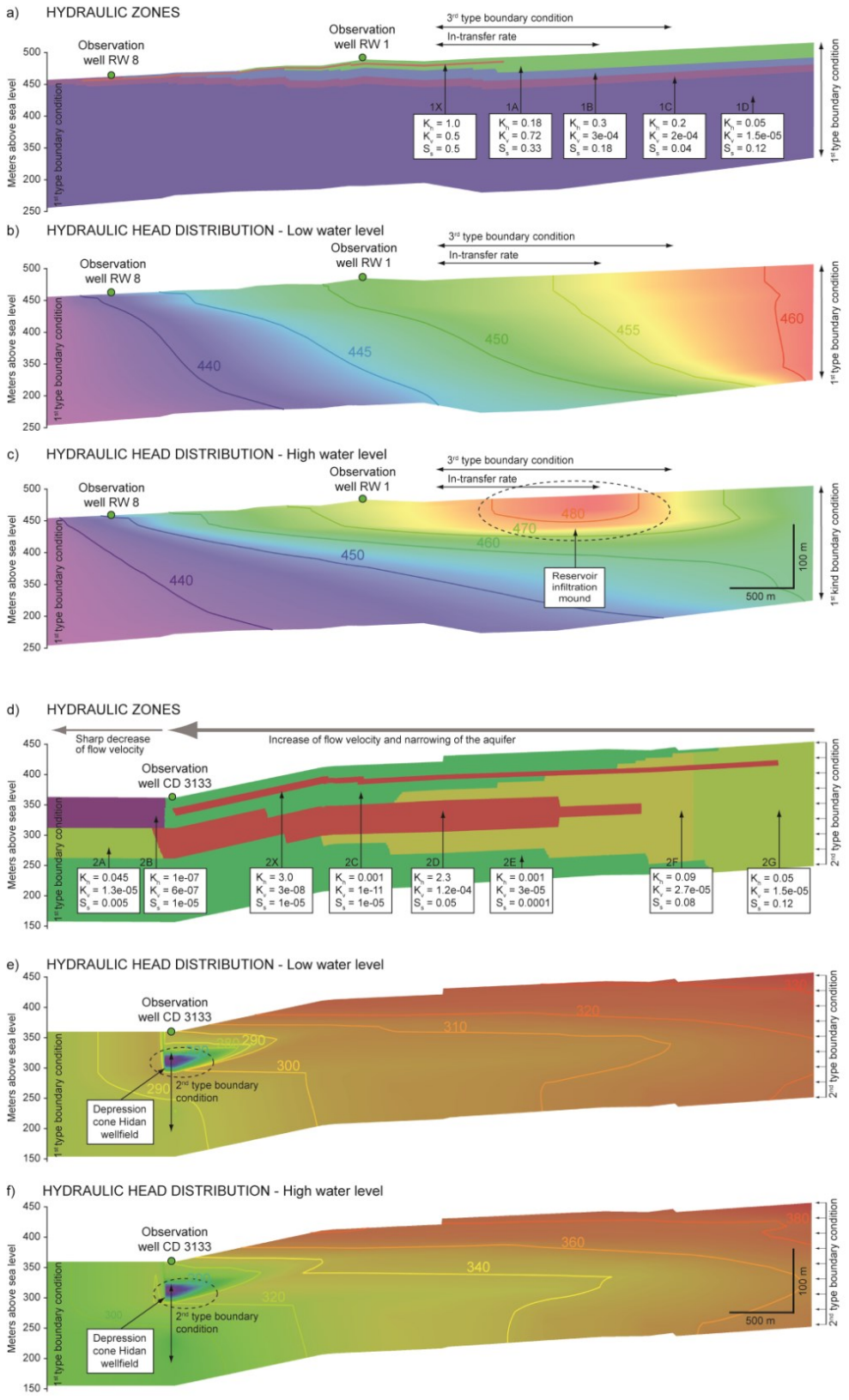

Fig. 3.3 Superelevated presentation of a) the distribution of hydraulic zones of the recharge model and b) the hydraulic head distribution during low groundwater level and c) high water level in the recharge model. d) Distribution of hydraulic zones of the abstraction model and e) hydraulic head during low groundwater level and f) high groundwater level in the abstraction model.

3.4 Results and discussion

Results from the pre-sensitivity analysis (see supplementary information SI1) showed that the behavior of the karst groundwater level fluctuations at the recharge wells in response to infiltration can be simulated with well-suited parameters. However, it must be noted that these parameter values, or parameter combinations, do not necessarily reflect realistic values of the hydrodynamic aquifer properties and may over- or underestimate the generated groundwater flux.

3.4.1 Model calibration and simulation

During calibration, various cases were tested to identify the most suitable distribution and dimensioning of the hydraulic zones (e.g. additional thin and high permeable zones) but also to adjust the in-transfer rate for the recharge model. Since automatic geometric adaptions and creation of time series is not possible, the automatic calibration with PEST was unpractical for both models. Accordingly, the calibration was performed manually while the hydraulic zones, the in-transfer rate and the three hydraulic parameters K_h, K_v and S_s were changed alternatingly in order to find the best fit between measured and simulated groundwater level.

3.4.1.1 The recharge model (upper section)

To allow a flexible adjustment of the simulated water level to the measured ones by adjustment of the hydraulic parameters, the recharge model was divided into four hydraulic sections (Fig. 3.3a). Their vertical extensions were derived from the range of water level fluctuations and adjusted during the calibration process. The lowest hydraulic section represents the part, which is not affected by water level changes and was therefore not further divided. The upper hydraulic section is equivalent to the Wadi Ghudran formation, where water level fluctuations take place. It was further divided into three sections according to the aquifer properties of the geological members (Table 3.1), which reveal a higher section in the middle and lower permeable layers above and below. This also allowed a more flexible adaption of the hydraulic parameters on fast flow and slow depletion. Additionally, a small high permeable zone within the upper section supports the very fast water level increase, as observed in RW 1 and RW 8. The spatial distribution of pressure head for low and high water level in the reservoir is shown in Fig. 3.3b and c.

The in-transfer rate required a time-dynamic setup because the thickness of the sediment layer in the reservoir increased over time and hence the in-transfer rate generally decreases according to Eq. (2). Furthermore, the relation between the reservoir water-level and infiltration from the reservoir is non-linear (Fig. 3.4a) since the influence of the sediments on infiltration rate increases as the water level in the reservoir decreases (Fig. 3.4b). Therefore, the in-transfer rate was adapted manually for each year.

Pedretti et al. (2011) detected the exponential decay of the infiltration rate to about 37% of the initial value, as a result of clogging during one infiltration event. In the present case, the effect of sedimentation causes a long-term exponential decay of the infiltration rate as a result of multiple infiltration events. Here, the exponential decay is more attributed to a reduction of the infiltration area at the flanks of the reservoir, owed to the V-shaped reservoir geometry (Fig. 3.4b), and less to direct clogging of infiltration paths through suspended material. An overall long-term reduction of the in-transfer rate of around 32% was observed from the maximum peaks from 2002 (1.0) to 2009 (0.68). However, the results indicate a slower growing impact of the sediments on the infiltration than in the early years as the sediment level reveals a lower growing rate due to the upwards widening reservoir basin. The lateral inflow is therefore much less reduced than in the beginning (Fig. 3.4b).

The simulation results showed generally satisfying accordance of measured and simulated groundwater level fluctuations at RW 1 and RW 8 (Fig. 3.5b) with correlation coefficients of 0.87 (Fig. 3.5d) and 0.82 respectively (from 2002 to 2012) (Fig. 3.5e).

Discrepancies exist from June 2011 onwards. These can be ascribed to the artificial injection through the recharge wells, which was not considered in the model due to uncertainties regarding the injection rates. Excluding the years 2011 and 2012 from the performance analysis, the correlation coefficients increase to 0.95 (RW 1) and 0.91 (RW 8) respectively (Fig. 3.5d and e).

According to the assumption of preferential flow paths along horizontal bedding planes, a high anisotropy for the hydraulic zones allowed obtaining the best fit between observation and simulations: K_v and K_h values range from 0.5 to 1×10^{-05} m/s and from 1.0 to 0.05 m/s, respectively; S_s values vary between 0.5 and 0.04.

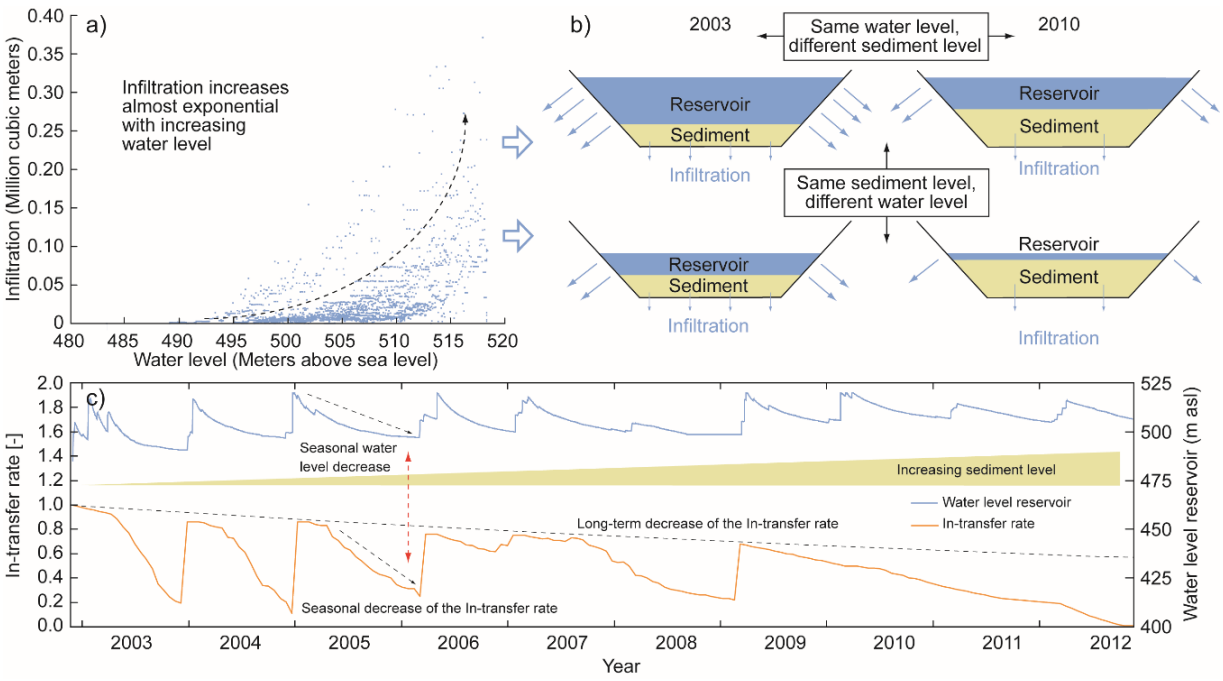

Fig. 3.4 a) Reservoir infiltration increases exponentially when the water level in the reservoir increases. b) Increased sedimentation and thicker sediment layer reduce the infiltration rate. c) The manually adapted in-transfer rate and its decrease over time in dependency of the water level in the reservoir.

3.4.1.2 The abstraction model (lower section)

The groundwater-level in well CD 3133 (Fig. 3.2b) indicates a fast groundwater flow and retardation at Hidan wellfield by strong vertical changes and fast reaction on reservoir infiltration, which required also a parameter adaption along the x-axis of the model. A productive aquifer zone in the middle was implemented with a high permeable layer (Fig. 3.3d), which promoted a faster reaction at the wellfield (enhanced infiltration) in response to water level changes in the reservoir. Strong water level increase was realized with a hydraulic barrier at the wellfield and a very low vertical hydraulic conductivity along the whole model. This corresponds to field observations that highlight both a fault at the wellfield and preferential horizontal flow path along bedding planes (Table 3.1). An additional high-permeability zone (representing a karst conduit) was implemented to promote fast flow in the upper section of the model (Fig. 3.3d). The spatial distribution of hydraulic head for low and high water level is shown in Fig. 3.3e and f.

For geometric reasons, radial flow toward pumping wells cannot be simulated in a straightforward way in 2D cross sectional models (Anderson et al. 2015; Wels et al. 2012). Therefore, the 2nd type BC was applied for groundwater abstraction, as recommended by Anderson et al. (2015) (see Section 3.3.3.2). It is common practice in groundwater modeling to calculate the "unit flow rate" of a representative 2D vertical section and multiply this value by a relevant width (typically the aquifer width) in order to obtain the real flow rate of the entire 3D flow system (e.g. Kresic 2006). In the present case, the

effective hydraulic width of the karst aquifer is unknown. Therefore, real abstraction rates had to be fitted to the model specific unit flow. The ratio of real- and simulated abstraction rates was empirically determined to be 5.75.

During the regarded period between 2002 and 2012 several new wells were drilled and both the abstraction depth and the location of the wells actually used for abstraction also changed over time. Therefore, an impact on the depression cone of the wellfield is most probable. The change was implemented in the model in 2006, 2008, 2009 and with the beginning of 2011 (Fig. 3.5c) with a shifting of the projected abstraction depth (Fig. 3.5k) into a lower depth, which resulted in a much higher correlation coefficient of 0.92 (Fig. 3.5g), instead of 0.33 (Fig. 3.5f) without any other changes. The increase of the abstraction proportion in the upper aquifer section (2C) demonstrated the sensitive reaction on changes of the average abstraction depth and the drilling of new wells. This correlates with indications of Humphreys (1991) stating a low productivity in the upper aquifer part. Still, it cannot be excluded that groundwater flux resulting from reservoir infiltration is overestimated during low water level in the reservoir, as stated above (Section 3.4).

The parameter distribution shows significant differences for the Kh values, which range from 2.3 to 1×10^{-7} m/s. This implies strong karstification in horizontal direction, whereby Kv values are significantly lower and range from 1.2×10^{-4} to 1×10^{-11} m/s. The storage coefficients turned out far lower than in the recharge model and range from 0.12 to 1×10^{-5}, which can be explained by the dense limestone matrix of the Wadi As Sir formation.

3.4.2 Model performance criteria

3.4.2.1 Uncertainty analysis

Model uncertainties have their origin in all aspects of model development and concern geological features, which affect the model geometry and the hydraulic parameter distribution, field data collection and the model setup itself (Freeze et al. 1992). Thus, the setup of both models depended partly on personal assessment and interpretation of the field data and therefore the degree of uncertainties is difficult to define, whereas the quality of the model setup was supported by several FEFLOW tools, such as a fine mesh discretization and a minimization of the interior angles of the triangles, as described in Section 3.3.3.

3.4.2.2 Model sensitivity

The iterative process of manual calibration includes already a sensitivity analysis by the stepwise adaption of hydraulic parameters and their spatial distribution. The calibration and simulation results of

the abstraction model revealed sensitivity to changing abstraction depths. A further structural sensitivity analysis was performed for the high permeable zone 2X and section 2B (Fig. 3.3d), while applying the three different steps of depth dependent abstraction as during calibration. In each case, the section 2B and the high permeable zone 2X was removed and replaced by the parameters from section 2C (Fig. 3.3d).

It can be shown that the horizontal high permeable zone 2X influences mainly the total magnitude of the groundwater level and thus accelerates the hydraulic signal from the reservoir to the wellfield. The water barrier (Section 2B) mainly controls the general seasonal vertical fluctuations, especially during 2008 (Fig. 3.5c).

3.4.3 Scenarios

For the dry period, the reservoir water level with a yearly inflow of about 4.6 MCM from 2012 was repeated for 10 years, and for the wet period the water level from 2010 with an annual inflow of about 10.9 MCM was applied, also for 10 years. The in-transfer rate required a manual adaption and was set between extrapolated exponential function of the maximum and minimum in-transfer values of the calibrated in-transfer rate from 2002 to 2012. The initial maximum value, which was 1.0 in 2003, decreased after 10 years (2012) to about 0.6. The extrapolation revealed a maximum value of about 0.3 in 2022 (Fig. 3.5h). The groundwater flow from both scenarios, which leaves the recharge model at the downstream boundary, served as inflow at the upstream boundary of the abstraction model.

To assess the effect of groundwater abstraction, simulations with the abstraction model were performed accounting for four scenarios: (#1a) applying abstraction rates from 2008 with an annual volume of 13.8 MCM for the wet period (#1), which lie above the annual average from 2002 to 2012 of 11.8 MCM, and another (#2a) with a 10% increase to about 15.2 MCM for the dry period (#2). For both climate scenarios, two different abstraction depths scenarios (#1b and #2b) were applied to identify the impact of the wellfield activities on groundwater level.

Groundwater levels of RW 1 and RW 8 were almost similarly affected during the wet and dry climate scenario applied for the recharge model. A lowering of the average annual groundwater level of around 2.7 m from 2013 to 2022 (Fig. 3.5i) indicates that the decrease in the in-transfer rate, caused by progressive sedimentation, has a greater influence on the decreasing infiltration rate from the reservoir than a lower maximum water level in the reservoir. This indicates that lateral infiltration from the reservoir is still high, even with a lower reservoir water level during the dry period.

For the abstraction model, the absolute values of long-term water level fluctuations and of decreasing long-term trend must be carefully examined as the conversion of the pumping rates affects also the

setting of hydraulic parameters (Section 3.3.3.2). Thus, values of mean lowering of the groundwater table, obtained by the scenarios, are seen as indications, not as absolute values, for the individual impact of each factor (reservoir infiltration, abstraction depth and abstraction rates) on long-term trends of groundwater level.

The mean lowering of the groundwater level at Hidan wellfield from 2013 to 2022 is almost equally affected by both climate scenarios when changing the abstraction depth no. 2 and no. 3 in the abstraction model. Thus, the difference in the lowering of mean groundwater level is 3.6 m during both wet scenarios and 3.0 m during both dry scenarios. However, the entire average groundwater level is significantly different with abstraction depth no. 3 (shallower abstraction). Here, the mean groundwater level dropped below the groundwater level reached in 2008 and is about 30–40 m lower than when simulation is performed with abstraction depth no. 2 (Fig. 3.5j).

A similar lowering of the mean annual groundwater level of about 6 m is observed for both climate scenarios when the same abstraction depth is applied. Thus, mean lowering of the groundwater level is 2.7 m (wet scenario) and 9.0 m (dry scenario) when abstraction depth no. 2 is applied. For abstraction depth no. 3, mean lowering of the groundwater is 6.3 m (wet scenario) and 12.0 m (dry scenario).

The scenarios identified a further decrease in infiltration from the reservoir for the next 10 years, but not so fast as in the first years (2002–2008). A considerable effect on long-term water level drop is caused by the decreasing reservoir infiltration, but also affected by the different abstraction depths and to a lesser extent by the abstraction rates.

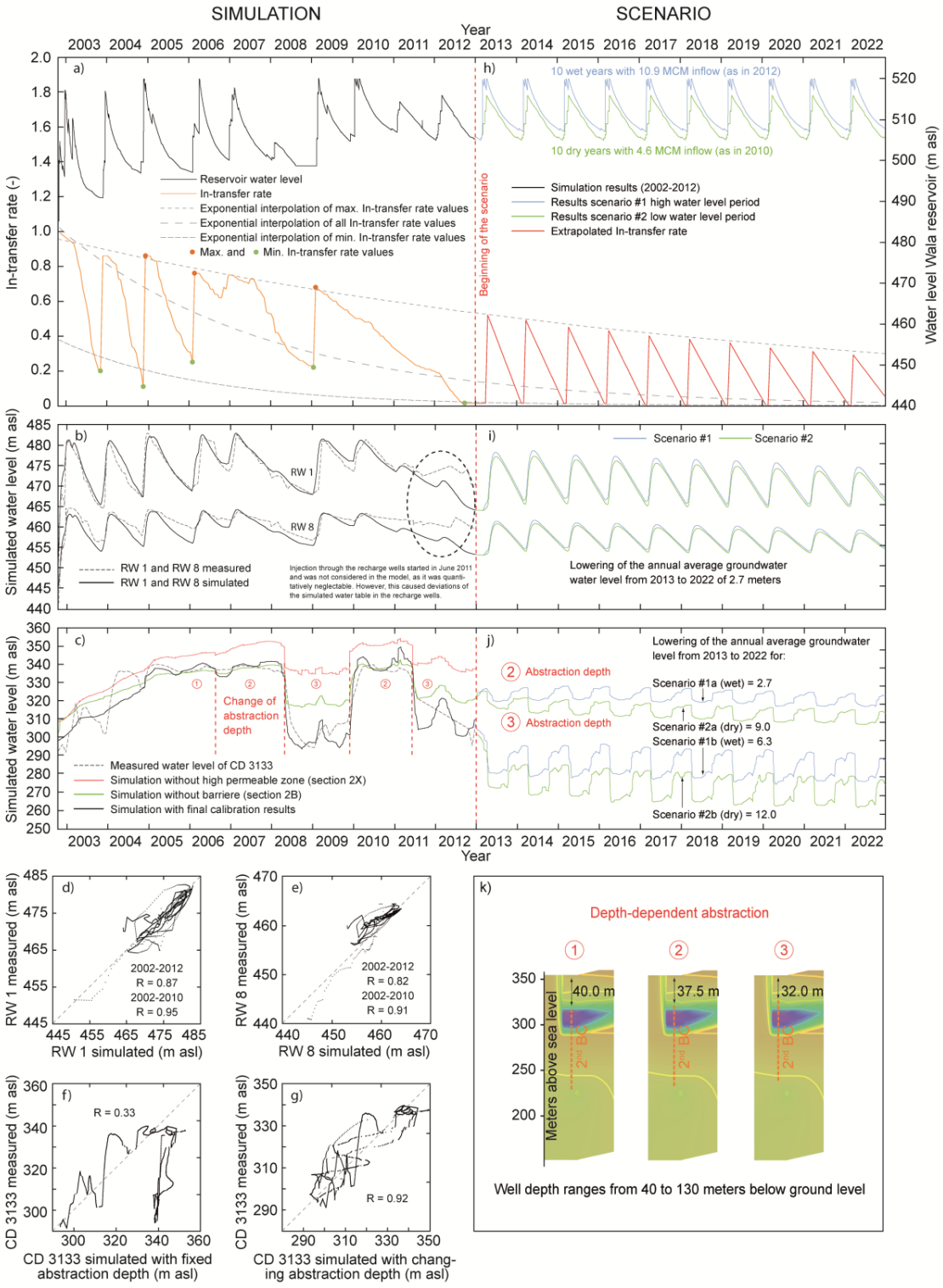

Fig. 3.5 a) Reservoir water level and in-transfer rate, b) measured and simulated hydraulic head at recharge well RW 1 and RW 8 and c) groundwater level simulations at CD 3133 and results of sensitivity analysis performed with the abstraction model when the high permeable zone 2X or the aquifer section 2B were removed and replaced by the hydraulic parameters from section 2C. The correlation between measurement and observation at d) RW 1, e) RW 8, f) CD 3133 with abstraction depth no 1 and g) changing abstraction depth. f) Sketch of the different abstraction depths no 1-3. Scenario period (2013-2022) of h) water level of Wala reservoir and in-transfer rate, i) water level at RW 1 and RW 8 and j) the impact of the four scenarios on water level at observation well CD 3133.

3.5 Conclusions

Numerical simulation of groundwater flow in karst aquifers using an equivalent porous medium (EPM) approach requires specific adaptations considering the heterogeneity and anisotropy of karst aquifers along with a generalization of the complex 3-dimensional aquifer setup, especially on intermediate and local scale simulations. In this study, which focuses on managed aquifer recharge (MAR) into a karst aquifer, satisfying match of simulated and measured groundwater levels was achieved by spatial subdivision into hydraulic sections corresponding to the prevailing geological and structural conditions of the aquifer beneath the wadi. They partly correspond to zones of preferential flow, which allowed simulating the characteristic hydrodynamic behavior of the karst with fast flow and slow depletion. Furthermore, the success of the model application is owed to the simplification of the complex 3D anisotropic aquifer structure to a 2D vertical projection and a further separation of the model domain into a recharge and abstraction model, which simplified the calibration procedure.

The results of the calibration, simulations and scenarios allow a more precise description of the hydraulic system and recommendations can be derived regarding an improved management of the MAR site. Thus, immediate measures are recommended to reduce the sedimentation rates and to remove sediments from the reservoir to restore or at least suspend the infiltration rates and reservoir storage capacity. A 2.7 m drop of the average groundwater level at the recharge wells and probably a greater depletion at the wellfield is projected to occur between 2013 and 2022. Based on the modeling results, it is recommended that artificial injection through the recharge wells takes place mainly during May and October, when groundwater level is low.

At Hidan wellfield, the model revealed a strong impact on water level fluctuations as a result of changing abstraction depth and differences in the monthly abstraction rates. However, statements about the magnitude of fluctuations have to be considered carefully, because of the inherent problems in representing pumping rates in a 2D vertical model. Since this affects also the hydraulic parameter combination in terms of uniqueness, water level fluctuations cannot be predicted precisely. However, the projected long-term drop of groundwater levels, caused by decreasing reservoir infiltration, can be regarded as reliable. Therefore, pumping from the upper aquifer section should be avoided and additional monitoring wells would help to identify an optimized well management to avoid strong water level declines. Based on the findings of the computed scenarios it can be concluded that mean annual abstraction rates higher than the actual mean annual abstraction rate (11.8 MCM/year) could lead to a significant long-term depletion in the groundwater levels.

The long-term experiences at Wadi Wala suggest that managed aquifer recharge can be a feasible and efficient technique for integrated water management, also in karst areas. Our modeling study

demonstrates that numerical simulations are powerful to achieve an optimized management of MAR sites and to make quantitative predictions concerning the impacts of technical measures, increasing water demand and climate change.

The long-term experiences at Wadi Wala suggest that managed aquifer recharge can be a feasible and efficient technique for integrated water management, also in karst areas. Our modeling study demonstrates that numerical simulations are powerful to achieve an optimized management of MAR sites and to make quantitative predictions concerning the impacts of technical measures, increasing water demand and climate change.

Acknowledgement

The German Federal Ministry of Education and Research (BMBF) is acknowledged for funding the SMART Project (Sustainable Management of Available Water Resources with Innovative Technologies) (FKZ 02WM1079-1086 and FKZ02WM1211-1212). The authors thank Zhao Chen from the Karlsruhe Institute of Technology for rewarding discussions and the associate editor Dr. Barbara Mahler and the reviewers for their valuable comments and suggestions.

Chapter 4

Contamination risk and drinking water protection for a large-scale managed aquifer recharge site in a semi-arid karst region, Jordan

Reproduced from: Xanke J, Liesch T, Goeppert N, Klinger J, Gassen N, Goldscheider N (2017) Contamination risk and drinking water protection for a large-scale managed aquifer recharge site in a semi-arid karst region, Jordan. Hydrogeol. J. 1–15. http://dx.doi.org/10.1007/s10040-017-1586-0.

Abstract

Karst aquifers in semi-arid regions are particularly threatened by surface contamination, especially during winter seasons when extremely variable rainfall of high intensities prevails. An additional challenge is posed when managed recharge of storm water is applied, since karst aquifers display a high spatial variability of hydraulic properties. In these cases, adapted protection concepts are required to address the interaction of surface water and groundwater. In this study a combined protection approach for the surface catchment of the managed aquifer recharge site at the Wala reservoir in Jordan and the downstream Hidan wellfield, which are both subject to frequent bacteriological contamination, is developed. The variability of groundwater quality was evaluated by correlating contamination events to rainfall, and to recharge from the reservoir. Both trigger increased wadi flow downstream of the reservoir by surface runoff generation and groundwater seepage, respectively. A tracer test verified the major pathway of the surface flow into the underground by infiltrating from pools along Wadi Wala. An intrinsic karst vulnerability and risk map was adapted to the regional characteristics and developed to account for the catchment separation by the Wala Dam and the interaction of surface water and groundwater. Implementation of the proposed protection zones for the wellfield and the reservoir is highly recommended, since the results suggest an extreme contamination risk resulting from livestock farming, arable agriculture and human occupation along the wadi. The applied methods can be transferred to other managed aquifer recharge sites in similar karstic environments of semi-arid regions.

4.1 Introduction

Many countries in the Middle East and North Africa are facing the challenge of population growth and the associated increase in water demand. Most of these countries are located in a semi-arid climate, which exacerbates the situation due to natural water scarcity (Alsharhan et al. 2001; Kliot 2005; Amery and Wolf 2010). A continuous water supply is difficult to maintain since many aquifers are exhausted by overexploitation and both recharge and the availability of surface water is highly dependent on the seasonal variability of rainfall (Wada et al. 2010; Voss et al. 2013; Joodaki et al. 2014). Rainfall usually occurs at high intensities during relatively few days in the winter months, which often results in flash floodings—thus, only a small proportion contributes to groundwater recharge (Bou-Zeid and El-Fadel 2002).

In the past decades, water management was often promoted with the construction of surface reservoirs to capture the flash floods in winter and save the water for domestic and agricultural purposes in summer, when the water demand increases (Alsharhan et al. 2001; Sowers et al. 2011). However, in many countries, growing urbanization and exploitation of rural areas for agriculture progressively expose catchments of surface reservoirs (and groundwater reservoirs) to the impacts of anthropogenic activities (Foley et al. 2005; Scanlon et al. 2005), which exacerbates loading with, e.g., waste water and fertilizers, consequently impacting water quality (Vidal et al. 2000; Coxon 2011). A significant portion of the surface reservoir water is lost by evaporation, as a result of high temperatures.

To reduce these effects, managed aquifer recharge (MAR) presents a promising alternative to surface storage of flood water in semi-arid and arid regions since it requires less infrastructure, reduces evaporative losses and contamination of water, and enhances the natural purification of the water during the infiltration process and residence time in the underground; furthermore, MAR counteracts declining water tables (Bouwer 2000, 2002). The different purposes and techniques for MAR are presented and discussed by Dillon (2005) and Dillon et al. (2009), wherein most of the examples occur in unconsolidated aquifers. Karst aquifers still play a minor role, due to their characteristic variability of hydraulic properties which affect storage and flow conditions (Bakalowicz 2005; Daher et al. 2011). Indeed, these hydraulic properties often make them a productive source of fresh water in the Middle East (Alsharhan et al. 2001; Margane et al. 2002; MWI 2004; El-Hakim and Bakalowicz 2007), but challenge their sustainable management and protection. In karst, rapid and voluminous infiltration through surface features (e.g. dolines, sinkholes, swallow holes) poses a contamination risk as water quickly reaches the phreatic zone with little purification. Therefore, in terms of MAR application, surface infiltration through the epikarst zone is favored instead of direct injection into the underground (Daher et al. 2011). Either way, protection concepts must address both drainage systems of surface

water and groundwater, as well as their interaction, and must be adapted to the regional characteristics of the karst aquifer.

To quantify this risk of surface water and groundwater contamination, the spatiotemporal occurrence and sources of contaminants must be identified. The presence of fecal bacteria is commonly regarded as an indicator for other pathogenic microorganisms originating from human or animal waste. Because their occurrence often varies temporally, controlled by rainfall events or floods (Auckenthaler and Huggenberger 2013), a qualitative detection and correlation with these events is necessary in order to reveal causal relationships and identify trigger events. Furthermore, natural and artificial tracers are valuable tools to simulate the hydraulic behavior of aquifers and identify flow paths and transit times in the underground (Käss 2004; Leibundgut et al. 2011). Their application and the type of substance used for tracing, depends on various aspects of the environmental setting, toxicology of the tracer, and economic and logistical factors (Behrens et al. 2001; Schudel et al. 2002; Nguyet and Goldscheider 2006).

Groundwater vulnerability and risk mapping provide valuable information on the protective function of the geological environment against infiltration of hazardous substances into groundwater. As a first method for karst environments, the EPIK approach (Doerfliger and Zwahlen 1998) established the scope for the European initiative COST Action 620. This action developed an "improved and consistent European approach for the protection of karst groundwater" based on the origin-pathway-target model (Zwahlen 2004). In this context, numerous methods were developed, such as the PI method (Goldscheider et al. 2000), COP method (Vías et al. 2006), VURAAS method (Laimer 2005), Slovene approach (Ravbar and Goldscheider 2007) or the duality method (Nguyet and Goldscheider 2006). They address the vulnerability of either source (springs, wells) or resources (entire aquifers) in light of various hydrogeological aspects, often adapted to regional characteristics. In areas of Jordan, karst groundwater protection is increasingly assessed by vulnerability mapping (Al-Adamat et al. 2003; El-Naqa 2004; Al-Kuisi et al. 2006; Werz and Hötzl 2007; Al-Hanbali and Kondoh 2008; Hammouri and El-Naqa 2008; Awawdeh and Jaradat 2010).

For this study, a combined protection approach for the surface catchment of Wala reservoir and Hidan wellfield in Jordan is developed. The Wala reservoir poses a successful example of large-scale MAR into a karst aquifer, where flood water is stored and discharged to the underground to recharge the Hidan wellfield 7 km downstream (Xanke et al. 2015, 2016). However, frequent contamination of the groundwater by coliform bacteria has been observed in the past, and this requires an adapted protection concept for the MAR scheme to address the interaction of surface water and groundwater. This study aims to (1) characterize the natural vulnerability to contamination of the groundwater by monitoring coliform bacteria, (2) to identify through tracer testing the major impact pathways and (3) to develop a

pragmatic protection approach. This includes a vulnerability mapping method based on the COST action 620 approach (Zwahlen 2004), which requires minimal data as input for a risk map and conceptual protection zones, and addresses the interaction of the surface reservoir and the karst aquifer.

4.2 Site description

4.2.1 Geographical setting

The Wala surface catchment is located around 50 km south of Jordan's capital Amman, and covers an area of about 1,770 km2. Elevation ranges from 1,000 m above sea level (asl) at the northern, eastern and southern peripheries, down to 400 m asl in the west. Mean annual rainfall decreases from about 500 mm (north) to about 100 mm (south), of which 85–93% evaporates (El-Naqa 1993) as a result of high temperatures (Margane et al. 2009). Only 3–11% of the rainfall contributes to natural groundwater recharge (El-Naqa 1993), and 0.5–10% generates surface runoff; hence, natural groundwater recharge takes place mainly in the northern part of the large surface catchment where most of the rainfall occurs.

Since the construction of the Wala Dam in 2002, the surface catchment has been divided into two parts, upstream and downstream of the reservoir. The additional total groundwater recharge by reservoir infiltration was about 74 million cubic meters (MCM) from 2002 to 2012. Here, the annual average infiltration of about 6.7 MCM (Xanke et al. 2015) partially offsets an average yearly extraction at Hidan wellfield of about 11.7 MCM before 2012 and raised the groundwater level about 20–30 m; however, since the reservoir infiltration is highly variable, water level dropped down again in 2008, 2011 and 2012. Assuming a constant water level, the minimum amount of groundwater flow contributed by the catchment would be about 5 MCM. The loss from the reservoir by evaporation is about 0.7 MCM. The Wala Dam reveals a length of about 265 m and a height of about 42 m and a lake surface of about 0.77 km2 at its highest storage. The most constraining factor for the reservoir is the heavy sedimentary load which reduced the storage capacity by about 1.6 MCM from primary 9.3 MCM to about 7.7 MCM in 2012.

Additionally to the natural recharge by reservoir infiltration, injection into eight recharge wells (Fig. 4.2f) was first conducted in June/July 2011 (Xanke et al. 2015) with a total volume of about 138,000 m3 and in November/December 2011 with a total volume of about 32,000 m3. A further injection was conducted in 2012 with about 11,000 m3 in May, 116,000 m3 in June, 74,000 m3 in July and 115,000 m3 in August. The water is released from the reservoir by gravity force through a pipe and is passed through sand filters to avoid clogging of the recharge wells. The depth of the recharge wells is 175 m with a diameter of about 0.5 m (Fig. 4.1b); however, the monthly recharge from the reservoir between

May and August 2012 ranged between 382,000 and 415,000 m3 and therefore exceeds the artificial recharge.

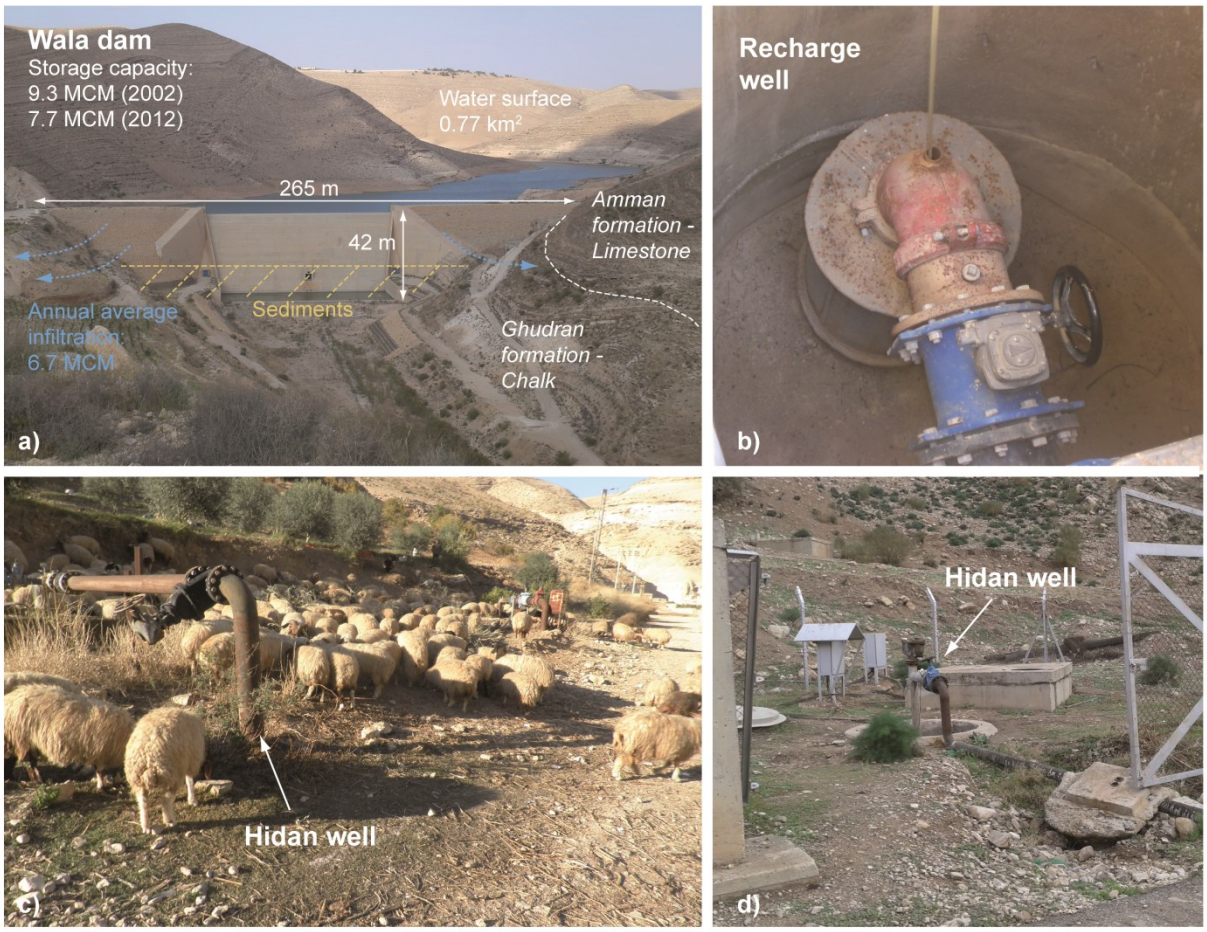

Fig. 4.1 a) View of the Wala Dam and b) a recharge well. c) Sheep herd at Hidan wellfield between unprotected wells and d) well with destroyed fence.

The additional recharge from the Wala reservoir counteracts the declining water table at Hidan wellfield and contributes to a constant drinking water supply for the cities of Amman and Madaba and adjacent communities. In addition to the wellfield, several production wells located a little bit further away from the wadi (> 100 m) compared to the Hidan wells (Fig. 4.2f) are used for local irrigation and drinking water supply (Xanke et al. 2015; however, most of the Hidan and Wala wells are of poor construction since proper wellhead protection (e.g. fences) is often missing (Fig. 4.1a,b).

The management of the reservoir and the wellfield includes the observation of daily changes in the storage volume caused by inflow, infiltration into the aquifer and evaporation; furthermore, the monthly abstraction rates at Hidan wellfield are documented (Xanke et al. 2015). The measured physical, chemical and microbial parameters at Wala reservoir, Hidan and Wala wells are water level, pH, electrical conductivity and temperature as well as the major ions, tritium, oxygen-18 and deuterium, and carbon-14 and -13. Since water sampling is done irregularly, mainly on a monthly

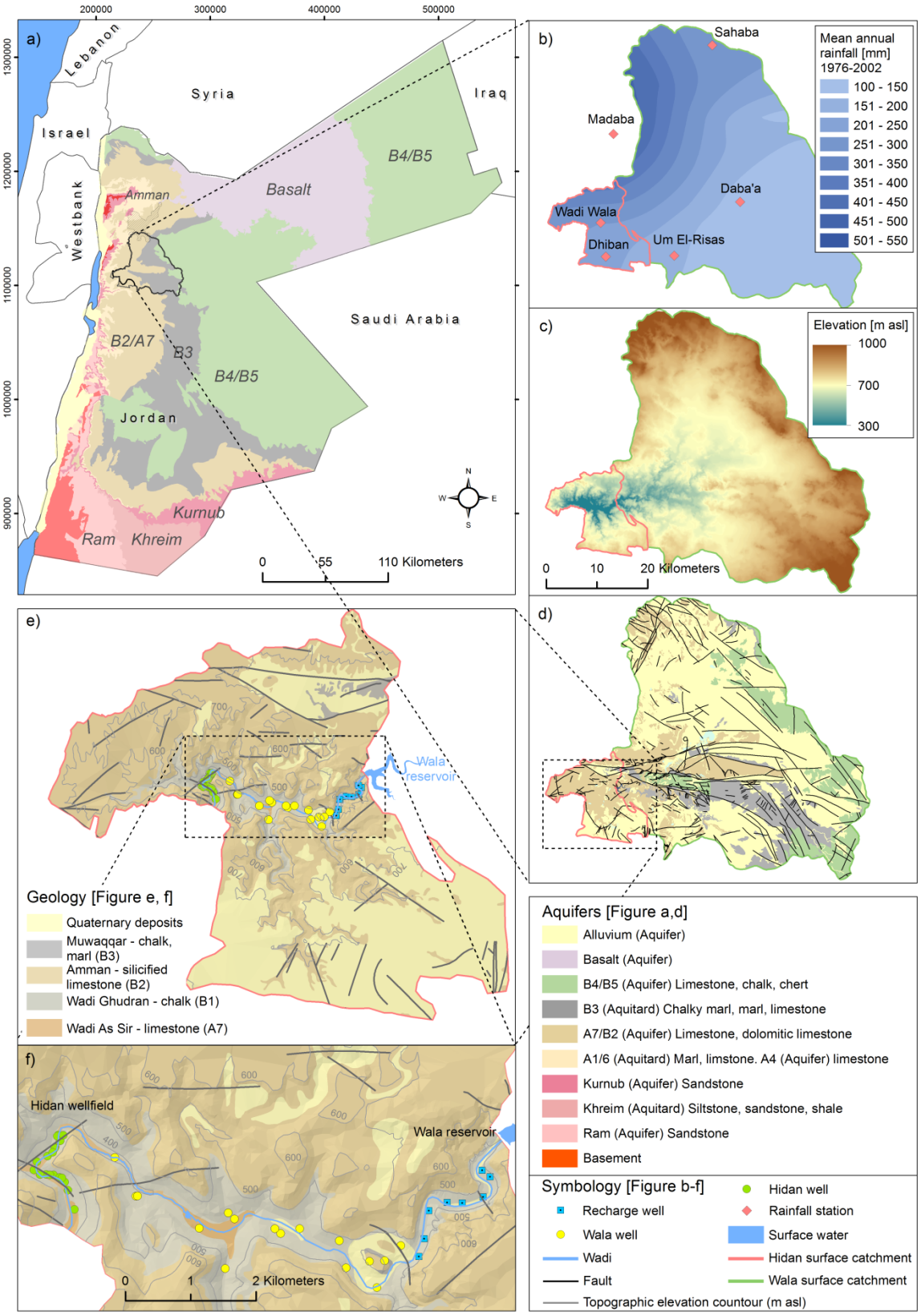

Fig. 4.2 a) Location of Wala surface catchment relative to Jordan's major aquifer systems. b) Mean annual rainfall distribution in the Wala catchment and its wadi channel network, c) topography and d) outcropping aquifer systems and geological structures. e–f) Geological map and location of Wala reservoir, recharge and production well.

basis, the data time series often reveal large gaps. A general water chemistry assessment is presented in Xanke et al. (2015), which revealed only small changes in salinity (<200 µS/cm) as a result of MAR from the reservoir.

The risk of contamination at Hidan wellfield, but also at the Wala wells, is mainly related to microbial pollution and turbidity; however, not all of these parameters are measured regularly, and only the data from total coliforms and Escherichia coli (E. coli) are available as indicators for such contaminations. Nevertheless, the simultaneous occurrence of E. coli and turbidity is observed in many karst areas (Heinz et al. 2009) and was also detected at Hidan wellfield and Wala wells. Therefore, the wells are switched off when turbidity occurs and hence sampling is not conducted. Data for contamination events prior to the construction of the Wala Dam are not available, but it is assumed that they occurred mainly during heavy flash floods in winter as well as related to rainfall; therefore, additional risk is associated with reservoir infiltration and the seepage into the wadi. Post-treatment of the groundwater used for drinking is done by chlorination.

4.2.2 Geology and hydrogeology

The geological setting of Jordan consists of Precambrian crystalline basement, sandstone formations of Cambrian to Lower Cretaceous, carbonate rocks of Upper Cretaceous to Tertiary, and Quaternary alluvial and igneous rocks. About 70% of the non-Quaternary surface exposures in Jordan are carbonate rocks, followed by basalt (13.2%) in the north, sandstone (10.7%) and the crystalline basement (2.5%) in the south (Fig. 2a) and sedimentary deposits (2.5%) in the Jordan Valley. Their physiographical appearance was mainly formed in the past 12 million years by the tectonic evolution of the Jordan Rift Valley (Bayer et al. 1988).

Outcropping formations in the Wala and Hidan catchment range from Upper Cretaceous to Eocene and comprise the B4/B5 and B2/A7 aquifer systems (Fig. 2a,d). The latter consist of the Wadi As Sir limestone formation (A7) and the chert and limestone sequences of the Amman (B2b) and Al Hisa (B2a) formations. At the Wala Dam, the A7 is the main aquifer and displays an average thickness of about 150 m with a 30–50 m thick production zone in the middle. In some areas, the chalky deposits of Wadi Ghudran (B1) formation are well developed and act as an impermeable layer between A7 and B2. Likewise, the chalky Muwaqqar formation (B3) separates the B2/A7 from the B4/B5 aquifer system. The latter is formed by limestone deposits of the Rijam formation (B4) and the chalky, marly limestone of the Wadi Shallala formation (B5). The Wala reservoir is located on the Wadi Ghudran formation, whereas the Hidan wellfield is drilled into the outcropping Wadi As Sir formation (Fig. 2e). Permanent groundwater seepage downstream the reservoir generates variable runoff towards the

wellfield (Xanke et al. 2015), which behaves as a losing stream since water successively sinks at different infiltration pools along the wadi.

4.3 Methodology

4.3.1 Data acquisition

Geological and hydrogeological data were obtained during field investigations in 2012 and 2013 and complemented with historical data from the Ministry of Water and Irrigation (MWI) in Amman. Data collection, analytical methods and periods of data record are described below:

Field investigations

- Daily water levels of the Wala reservoir were measured from January to July 2012 using a diver pressure sensor.
- In the framework of a tracer test with sodium chloride (NaCl), 42 samples were taken between 29 May and 1 June 2013 from well CD 3368, CD 3243 and CD 3475 and analyzed for chloride (Cl) using ion chromatography.
- For hazard mapping, the locations of houses, livestock grazing, and agriculture fields were mapped in 2012 and 2013 and complemented with information from digitized aerial photos (DigitalGlobe via Google Earth).

Data provided by MWI

- Data on total coliform and E. coli are available from 18 Hidan wells (2003–2012) and 2 Wala wells (2003–2012) and for Wala reservoir (2008–2009, 2011–2012). Total coliforms and E. coli were analyzed using the Multiple Tube Fermentation method (Rompré et al. 2002). The samples for total coliforms and E. coli were taken from a tap which is attached to the wellhead. The taps were sterilized by a flame before samples were taken and filled into glass bottles (250 ml) and transported into a cooling box. The sampling was conducted using sterile gloves. The analyses were started during the same day in the laboratory.
- Monthly precipitation data (rainfall collector) were available from the Sahaba, Madaba, Wadi Wala, Daba'a, Um El-Risas and Dhiban stations (1976–2002) and daily values from the Wadi Wala station (2005–2012).
- Mean monthly runoff data were available at Wadi Wala (1976–2002).
- Daily data of injection into recharge wells were available (May–June 2012).

4.3.2 Methods for assessing groundwater contamination

4.3.2.1 Correlation of rainfall and microbial occurrence

To characterize the natural vulnerability of water quality to contamination, total coliforms and E. coli were used as indicators of the impact of human wastewater and animal waste on surface water and groundwater. To assess triggering events during 2002 and 2012, their occurrence in Hidan and Wala wells were correlated to rainfall events, to artificial injection and to natural infiltration from the reservoir into the karst aquifer. Based on the sampling intervals of the available data, it cannot be excluded that additional contamination events occurred during the study, since no continuous bacterial analysis were conducted, especially during summer; thus, data from the reservoir are only available for the years 2008, 2009, 2011 and 2012.

4.3.2.2 Tracer test

To identify surface-water/groundwater interactions through the losing stream (section 'Geology and hydrogeology') along Wadi Wala (Fig. 4.3a), a tracer test was conducted at Hidan wellfield using dissolved sodium chloride (NaCl). Its easy direct detection by ion chromatography or indirect measurement in-situ via electrical conductivity measurements makes it a cost effective alternative to other artificial tracers such as fluorescent dyes. However, the occurrence of NaCl in groundwater undergoes natural fluctuations and therefore relatively large amounts are required to identify injection-induced changes in the ion concentration; therefore, the use of NaCl as a tracer is suitable only for short distances (Käss 1998; Goldscheider et al. 2008).

A dry pool in the karstified streambed north of Hidan wellfield (Fig. 4.3b), between wells CD 3368, CD 3475 and 3243, was selected as the injection point to investigate the direct vertical infiltration path from the wadi to the extraction wells. The horizontal distance to the wells is between 15 and 40 m. An amount of 300 kg NaCl was pre-dissolved in 2 m3 of water, which corresponds to a chloride concentration of about 90,000 mg/L. The pool was filled with about 90 m3 of water from well CD 3368 on 29 May 2013 and mixed with the pre-dissolved salt. This corresponds to a chloride concentration of about 2,000 mg/L. The three wells were manually sampled for chloride (Cl^-) each hour after injection and an electrical conductivity meter was used for on-site monitoring to indicate salinity increase. The normal pumping rate of the three wells (and during the testing) is between 100 and 230 m3/h.

The tracer test represents a realistic scenario of a contamination events caused by flash floods and increased wadi runoff, respectively. It simulates the filling of dry pools that are located in the wadi close to the wellfield and the following percolation of large quantities of water into the underground

(Fig. 4.3c); however, it is not representative for diffuse infiltration along the wadi course through joints and fractures, as well as not for direct rainfall infiltration at unprotected Hidan wellheads. The uncontrolled injection and the infiltration through the unsaturated zone are not ideal experimental conditions in terms of a quantitative evaluation; therefore, a conventional advection dispersion model (ADM) was applied using CXTFIT (Toride et al. 1999) to robustly estimate parameters by modeling the breakthrough curve (BTC) of the tracer.

The time of the first tracer detection and its peak, and the corresponding maximum velocity and peak velocity were directly taken from the BTC. The recovered tracer mass (only chloride is considered) was calculated from the pumping rate (Q), the measured concentrations (c) and the injection mass (M). The ADM model was used to determine mean flow velocity (v), mean transit time (t0), longitudinal dispersion (D) and longitudinal dispersivity (α). Note that the parameters obtained by the ADM are not transferable to other locations, such as to the Wala reservoir, as they represent only site-specific infiltration conditions and groundwater flow along the wadi, which is induced by pumping wells. The problem setting for the ADM was set to be a Dirac delta input.

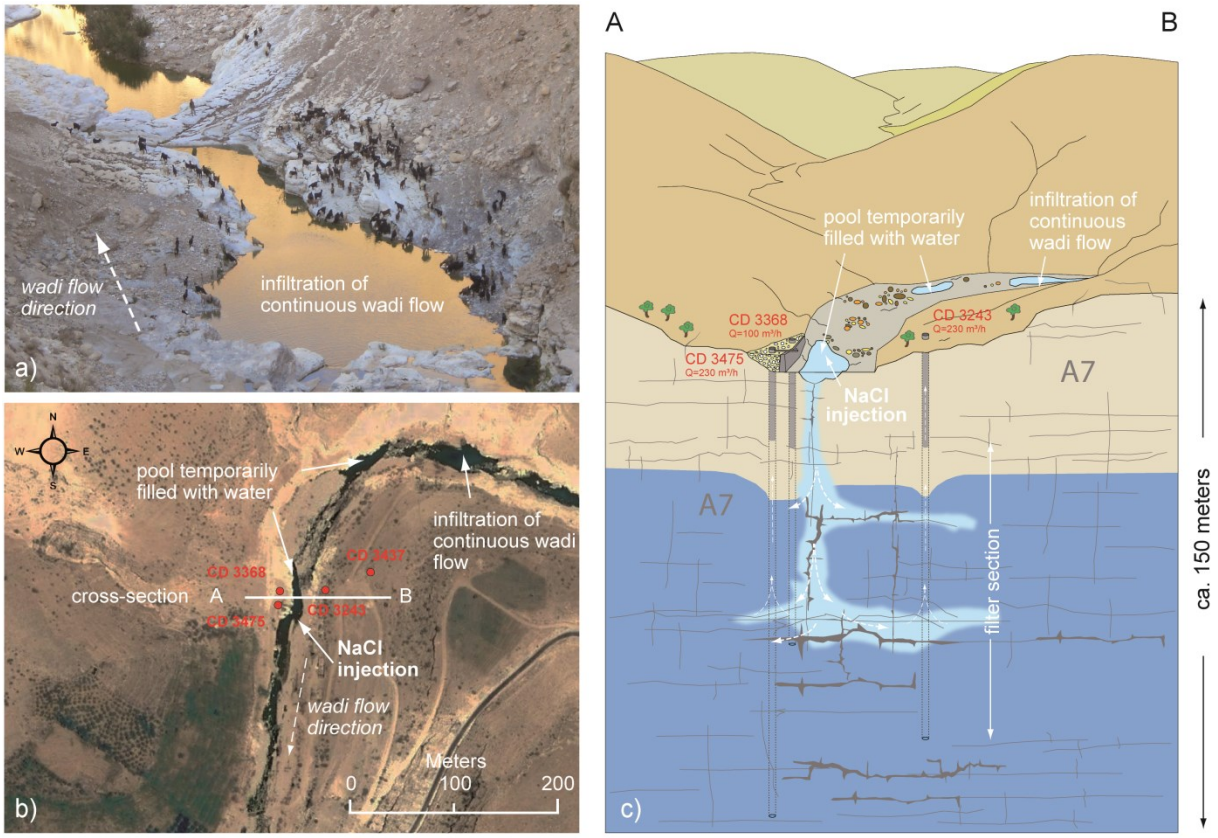

Fig. 4.3 a) Goat herd at a pool, which is continuously filled with water. b) Location of tracer injection between the abstraction wells of Hidan wellfield. The selected dry pool is only filled with water after rainfall or flood events. Pools north of the wellfield receive continuous wadi flow. c) Schematic cross section of Hidan wellfield with the selected pool between well CD 3475 and CD 3243 and the assumed infiltration path of the NaCl solution.

4.3.2.3 Vulnerability and risk assessment

To assess groundwater vulnerability at Hidan wellfield and to identify areas that facilitate the mobilization of contaminants (e.g. coliform bacteria) after rainfall events, a simplified intrinsic vulnerability mapping method based on the COST action 620 approach (Zwahlen 2004) was adapted to the hydrogeological characteristics of the study area. More detailed explanations are given by Nguyet and Goldscheider (2006). The adaptions are shown in Fig. S1 of the electronic supplementary material (ESM). Based on these results, an improved protection zone concept was compiled for Hidan wellfield and Wala reservoir integrating aspects of the existing protection concepts for Hidan wellfield (Gassen et al. 2013) and Wala reservoir (Margane et al. 2009) as well as the general guidelines of Jordan (MWI 2004; Margane et al. 2010) for surface water and groundwater. Furthermore, land use data were gathered to compile a hazard map of the Hidan wellfield catchment and to assess the contamination risk by overlaying this map on the vulnerability map.

The groundwater vulnerability mapping method is based on two principal factors, the overlying layers (O factor) and concentration of flow (C factor), which characterize the allogenic and autogenic recharge processes in karstic environments. The layers of the unsaturated zone and their protection against direct water infiltration and percolation (autogenic recharge) are described by the O factor. The C factor describes the concentration of flow and considers allogenic recharge processes, where non-karstic areas drain towards the karst.

To account for the special influence of the MAR site and its function as a physical barrier for surface runoff, an additional zone factor was included. Here, an inner zone (IZ) addresses direct impact of surface runoff to the Hidan wellfield and an outer zone (OZ) addresses runoff towards the Wala reservoir. The OZ downgrades the vulnerability of Wala catchment by one order (e.g. from moderate to low) as there is no direct surface runoff to the wellfield (see SF1). Similar considerations of different zones addressing direct and indirect drainage to the source (e.g. wells) are described by Andreo et al. (2009) and DoELG/EPA/GSI (1999).

To suit the local hydrogeological characteristics (e.g. extensive plateaus, deeply incised wadis), the method was adapted to the semi-arid Jordan region; hence, short but strong rainfall events are expected to generate higher runoff on carbonate formations, especially along the steep slopes of the deeply carved wadis, than is assumed by the original Nguyet and Goldscheider (2006) model. Conversely, less runoff is expected from the extensive plateaus when formations of intermediate infiltration are present. Consequently, adaptions in the matrix system for the O factor and the vulnerability are made and presented in Fig. S1 of the ESM. Adjustments to the risk assessment were made since hazards of high potential (e.g. urban areas, livestock and houses) and moderate potential (agriculture) might be

classified to be of high risk even when they are located on the plateau, far away from the wellfield. Thus, they are only of extreme and high risk when they are located in areas of extreme or high vulnerability (e.g. along the wadi); otherwise (e.g. at the plateau), they are downgraded by one order. This is necessary since the resource vulnerability character does not consider the distance to the wellfield.

4.4 Results

4.4.1 Correlation of rainfall and microbial occurrence

Rainfall in the study area mainly occurs between October and May with peak values in January and February (Fig. 4.4a) of varying intensities, whereas the maximum values of mean monthly runoff are found in December (Fig. 4.4b). With the construction of the Wala Dam, surface runoff generation changed and runoff towards Wala reservoir is only generated by rainfall upstream of it, whereas wadi flow towards Hidan wellfield can be influenced by:

- Rainfall in the catchment downstream the reservoir
- Spilling of the reservoir
- Groundwater seepage along Wadi Wala (downstream Wala reservoir), which increases during high reservoir infiltration and/or injection into recharge wells

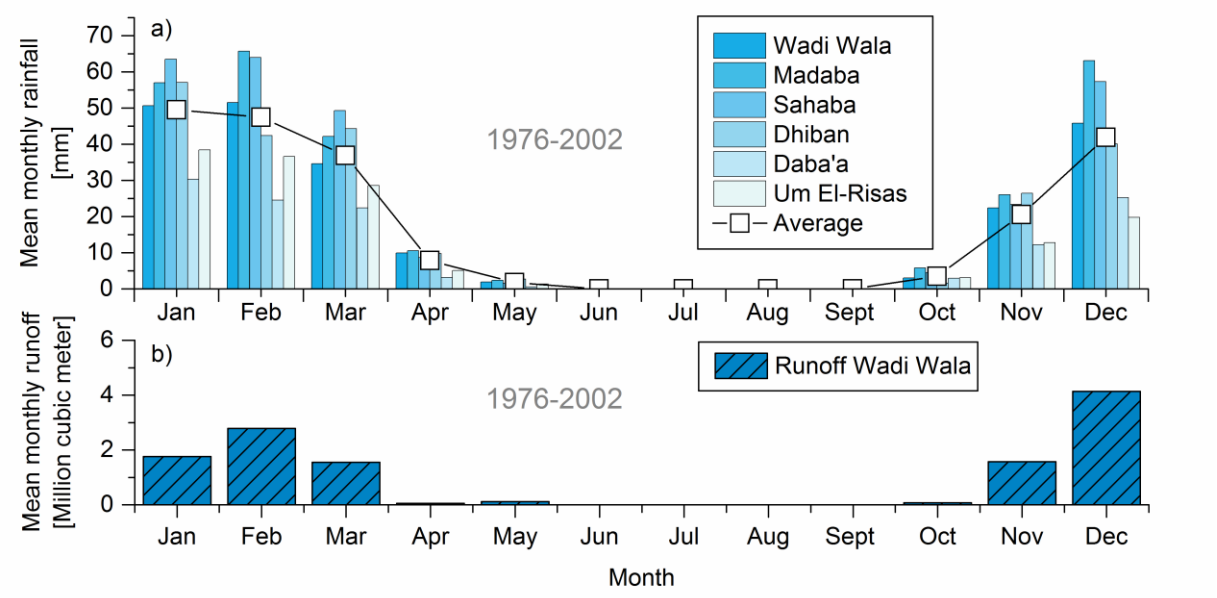

Fig. 4.4 a) Mean monthly rainfall at different stations within the Wala catchment (Fig. 1b) and b) the resulting mean monthly surface runoff of Wadi Wala.

The wadi runoff, caused by seepage as well as direct infiltration of rainfall and recharge from the reservoir, is assumed to cause groundwater contamination at Hidan wellfield. Rainfall is assumed to

flush contaminants directly from the surface into Hidan and Wala wells that are in bad conditions (Fig. 4.1c). Moreover, runoff generated by rainfall or seepage infiltrates along the wadi both diffuse through fractures and distinctly through pools. Furthermore, reservoir infiltration and injection into the recharge wells may transport contaminants through groundwater flow towards the Hidan wellfield.

In 2003, 2004 and 2005 coliform bacteria in groundwater were sampled monthly and indicated a constant contamination almost during the entire year. This can be explained as a result of high infiltration rates from the reservoir (when sedimentation in the reservoir was still low) and thus a direct contamination through groundwater flow. Though bacteriological contamination in the reservoir was not documented before 2008, it is most likely as documented in 2008/2009 and 2011/2012 (Fig. 4.5b); however, it is assumed that this contamination path gets less dominant with increasing sedimentation in the reservoir. This assumption is confirmed by the fact that in the years of low recharge (e.g. 2011 and 2012), background load cannot be clearly derived from the data.

A second contamination path is increased runoff in the wadi, either caused by rainfall or by seepage into the wadi, which infiltrates through the numerous pools close to the wellfield or directly at the wellheads as described in the preceding. Therefore, an ongoing contamination of groundwater with coliform bacteria was assumed for the years 2006, 2007, and 2009 to 2012, with an increasing influence of contamination by runoff events, which is also confirmed by several sampling campaigns, despite irregular sampling. In 2008, the reservoir dried out and no trigger event occurred.

Additionally to the background load by reservoir infiltration and occasional seepage, values of total coliform and E. coli in Hidan and Wala wells often showed a clear increase coincidental with rainfall events in the Wadi Wala area (Fig. 4.5a). The coliform peak after rainfall events usually appears at a time lag of less than 24 h (Fig. 4.5c), but may be much shorter since sampling was not always conducted directly after the rain started. The short time lag indicates an infiltration near the wells, which is plausible since many pools are located in the wadi close to the Hidan wells; however, not all rainfall events trigger a bacteria occurrence since runoff generation depends also on the rainfall intensity. The contamination in January, February and March 2012 (Fig. 4.5b) showed a decrease of E. coli concentration in groundwater within about 2 weeks following rainfall events (Fig. 4.5c). Here, the Hidan wells show much higher concentrations (>1,000 MPN/100 ml; MPN = most probable number) than Wala wells (<1,000 MPN/100 ml), indicating a distinct hydraulic connection to the surface for the wellfield. In fact, Wala wells are away from the wadi course (>100 m) and appear not to be well connected to the karstified wadi zone.

Contamination in April, May and June 2012 could not be related to rainfall or other events but it cannot be ruled out that rainfall events were not documented, since the data curve shows similar

behavior like previous rainfall events. The contamination event in April 2012 can be caused by reservoir infiltration in March since the E. coli load in the reservoir is in the same range (Fig. 4.5d). In May 2012, bacteriological pollution in the wellfield appeared to be coincident with water injection from Wala reservoir into the recharge wells. Here, the injection may have caused increased groundwater seepage into the wadi. Additional contaminants are mobilized by the increased wadi runoff, which is then infiltrating again close before the wellfield, which is assumed since the lag time is very short and the E. coli load in the reservoir is lower at this time.

The overall results of the coliforms samples indicate that total coliform and E. coli occurrence in groundwater can be related to both direct infiltration at the Hidan abstraction wells or close to them, and to infiltration from the reservoir and the recharge wells, respectively. However, infiltration from the reservoir is assumed to cause a constant load with total coliforms at the wellfield during high infiltration rates, but since water is treated with chlorine this may not have a negative impact as long as no turbidity is associated. The latter is the case when increased runoff (caused by rainfall, seepage or reservoir spilling) causes direct infiltration through pools and diffuse infiltration along the wadi.

Even though turbidity sampling has not been carried out, a constant high turbidity during the year is ruled out, since wells are then usually switched off. Precipitation (and associated runoff) and spilling events represent the main problem since they are assumed to be associated with turbidity occurrence. With daily abstraction rates of about 0.03 MCM, this results in a loss of about 0.42 MCM within 2 weeks, as the duration of contamination showed in 2011 and 2012 (Fig. 4.5b,c). In the case of several precipitation events per year, this adds up to a considerable sum that is missing from the drinking water supply; however, the avoidance of such runoff events is difficult since there are multiple infiltration pathways along the wadi. To drill deeper injection wells or relocate them further downstream the reservoir is not an option since the total aquifer depth is already reached. Optimized injection management would help to avoid groundwater seepage, whereas the removal of sediments from the reservoir to restore its storage capacity would help to reduce the risk of overflow.

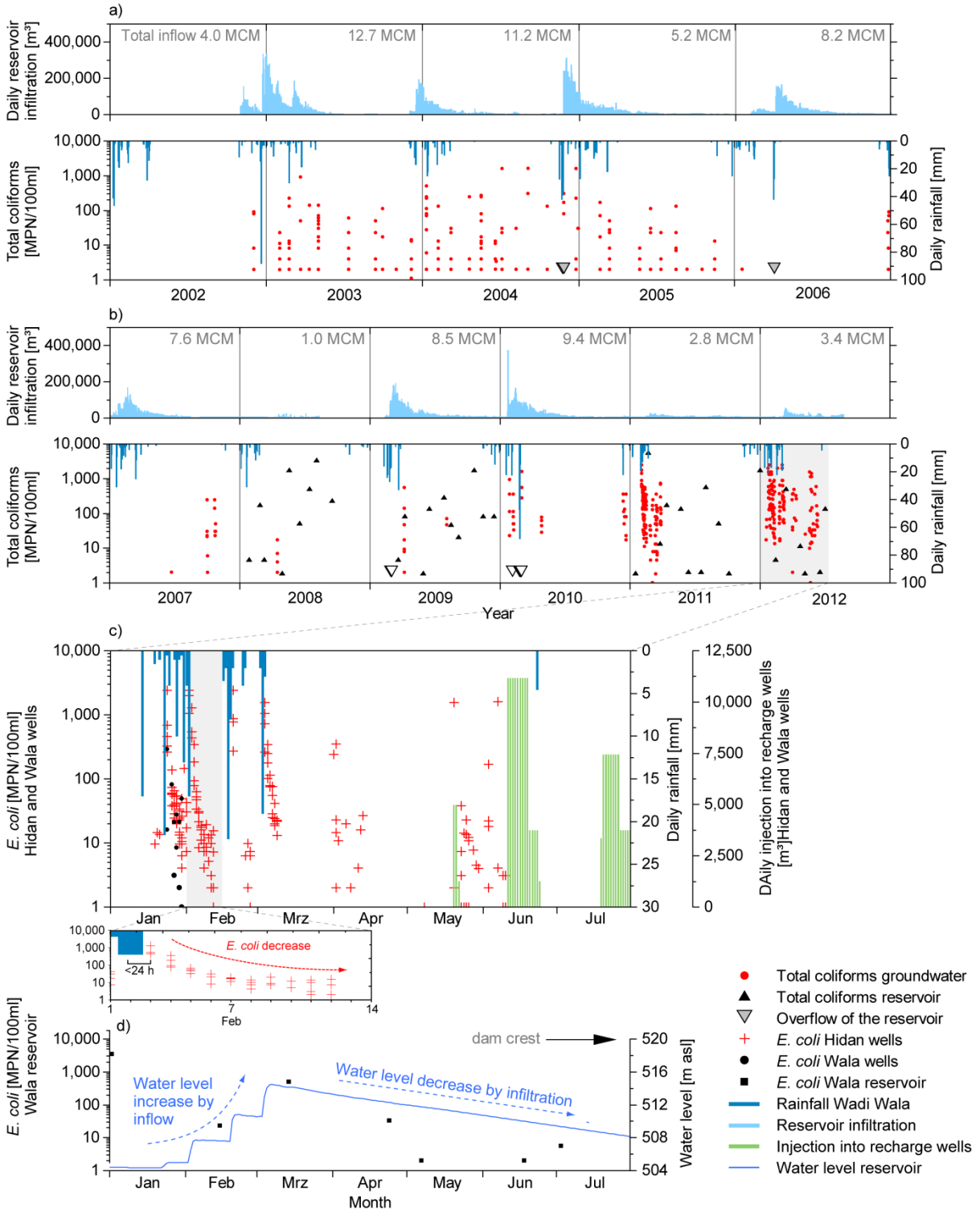

Fig. 4.5 Comparison of daily reservoir infiltration, rainfall and total coliforms at Wala and Hidan wells a) from 2002 to 2006 and b) from 2007 to 2012. C) Comparison of E. coli with rainfall and injection into recharge wells from January to July 2012 and with rainfall and E. coli in February 2012. The lag time between rainfall and E. coli is less than 24 h. d) Water level of Wala reservoir and E. coli occurrence in the reservoir from January to July 2012.

4.4.2 Tracer test

The water used for the wadi runoff simulation was completely infiltrated after around 7 h and a first arrival of the tracer in well CD 3243 (east of the injection pool) was observed after 1.0 h (1.1 mg/L), whereas a more distinct increase of about 5.8 mg/L was detected after 2.8 h. The tracer peak, with an increase of around 19.3 mg/L, was reached after 8.9 h (Fig. 4.6). Flow velocities derived from the BTC show a maximum of 14.3 m/h and a peak velocity of 4.5 m/h (Table 1). The recovery of the tracer of about 65.2% corresponds to about 117.3 kg of chloride, while the remaining part might be transported by groundwater flow to the west or has followed other discrete conduits or fractures that are not connected to the wells. A significant influence on the flow path, on the maximum or mean flow velocity due to density effects of the tracer solution is not expected, as the maximum peak with a chloride increase of 19 mg/L shows a strong mixing. A comparable salt tracer study conducted by Robert et al. (2012) in a fractured limestone aquifer in Belgium over a similar distance, but with much higher input concentrations (38 and 154 mg/L), did not show any density-driven sinking effects using electrical resistivity tomography (ERT). Dilution effects were of greater importance due to the high horizontal flow rates. Even in the present study, the advective and dispersive transport processes have a much stronger impact since horizontal groundwater flow velocity is reinforced by the pumping wells. Predominant processes could not be detected since the Peclet number (ratio of advective transport to dispersion) was calculated to be 2.4.

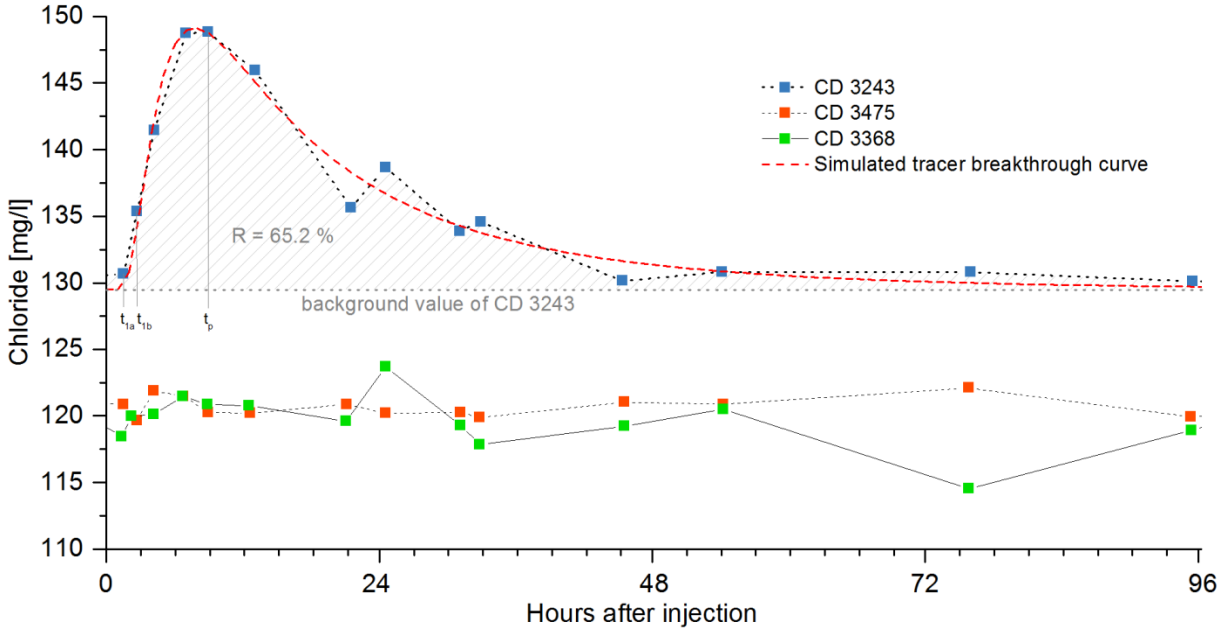

Fig. 4.6 Chloride concentrations during the tracer test in well CD 3243, CD 3475 and CD 3368 of Hidan wellfield. A distinct tracer breakthrough was detected after around 2.8 h and the maximum peak after around 8.6 h.

Since the mechanical dispersion, as a result of the dual porosity character of karst aquifers, increases with the distance between the tracer input and recovery point, it is not assumed that this impacts the tracer results on the short horizontal distance to the well of about 40 m. The ADM provides a fitted curve with a correlation coefficient of 0.96. Mean flow velocity and transit time were estimated to be 1.8 m/h and 22.6 h respectively, with a longitudinal dispersion of 30.5 m2/h and longitudinal dispersivity of 16.9 m. Both values are in a plausible range for karst aquifers since they are usually higher than in porous aquifers (Käss 2004). A summary of the results is presented in Table 1.

Table 4.1 Results from the NaCl tracer test.

Phase	Property	Symbol	Unit	Value
Basic data	Injection quantity	M	kg	180
	pumping rate	Q	L/s	69
	Distance to injection point	L	m	40
	Time of first detection	$t_{1a/b}$	h	1.0 to 2.8
	Peak time	t_p	h	8.9
	Maximum velocity	v_{max}	m/h	40.0 to 14.3
	Peak velocity	v_p	m/h	4.5
	Recovery	R	%	65.2
ADM	Mean flow velocity	v	m/h	1.8
	Mean transit time	t_0	h	22.6
	Longitudinal dispersion	D	m^2/h	30.0
	Longitudinal dispersivity	α	m	16.9
	Coefficient of determination	R^2	-	0.96

The results demonstrate the direct connection to well CD 3243, whereas the other two wells were not affected. Given the expected highly anisotropic and inhomogeneous characteristics of the karst aquifer, this is not unusual. The fast reaction (within several hours) confirms the hypothesis from the results of the total coliform and E. coli analysis of a fast connection of surface water and groundwater through infiltration pools and underlying conduits and confirms the high vulnerability of the A7 aquifer along the wadi. Similar conditions for other pools within the wellfield are expected. Here, the sealing of pools that are known to promote fast infiltration of large amounts of surface runoff may help to diminish contamination events.

4.4.3 Vulnerability and risk assessment

4.4.3.1 Groundwater vulnerability

A highly protective function was attributed to the Quaternary deposits, the Ghudran and Muwaqqar formations, and the Wadi Shallala formation. Although these formations are connected to the regional aquifer systems, the Muwaqqar and Ghudran formations are considered as aquitards, and the Shallala formation as a semi-permeable aquifer. Moderate protection was ascribed to the Amman and Al Hisa formation, and low protection to the Wadi As Sir formation, which constitutes the main karstic aquifer system and was identified by the tracer test to promote fast infiltration. Results for the O-factor and C-factor are presented in the supplementary material SF2 (ESM).

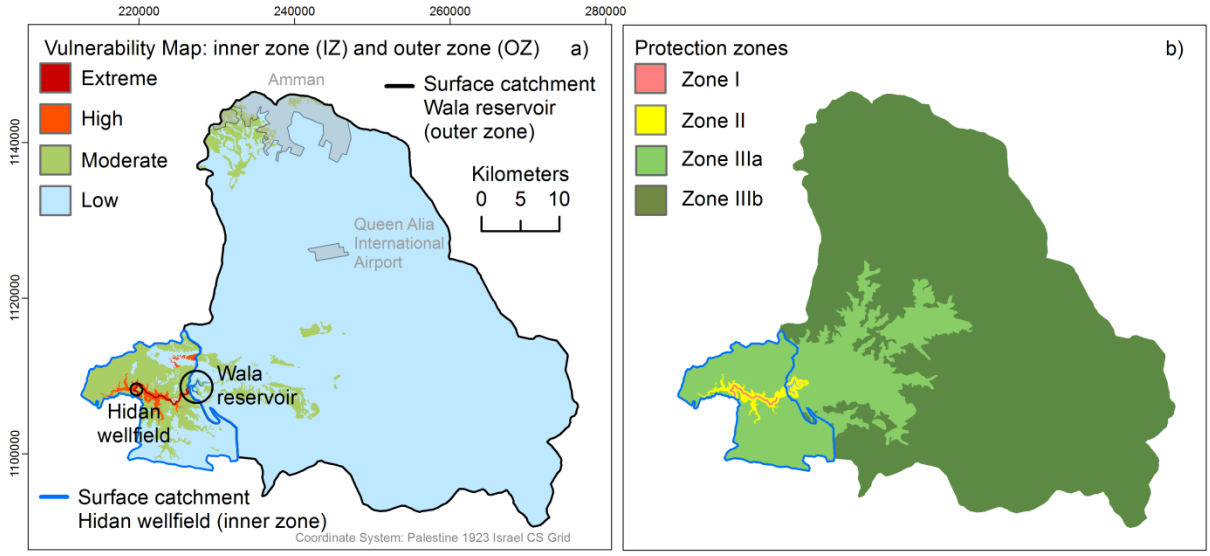

Fig. 4.7 a) Resulting vulnerability map from the combination of the O and C map and b) the derived protection zones (see also Fig. 4.8c).

Including the OZ factor, almost 96% of the Wala catchment reveals low and about 4% moderate vulnerability, mainly in the northern and central parts of the catchment. In the Hidan catchment, vulnerability is low in 42%, moderate in 50%, high in 6% and extreme in 2% of the area. High and extreme values can coincident with the outcrops of Wadi As Sir limestone along the wadi (Fig. 4.7a).

The vulnerability map was directly transformed, with small adjustments, into a protection zone map for the wellfield. Thus, protection Zone I was directly derived from Zone 1 of the C factor and follows Wadi Wala with its 100 m buffer on each side, and a 50 m buffer around each extraction well. It extends from the southern border of the wellfield to recharge well 6 from which groundwater seepage generates surface runoff during most of the year. The relatively long extent of Zone I was chosen since water in the wadi is in direct contact with hazardous activities (housing, agriculture and farming) and consequently reaches the wellfield quickly. The outer border of protection Zone II was delineated

according the top of the Ghudran formation (Figs. 4.7d and 4.8e) with a minimum distance to the wadi of 350 m, as proposed by MWI (2006). This covers the steep slopes along Wadi Wala, where rainfall does not infiltrate and generates fast runoff. Protection Zone IIIa comprises the rest of Hidan wellfield catchment (Fig. 4.7b).

For the reservoir catchment, protection zone II corresponds to the highest water level of the reservoir plus a buffer zone of 350 m, zone IIIa reaches up to 700 m asl topographic contour, and zone IIIb covers the rest of the Wala catchment. These proposed protection zones represent a refinement of those from previous studies by Margane et al. (2009), and Gassen et al. (2013).

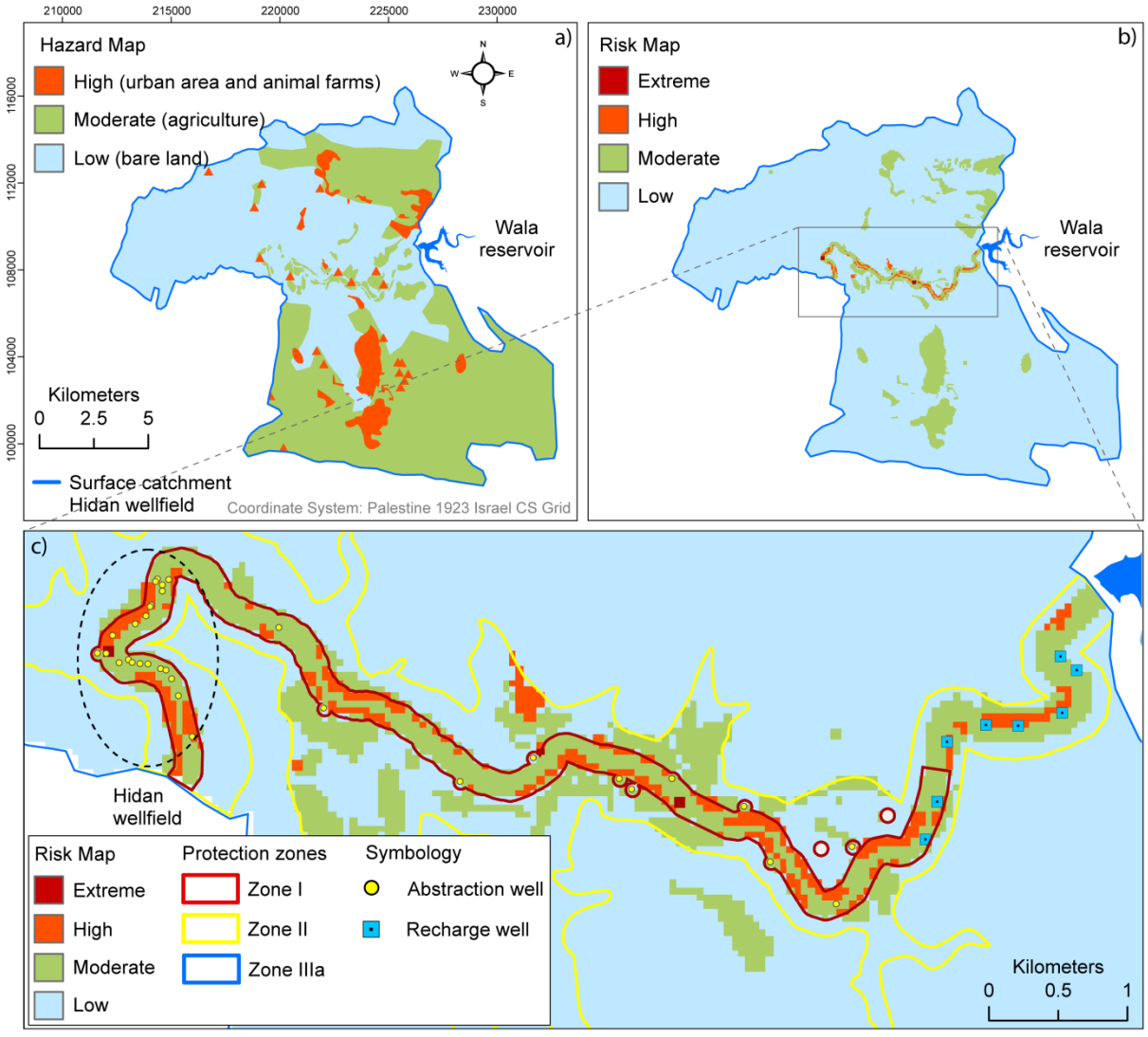

Fig. 4.8 a) Hazard map based on land use, b the resulting risk map and c proposed protection zones I and II and the risk areas.

4.4.3.2 Assessment of contamination risk

Land use and hazards

Large areas of the Wala and Hidan catchment serve as open rangeland or bare land (47%) or are used for rain-fed cultivation of cereals (38%)—mainly wheat and barley. Only small areas are irrigated (3%). Populated areas (7% see Al-Bakri and Al-Jahmany 2013) are distributed over the catchment as small settlements and villages or individual or groupings of houses. Additionally, livestock farming is practiced, including free-range grazing of goats and sheep (SF3b). Both livestock farming and human housing are classified as high hazard, whereas moderate values are assigned to cultivation activities. Low hazard is assigned to open rangeland and bare land (Fig. 4.8a).

Contamination risk

In this study, only Hidan wellfield catchment was considered for the risk map since it has high vulnerability, with the major contributors to contamination are located nearby. It can be concluded that especially the agriculture, housing areas and livestock farms represent moderate to high risk for Hidan wellfield when they are located close to Wadi Wala (Fig. 4.8b) and, hence, within protection zones I and II (Fig. 4.8c).

Beside the aforementioned technical measures (sections ‘Correlation of rainfall and microbial occurrence’ and ‘Vulnerability and risk assessment’) to avoid or at least to diminish infiltration at the wellfield, the replacing of the potential hazards (e.g. livestock farming) from protection zone I to zone II, or zone III, is unavoidable. However, to not neglect the traditional habits and needs of the local people, the installation of alternative watering places in zone II for sheep and goat herds would be an alternative to a complete prohibition of livestock farming. A restricted use of fertilizer in zone II during the winter months could also be an adapted measure.

4.5 Conclusions

The present study proposes a combined protection approach for large-scale managed aquifer recharge into a karst groundwater system at the Wala reservoir, Jordan. The characteristic vulnerability of the surface water and groundwater interaction at the reservoir and the downstream Hidan wellfield were addressed by monitoring rainfall events, recharge from the reservoir, and the potential for, and variability of, contamination as characterized using coliform bacteria and a tracer test. Furthermore, a vulnerability and risk assessment served as the basis for a protection zone concept for Wala reservoir and Hidan wellfield.

Infiltration from the reservoir, groundwater seepage (produced by managed aquifer recharge), rainfall and natural flash floods were identified as trigger events for groundwater contamination. The principal contamination pathway to the wellfield is through groundwater flow and karstic conduits fed by infiltration through surface pools. Here, high reservoir infiltration is assumed to cause background contamination in groundwater with total coliforms but is assumed to be less critical since water is chlorinated before being distributed for drinking water supply. However, diffuse rainfall and local runoff infiltration along the wadi is known to also cause turbidity which makes groundwater unusable for drinking; therefore, it is recommended that injection of reservoir water into recharge wells has to be carefully managed in order to avoid groundwater seepage and activation of these coupled surface-water/groundwater pathways. At a minimum, the possibility of sealing certain infiltration pools up-gradient of the wellfield should be considered, despite the technical challenges. This will not prevent contamination but at least it will diminish the extent of pollution and reduce treatment costs. Overflow of the dam could be reduced by the removal of sediments from the reservoir to restore its capacity. Relocation of the recharges wells, or drilling them deeper, is not recommended since the total aquifer depth is already reached and the water table is generally high along the wadi course. A high priority should be also given to the physical maintenance of the wells and to improved wellhead protection. The delineation of the proposed protection zones is strongly recommended, as it entails the removal of hazards within protection zone I. Also important are the prohibition of livestock farming and controlled use of fertilizers in zone II or at least a relocation of livestock farming and the implementation of alternative watering places for sheep and goat herds downstream the abstraction wellfield or to selected sites within zone II. While critical for study area, the methodology described in the preceding is also transferable to other managed aquifer recharge sites in karstic and semi-arid environments.

Acknowledgement

The authors thank the Ministry of Water and Irrigation of Jordan (MWI) for the provision of the data, the Jordan Valley Authority (JVA) and the Water Authority of Jordan (WAJ) for their support during field work. Furthermore, the German Federal Ministry of Education and Research (BMBF) is acknowledged for funding the SMART Project (Sustainable Management of Available Water Resources with Innovative Technologies) (FKZ 02WM1079-1086 and FKZ02WM1211-1212). The authors also thank the Federal Institute for Geosciences and Natural Resources (BGR) for a successful cooperation in Jordan. Special thanks go to Prof. Tim Bechtel for language editing.

Chapter 5

Synthesis

5.1 Conclusion

The Wala reservoir represents a successful example of managed aquifer recharge (MAR) into karst and demonstrates the promising potential that comes along with this technique regarding karst groundwater management in semi-arid regions. At the study site, flood water is captured and recharged into the karst aquifer helping to cover the increased water demand in summer by providing additional water to the downstream Hidan wellfield. However, MAR into karst poses a particular challenge due to the distinct hydraulic characteristics of the underground and therefore requires adapted methods for a comprehensive hydrogeological evaluation, a sustainable management and the protection of the MAR site. This study investigated the hydrogeological setting at the Wala reservoir and developed a numerical model to assess the impact of climate change and of decreasing infiltration from the reservoir as a result of progressing sedimentation on the long-term groundwater level trend. Furthermore, a combined protection concept was developed to address the surface water and groundwater interaction at the reservoir and the wellfield.

The hydrogeological characterization of the study site (chapter 2) demonstrates the importance of a combined investigation using hydrochemical, isotopic and hydraulic data to gain a comprehensive understanding of the prevailing hydraulic conditions and function of the MAR site. The semi-arid characteristic landscape of the catchment with a dry soil and sparse vegatation led to high sedimentation rates in the reservoir and progressively decreasing infiltration rates and storage capacity. Therefore, the removal of sediments and technical measures to reduce the sedimentation rate (e.g. check dams upstream the reservoir) are strongly recommended. The drilling of additional abstraction wells at the wellfield, along the wadi or upstream the reservoir is not recommended since this will directly affect the wellfield by groundwater level drop. Furthermore, temporal changes in the groundwater salinity are not expected to exceed the fluctuations observed between 2002 and 2012 of about 200 µS/cm since they are assumed to be a result of reservoir infiltration and an associated mobilization of fine material in the aquifer and dissolution of easily soluble salts. Hence, it will not negatively affect groundwater quality in terms of its use for drinking. However, a long-term increase in the average groundwater salinity, as it was observed since the 1980s, is not excluded since the cause cannot be determined precisely, but is assumed to be related to a progressing groundwater overexploitation and the impact of wastewater in the entire catchment.

The presented numerical simulation of the aquifer section between the Wala reservoir and the Hidan wellfield (chapter 3) emphasizes and confirms the importance of numerical models for groundwater management, although the implementation in karst settings is challenging. The successful application of an equivalent porous medium (EPM) approach is demonstrated with specific adaptations to the heterogeneity and anisotropy of the karst aquifer, which allows an identification of the relevant hydraulic characteristics and the major reasons for strong groundwater level fluctuations. Results show that an adequate match of simulated and measured hydraulic head is realizable when the multifaceted 3-dimensional aquifer setup is projected onto a 2-dimensional vertical profile and when the karst characteristic duality in discharge pattern is considered by subdividing the profile into hydraulic zones of preferential flow. Furthermore, the calibration process can be simplified when the two hydraulic processes, recharge from the reservoir and abstraction from the wellfield, are simulated separately with two models. The simplified model structure using an EPM approach can be used as the basis for a later extension to a 3-dimensional model. The results confirmed the recommendations from chapter 2 to reduce the sedimentation rates in the reservoir otherwise a long-term decrease of the groundwater level is unavoidable. Furthermore, the computed scenarios suggest to not increase mean annual abstraction rates of 11.7 MCM and to avoid pumping from the shallow aquifer part to prevent a significant long-term depletion in the groundwater levels. Since most of the reservoir water is infiltrating naturally by gravitation, especially in winter, artificial injection through the recharge wells is recommended to be conducted during May and October. An important remark is that 2-dimensional vertical models are limited in the simulation of pumping wells, and therefore quantitative statements about the magnitude of groundwater level fluctuations must be evaluated carefully.

Managed recharge of storm water into karst aquifers requires adapted protection approaches, since it represents a strong intervention into natural runoff and groundwater flow processes. The presented study in chapter 4 proposes a combined protection approach which addresses the site characteristic vulnerability as a result of the surface water and groundwater interaction and the separation of the surface catchment by the Wala reservoir. A comprehensive hydrogeological evaluation and the identification of trigger events for groundwater contamination as well as their major impact pathways is fundamental for a site specific vulnerability and contamination risk assessment. It is shown that the occurrence of coliform bacteria is a valuable indicator for groundwater contamination, and their major impact pathways can be proved by tracer tests. It is recommended to enforce the protection zones and their restrictions on land use and settling in order to avoid or at least reduce further contamination. This includes a proper rehabilitation of the wells and protection zone I.

A general proposal is made for the improvement of the management related to a fine-tuning at the decision-making level addressing the operational business of the reservoir and the wellfield since this

is organized with different authorities. Hence, the Jordan Valley Authority (JVA) is responsible for the operation and maintenance of the reservoir and the injection wells, but the water supply from the wellfield and its quality is managed by the Water Authority Jordan (WAJ) and the Ministry of Water and Irrigation (MWI). Here it is recommended to find a solution to leave the supervision of the reservoir and the wellfield with one entity to ensure a consistent data gathering and coordinated operation of the MAR site.

The investigations presented in chapter 2-4 provide a step-by-step approach towards an improved and sustainable management of managed aquifer recharge into karst using hydrogeological and hydrochemical data (Chapter 2), a numerical evaluation (chapter 3) and a vulnerability- and risk assessment (chapter 4). The presented methods and tools shows the importance of combined investigations using different approaches and are transferable to other managed aquifer recharge sites or can be consulted for planned projects in karstic environments of semi-arid regions.

5.2 Perspective and Outlook

In addition to the local specific challenges that are discussed in this thesis and concluded in chapter 5.1, also further research questions are raised that address the transferability of the findings to other test sites in the region or beyond. Thus, future research in Jordan could focus on the identification of additional locations in karstic environment that are suitable for MAR and to quantify the potential of this technique to increase groundwater availability. Here, additional studies may emphasis on an initial step on the selection criteria on regional and catchment scale before investigating the local specific hydrogeological setting. Hence, suitable topographical structures that promote runoff generation and its capturing, the estimation of mean annual rainfall and related flow accumulation, the thickness of the unsaturated zone and the resulting storage capacity are essential to be determined. The approach for the selection of potential MAR sites on catchment scale can be also applied to the Wala reservoir catchment, which then can be used to verify the method. The results would be a sound basis on which decision-makers could promote more detailed studies.

In a second step, potential MAR sites need to be assessed in terms of the infiltration and recovery conditions on a local- and intermediate scale despite this is more challenging. The distance between point of recharge and abstraction must be sufficient to avoid direct contamination at the recovery point (e.g. a well or spring), but close enough to allow an adequate storage time to use the water within the same year, e.g. to cover the increased demand during summer. Here, the application of tracers is highly recommended to identify groundwater flow path and time. Furthermore, structural geological conditions must be identified since they can favor the application of MAR or make it obsolete. Additionally, the feasibility of complementing existing surface reservoirs in karst environments with

injection- and abstraction wells can be studied. Furthermore, the sediment transport into reservoirs has to be considered to avoid the reduction of the storage capacity and infiltration rates. In addition, the risk of groundwater contamination represents an important task and must be examined too.

The identification criteria for MAR on regional and catchment level can also be extended to karstic environments that are located in other semi-arid or arid regions, such as to large parts of the Middle East and North Africa, but also to the dry sub-humid and humid regions along the northern Mediterranean coast (Fig. 5.1). Studies are required to evaluate the availability of surface runoff at karstic environments and to quantify their potential for MAR on the basis of the same selection criteria as stated above. The possible benefit of MAR on regional or local water supply and on economical or environmental aspects is of further interest. This depends on the purpose of MAR in the different regions since the intentions can be of different nature, such as to improve groundwater availability, to avoid seawater intrusion in coastal regions, to maintain or restore the ecological balance of groundwater-dependent ecosystems or to reduce the risk of flood damages.

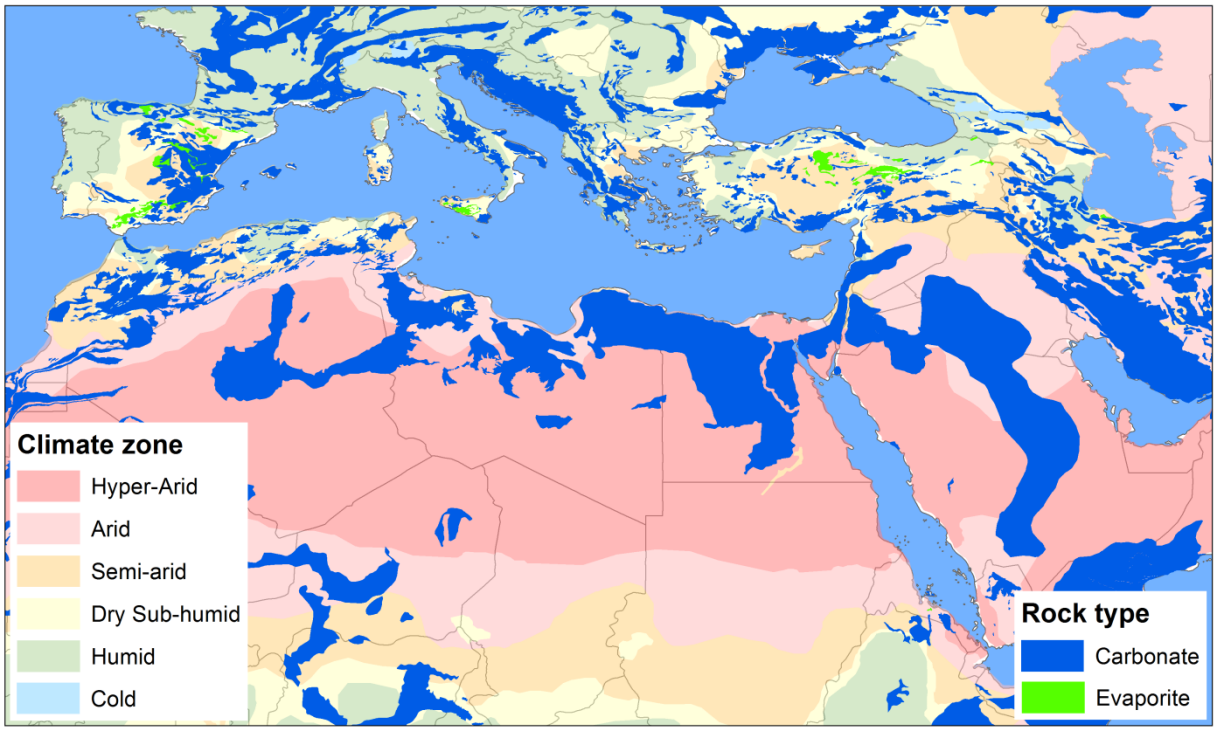

Fig. 5.1 Humidity index of semi-arid, arid and hyper arid zones of the Mediterranean region and Middle East in relation to outcrops of carbonate rocks (carbonate map by Chen et al. (2017); humidity data from University of Auckland, New Zealand: http://web.env.auckland.ac.nz/our_research/karst/; humidity data from UNEP (2016)).

Overall, MAR using flood water bears a great potential to augment and sustain groundwater availability and thus assure the vital drinking water supply in semi-arid and arid regions. The example of the Wala reservoir shows that it can be also applied in karstic environments, though it must be implemented and managed carefully.

Acknowledgement

My sincere thanks go out to Nico Goldscheider who gave me the opportunity to gain considerable experience in the frame of my PhD thesis and to be part of the SMART project team. It was possible at any time to count on his advice and support and learn from his experience and knowledge.

Furthermore, special thanks go to Tanja Liesch for her the scientific support and help during the past years.

Many thanks go to Hervé Jourde and Michel Bakalowicz for their warm welcome in Montpellier and their great support and advices during the 3-month stay at the Laoboratoire Hydroscience of the Montpellier University. Both brought my work a big step further and I am pleased to have Hervé Jourde as the second examiner of my PhD thesis.

Jochen Klinger is acknowledged for the coordination of the SMART Project and his tireless efforts for the smooth running of the project, which provided the basis for a successful work. The fieldwork in Jordan was facilitated and supported in a variety of ways by many people: Ali Sawarieh, Ali Subah, Khair Hadidi, Nayef Seder, Hesham Al-Hesa, Niklas Gassen.

Many thanks go to Heinz Hötzl, there is hardly anyone who knows the Jordan region better than him and it was always a pleasure to discuss with him. A very special thank goes to Wasim Ali, who brought me closer to the culture and the people in Jordan, Palestine and Israel. Thanks for letting me benefit from your contacts and experience.

Many thanks go to Nadine Göppert for her help and advice during the past years.

I am very grateful to Paulina Alfaro, Felix Grimmeisen and Moritz Zemann for sharing the stressful and funny moments in the office and during fieldwork in Jordan.

Thanks to Zhao Chen and Simon Frank for all the discussions during lunch break.

Special thanks go to Daniela Blank, Chris Buschhaus and Christine Roske-Stegemann for their support in the laboratory and Petra Linder for her administrative support at the Institute.

Marian and Tim Bechtel are acknowledged for language editing of chapter three and four.

Thanks go to Klaus Schäfer for the language check of chapter one and five.

The German Federal Ministry of Education and Research (BMBF) are acknowledged for funding the SMART Project (FKZ 02WM1079-1086 and FKZ02WM1211-1212).

Finally, I thank my family, especially my Mother, for their support during all time, my girlfriend Bianca for motivating me and cover my back in the past years.

Declaration of Authorship

Study 1

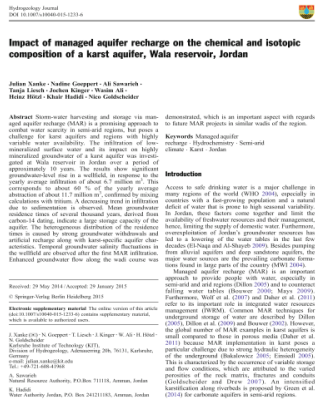

Impact of managed aquifer recharge on the chemical and isotopic composition of a karst aquifer, Wala reservoir, Jordan

Citation: Xanke J, Goeppert N, Sawarieh A, Liesch T, Kinger J, Ali W, Hötzl H, Hadidi K, Goldscheider N (2015) Impact of managed aquifer recharge on the chemical and isotopic composition of a karst aquifer, Wala reservoir, Jordan. In: Hydrogeology Journal 23 (5), S. 1027–1040. 1–14. http://dx.doi.org/10.1007/s10040-015-1233-6.

Declaration of authorship: Julian Xanke (JX) evaluated the data in consultation with Nadine Goeppert, Ali Sawarieh, Tanja Liesch, Jochen Klinger, Wasim Ali, Heinz Hötzl and Nico Goldscheider. JX wrote the manuscript, which was reviewed by all authors.

Study 2

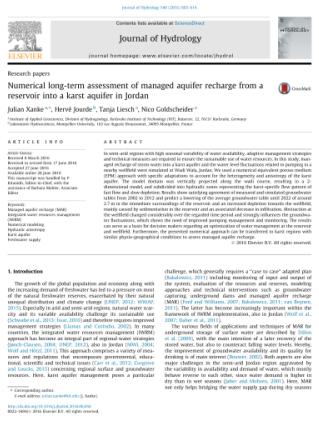

Journal of Hydrology

Numerical long-term assessment of managed aquifer recharge from a reservoir into a karst aquifer in Jordan

Citation: Xanke J, Jourde H, Liesch T, Goldscheider N (2016) Numerical long-term assessment of managed aquifer recharge from a reservoir into a karst aquifer in Jordan. Journal of Hydrology, 540, 603-614. http://dx.doi.org/10.1016/j.jhydrol.2016.06.058.

Declaration of authorship: Julian Xanke (JX) developed the numerical model in consultation with Hervé Jourde, Tanja Liesch and Nico Goldscheider. JX wrote the manuscript. The final manuscript was reviewed by all authors.

Study 3

Contamination risk and drinking water protection for a large-scale managed aquifer recharge site in a semi-arid karst region, Jordan

Citation: Xanke J, Liesch T, Goeppert N, Klinger J, Gassen N, Goldscheider N (2017) Contamination risk and drinking water protection for a large-scale managed aquifer recharge site in a semi-arid karst region, Jordan. In: Hydrogeology Journal 23 (5), S. 1027–1040. 1–14. http://dx.doi.org/10.1007/s10040-017-1586-0.

Declaration of authorship: Julian Xanke (JX) evaluated the data in consultation with Tanja Liesch, Nadine Goeppert, Jochen Klinger, Niklas Gassen and Nico Goldscheider. The Tracer test were planned, conducted and evaluated from JX and Niklas Gassen. The vulnerability and risk map was developed and evaluate in consultation with Tanja Liesch, Nadine Goeppert and Nico Goldscheider. The manuscript was written by JX and reviewed by all authors.

References

Abusaada M, Sauter M (2013) Studying the flow dynamics of a karst aquifer system with an equivalent porous medium model. *Groundwater*, 51(4), 641-650.

Agnew CT, Anderson E, Lancaster W, Lancaster F (1995) Mahafir: A water harvesting system in the Eastern Jordan (Badia) Eesert. *GeoJournal*,37(1), 69-80.

Al Hunjul NG (1993) Geological Map of Madaba. Madaba 3153 II, Scale 1:50 000. Geological Mapping Division, National Mapping Project.

Al-Adamat RAN, Foster IDL, Baban SMJ (2003) Groundwater vulnerability and risk mapping for the Basaltic aquifer of the Azraq basin of Jordan using GIS, Remote sensing and DRASTIC. In: *Applied Geography* 23 (4), S. 303–324.

Al-Assa'd TA, Abdulla FA (2010) Artificial groundwater recharge to a semi-arid basin: case study of Mujib aquifer, Jordan. *Environmental Earth Sciences*, 60(4), 845-859.

Al-Bakri J, Al-Jahmany Y (2013) Application of GIS and Remote Sensing to Groundwater Exploration in Al-Wala Basin in Jordan. In: *Journal of Water Resource and Protection* 2013.

Al-Hanbali A, Kondoh A (2008) Groundwater vulnerability assessment and evaluation of human activity impact (HAI) within the Dead Sea groundwater basin, Jordan. In: *Hydrogeology Journal* 16 (3), S. 499–510.

Al-Kuisi M, El-Naqa A, Hammouri N (2006) Vulnerability mapping of shallow groundwater aquifer using SINTACS model in the Jordan Valley area, Jordan. In: *Environmental Geology* 50 (5), S. 651–667.

Alsharhan AS, Rizk ZA; Nairn AEM, Bakhit DW, Alhajari SA (2001) Hydrogeology of an arid region: the Arabian Gulf and adjoining areas: Elsevier, Amsterdam

Amery HA, Wolf AT (2010) Water in the Middle East: a geography of peace: University of Texas Press. Austin, TX

Anderson MP, Woessner WW, Hunt RJ (2015) Applied groundwater modeling: simulation of flow and advective transport. Elsevier 2015.

Anderson MP, Woessner WW (1992) Applied Groundwater Modeling: Simulation of Flow and Advective Transport. Academic Press, 281 p.

Andreo B, Ravbar N, Vías JM (2009) Source vulnerability mapping in carbonate (karst) aquifers by extension of the COP method: application to pilot sites. In: *Hydrogeology Journal* 17 (3), S. 749–758.

Auckenthaler A, Huggenberger P (2013) Pathogene Mikroorganismen im Grund-und Trinkwasser: Transport—Nachweismethoden—Wassermanagement: Springer, Heidelberg, Germany

Awawdeh MM, Jaradat RA (2010) Evaluation of aquifers vulnerability to contamination in the Yarmouk River basin, Jordan, based on DRASTIC method. In: *Arabian Journal of Geosciences* 3 (3), S. 273–282.

Bajjali W (2006) Recharge mechanism and hydrochemistry evaluation of groundwater in the Nuaimeh area, Jordan, using environmental isotope techniques. *Hydrogeology Journal*, 14(1-2), 180-191.

Bajjali W, Abu-Jaber N (2001) Climatological signals of the paleogroundwater in Jordan. *Journal of Hydrology*, 243(1), 133-147.

Bakalowicz M, Boucheseiche C, Bouillin O, Cadilhac L, Gay D, Laurent A, Mettetal JP, Valencia G, Viprey F (1999) Connaissance et gestion des ressources souterraines en eaux souterraines dans les régions karstiques - guide technique n° 3, SDAGE Rhône-Méditerrannée-Corse - Agence de l'Eau Rhône-Méditerranée-Corse, Lyon, 40 p, 1999

Bakalowicz M (1994) Water geochemistry: water quality and dynamics. *Groundwater ecology*, 1, 97-127.

Bakalowicz M (2005) Karst groundwater: a challenge for new resources. *Hydrogeology Journal*, 13(1), 148-160.

Bakalowicz M (2011) Management of karst groundwater resources. In: *Karst Management*: Springer, S. 263–282.

Bakalowicz M (2015) Karst and karst groundwater resources in the Mediterranean. *Environmental Earth Sciences*, 74(1), 5-14.

Bakalowicz M, El Hakim M, El-Hajj A (2008) Karst groundwater resources in the countries of eastern Mediterranean: the example of Lebanon. *Environmental geology*, 54(3), 597-604.

Barrett ME, Charbeneau RJ (1997) A parsimonious model for simulating flow in a karst aquifer. In: *Journal of Hydrology* 196 (1), S. 47–65.

Bayer HJ, Hötzl H, Jado AR, Röscher B, Voggenreiter W (1988) Sedimentary and structural evolution of the northwest Arabian Red Sea margin. *Tectonophysics* 153(1):137–151

Behrens H, Beims U, Dieter H, Dietze G, Eikmann T, Grummt T, Hanisch H, Henseling H, Käß W, Kerndorff H, Leibundgut C, Müller-Wegener U, Rönnefahrt I, Scharenberg B, Schleyer R, Schloz W, Tilkes F (2001) Toxicological and ecotoxicological assessment of water tracers. In: *Hydrogeology Journal* 9 (3), S. 321–325.

Bender F (1968) Geologie von Jordanien, 230 (Geology of Jordan, 230). Gebrüder Borntraeger, Berlin.

Birk S, Geyer T, Sauter M (2008) Modellierung von Karstgrundwasserleitern. In: *Numerische GrundWasserModellierung*: Konzeption, S. 24.

Bouwer H (2000) Integrated water management: emerging issues and challenges. In: *Agricultural Water Management* 45 (3), S. 217–228. DOI: 10.1016/S0378-3774(00)00092-5.

Bouwer H (2002) Artificial recharge of groundwater: hydrogeology and engineering. In: *Hydrogeology Journal* 10 (1), S. 121–142. DOI: 10.1007/s10040-001-0182-4.

Bou-Zeid E, El-Fadel M (2002) Climate change and water resources in Lebanon and the Middle East. In: *Journal of water resources planning and management* 128 (5), S. 343–355.

Bögli A (2012) Karst hydrology and physical speleology. Springer Science & Business Media.

Carr G, Blöschl G, Loucks DP (2012) Evaluating participation in water resource management: A review. In: *Water Resources Research* 48 (11).

Chen Z, Auler A, Bakalowicz M, Drew D, Griger F, Hartmann J, Jiang G, Moosdorf N, Richts A, Stevanovic Z, Veni G, Goldscheider N (2017) The World Karst Aquifer Mapping Project – Concept, Mapping Procedure and Map of Europe. Hydrogeology Journal.

Clark ID, Fritz P (1997) Environmental Isotopes in Hydrogeology. Boca Raton, Florida: Lewis Publishers.

Cosgrove WJ, Loucks DP (2015) Water management: Current and future challenges and research directions. In: *Water Resources Research* 51 (6), S. 4823–4839.

Coxon C (2011) Agriculture and karst. In: *Karst management*: Springer, S. 103–138.

Craig H (1961) Isotopic variations in meteoric waters, *Science*, 133: 1702-1703.

Daher W, Pistre S, Kneppers A, Bakalowicz M, Najem W (2011) Karst and artificial recharge: Theoretical and practical problems: A preliminary approach to artificial recharge assessment. *Journal of Hydrology*, 408(3), 189-202.

Delleur JW (2006) The handbook of groundwater engineering. CRC press.

Diersch HJG (2002) FEFLOW reference manual. In: Institute for Water Resources Planning and Systems Research Ltd, S. 278.

Diersch HJG (2014) FEFLOW. Finite Element Modelling of Flow, mass and Heat Transport in porous and Fractured Media. Berlin: Springer.

Dillon P (2005) Future management of aquifer recharge. In: *Hydrogeology Journal* 13 (1), S. 313–316.

Dillon P, Pavelic P, Page D, Beringen H, Ward J (2009) Managed Aquifer Recharge. An Introduction. Waterlines Report Series No. 13, February 2009, p. 77.

DoELG/EPA/GSI (1999) Groundwater protection schemes. Department of the Environment and Local Government, EPA, Geol. Surv. of Ireland, Dublin, 24 pp.

Doerfliger N, Zwahlen F (1998) Practical guide: groundwater vulnerability mapping in karstic regions (EPIK). In: Swiss Agency for the Environment, Forests and Landscape (SAEFL), Bern 56.

Domenico PA, Schwartz FW (1998) Physical and chemical hydrogeology: Wiley New York.

DOS (2016) Department of Statistics, Jordan. *Online query 18.10.2016*. http://web.dos.gov.jo/

Dreybrodt W, Romanov D, Gabrovsek F (2002) Karstification below dam sites: a model of increasing leakage from reservoirs. *Environmental Geology*, 42(5), 518-524.

Eberts SM, Böhlke JK, Kauffman LJ, Jurgens BC (2012) Comparison of particle-tracking and lumped-parameter age-distribution models for evaluating vulnerability of production wells to contamination. *Hydrogeology Journal*, 20(2), 263-282.

Eichinger L (1983) A contribution to the interpretation of 14C groundwater ages considering the example of a partially confined sandstone aquifer.In Stuiver, M and Kra, RS, eds, Proceedings of the 11th International 14C Conference. Radiocarbon 25(2): 347–356.

Einsiedl F (2005) Flow system dynamics and water storage of a fissured-porous karst aquifer characterized by artificial and environmental tracers. *Journal of Hydrology*, 312(1), 312-321.

El-Naqa A (2004) Aquifer vulnerability assessment using the DRASTIC model at Russeifa landfill, northeast Jordan. In: *Environmental Geology* 47 (1), S. 51–62.

El-Naqa A (1993) Hydrological and hydrogeological characteristics of Wadi el Mujib catchment area, Jordan. Environmental Geology, 22(3), 257-271.

El-Naqa A, Al Kuisi M (2004) Hydrogeochemical modeling of the water seepages through Tannur Dam, southern Jordan. *Environmental Geology*, 45(8), 1087-1100.

El-Naqa A, Al-Shayeb A (2009) Groundwater protection and management strategy in Jordan. *Water resources management*, 23(12), 2379-2394.

El-Hakim M, Bakalowicz M (2007) Significance and origin of very large regulating power of some karst aquifers in the Middle East. Implication on karst aquifer classification. In: *Journal of Hydrology* 333 (2), S. 329–339.

Etcheverry D, Vennemann T (2009) Isotope im Grundwasser. Methoden zur Anwendung in der hydrogeologischen Praxis. Umwelt-Wissen Nr. 0930 (Isotopes in groundwater. Methods for use in hydrogeological practice. Environmental studies no. 0930). Bundesamt für Umwelt, Bern. 121 S.

Evans GV, Otlet RL, Downing A, Monkhouse RA and Rae G (1979) Some problems in the interpretation of isotope measurements in United Kingdom aquifers. In Isotope Hydrology II. Vienna, IAEA: 679–708.

Foley JA, DeFries R, Asner GP, Barford C, Bonan G, Carpenter SR, Chapin FS, Coe MT, Daily GC, Gibbs HK, Helkowski JH, Tracey H, Howard EA, Kucharik CJ, Monfreda C, Patz JA, Prentice IC, Ramankutty N, Snyder PK (2005) Global consequences of land use. In: *science* 309 (5734), S. 570–574.

Fontes JC, Garnier JM (1979) Determination of the initial 14C activity of the total dissolved carbon: A review of the existing models and a new approach. *Water Resources Research*, 15(2), 399-413.

Ford D, Williams PW (2007) Karst hydrogeology and geomorphology. John Wiley & Sons.

Freeze RA, James B, Massmann J, Sperling T, Smith L (1992) Hydrogeological decision analysis: 4. The concept of data worth and its use in the development of site investigation strategies. In: *Groundwater* 30 (4), S. 574–588.

Gassen N, Al-Hyari M, Hanbali B, Obaiat A, Kirsch H, Toll M, Xanke J (2013) Delineation of Groundwater Protection Zones for Hidan Well Field. Technical report No. 3. Project 'Water aspects in Land-Use-Planning', published by BGR and MWI; 98 S., Amman.

Gale IN, Macdonald DMJ, Calow RC, Neumann I, Moench M, Kulkarni H, Mudrakartha S, Palanisami K (2006). Managed aquifer recharge: an assessment of its role and effectiveness in watershed management: Final report for DFID KAR project R8169, Augmenting groundwater resources by artificial recharge: AGRAR.

Gat JR, Mazor E, Tzur Y (1969) The stable isotope composition of mineral waters in the Jordan Rift Valley, Israel, *J. Hydrology*, 76: 334-352.

Geyh MA (1970) Carbon-14 concentration of lime in soils and aspects of the carbon-14 dating of groundwater. Isotope Hydrology 1970. IAEA, Vienna, pp. 215–223.

Geyer T, Birk S, Licha T, Liedl R, Sauter M (2007) Multitracer Test Approach to Characterize Reactive Transport in Karst Aquifers. *Ground Water*, 45 (1): 36-45

Ghasemizadeh R, Hellweger F, Butscher C, Padilla I, Vesper D, Field M, Alshawabkeh A (2012) Review: Groundwater flow and transport modeling of karst aquifers, with particular reference to the North Coast Limestone aquifer system of Puerto Rico. In: Hydrogeology Journal 20 (8), S. 1441–1461.

Goeppert N, Goldscheider N (2007) Solute and Colloid Transport in Karst Conduits under Low- and High-Flow Conditions. *Ground Water*, 46 (1): 61-68

Goldscheider N (2005) Karst groundwater vulnerability mapping: application of a new method in the Swabian Alb, Germany. *Hydrogeology Journal*, 13(4), 555-564.

Goldscheider N (2015) Overview of methods applied in karst hydrogeology. In *Karst Aquifers - Characterization and Engineering* (pp. 127-145). Springer International Publishing.

Goldscheider N, Andreo B (2007) The geological and geomorphological framework. Methods in karst hydrogeology. International Contribution to Hydrogeology, IAH, 26, 9-23.

Goldscheider N, Drew D (2007) Methods in Karst Hydrogeology: IAH: International Contributions to Hydrogeology, 26: CRC Press.

Goldscheider N, Klute M, Sturm S, Hötzl H (2000) The PI method–a GIS-based approach to mapping groundwater vulnerability with special consideration of karst aquifers. In: Z Angew Geol 46 (3), S. 157–166.

Goldscheider N, Meiman J, Pronk M, Smart C (2008) Tracer tests in karst hydrogeology and speleology. In: *International Journal of Speleology* 37 (1), S. 3.

Goldscheider N, Hötzl H, Käss W, Ufrecht W (2003) Combined tracer tests in the karst aquifer of the artesian mineral springs of Stuttgart. *Environmental Geology*, 43 (8): 922-929

Gonfiantini R, Fröhlich K, Araguas-Araguas L, Rozanski K. (1998) Isotopes in groundwater hydrology. Isotope tracers in catchment hydrology, 203-246.

Gonfiantini R, Zuppi GM (2003) Carbon isotope exchange rate of DIC in karst groundwater. *Chemical Geology*, 197(1), 319-336.

Goode DJ, Senior LA, Subah A, Jaber A (2013) Groundwater-level trends and forecasts, and salinity trends, in the Azraq, Dead Sea, Hammad, Jordan Side Valleys, Yarmouk, and Zarqa groundwater basins, Jordan: U.S. Geological Survey.

Green RT, Bertetti FP, Miller MS (2014) Focused Groundwater Flow in a Carbonate Aquifer in a Semi-Arid Environment. In: *Journal of Hydrology*.

Hadadin N (2015) Dams in Jordan Current and Future Perspective. *Canadian Journal of Pure and Applied Sciences*, 9(1), 3279-3290.

Hadadin N, Qaqish M, Akawwi E, Bdour A (2010) Water shortage in Jordan—Sustainable solutions. Desalination, 250(1), 197-202.

Hammond WW (1993). Enhanced recharge and karst, Edwards aquifer, south central Texas. Geological Society of America, Abstracts with Programs; (United States), 25(CONF-9303212--).

Hammouri N, El-Naqa A (2008) GIS based hydrogeological vulnerability mapping of groundwater resources in Jerash Area-Jordan. In: *Geofísica internacional* 47 (2), S. 85–97.

Hartmann A, Goldscheider N, Wagener T, Lange J, Weiler M (2014) Karst water resources in a changing world: Review of hydrological modeling approaches. *Reviews of Geophysics*, 52(3), 218-242.

Heath RC (1983) Basic ground-water hydrology: US Geological Survey.

Heinz B, Birk S, Liedl R, Geyer T, Straub KL, Andresen J, Bester K, Kappler A (2009) Water quality deterioration at a karst spring (Gallusquelle, Germany) due to combined sewer overflow: evidence of bacterial and micro-pollutant contamination. *Environmental Geology* 57(4):797–808

Herczeg AL, Rattray KJ, Dillon PJ, Pavelic P, Barry KE (2004) Geochemical processes during five years of aquifer storage recovery. *Ground Water*, 42(3), 438-445.

Hiller T, Kaufmann G, Romanov D (2011) Karstification beneath dam-sites: From conceptual models to realistic scenarios. *Journal of Hydrology*, 398 (3), 202-211.

Hinkelmann R (2006) Efficient numerical methods and information-processing techniques for modeling hydro-and environmental systems: Springer Science & Business Media.

Humphreys H, Partners (1991) Dams on Wadi Wala and Wadi Mujib, Draft final report, Part IV Site Investigation. Internal report of the Jordan Valley Authority of Jordan, Amman.

Hussein, I.A., T.M. Abu Sharar, and A.M. Battikhi. 2005. "Water Resources Planning and Development in Jordan." In Food Security Under Water Scarcity in the Middle East: Problems and Solutions, edited by A Hamdy and R Monti, 183–97. Options Mediterraneennes: Serie A. Seminares Mediterraneens 65. Bari: CIHEAM.

Issar AS (2010) The Past is the Key to the Future: Springer.

Jaber JO, Mohsen MS (2001) Evaluation of non-conventional water resources supply in Jordan. In: *Desalination* 136 (1), S. 83–92.

Jønch-Clausen T (2004) Integrated water resources management (IWRM) and water efficiency plans by 2005: Why, what and how. In: Why, what and how.

Joodaki G, Wahr J, Swenson S (2014) Estimating the human contribution to groundwater depletion in the Middle East, from GRACE data, land surface models, and well observations. In: *Water resources research* 50 (3), S. 2679–2692.

Jurgens BC, Bexfield LM, Eberts SM (2014) A Ternary Age-Mixing Model to Explain Contaminant Occurrence in a Deep Supply Well. *Groundwater*.

Käss W (1998) Tracing technique in geohydrology. Balkema, Rotterdam, The Netherlands, 581 pp

Käss W (2004) Geohydrologische Markierungstechnik [Hydrogeological tracer techniques]. Borntraeger, Berlin, 557 pp

Kattan Z (1995) Chemical and environmental isotope study of the fissured basaltic aquifer system of the Yarmouk basin (Syrian Arab Republic. In: Proceedings of a symposium on isotopes in water resources management. IAEA-SM-336/28, vol. 2, Vienna.

Kattan Z (2001) Use of hydrochemistry and environmental isotopes for evaluation of groundwater in the Paleogene limestone aquifer of the Ras Al-Ain area (Syrian Jezireh). *Environmental Geology*, 41(1-2), 128-144.

Kinzelbach W, Bauer P, Siegfried T, Brunner P (2003) Sustainable groundwater management - problems and scientific tool. Episodes-Newsmagazine of the International Union of Geological Sciences, 26(4), 279-284.

Kliot N (2005) Water resources and conflict in the Middle East: Routledge.

Kresic N (2006) Hydrogeology and groundwater modeling. CRC press, S. 807

Kresic N (2013) Water in karst. Management, Vulnerability and Restoration. McGraw-Hill Professional, S. 708.

Kresic N, Papic P, Golubovic R (1992) Elements of groundwater protection in a karst environment. In: *Environmental geology and water sciences* 20 (3), S. 157–164.

Kruseman GP, De Ridder NA (1994) Analysis and Evaluation of Pumping Test Data (2nd edn.) International Institute for Land Reclamation and Improvement. Wageningen, The Netherlands.

Laimer HJ (2005) Die Erfassung der Karstgrundwasser-Vulnerabilität mit der Methode „VURAAS". In: *Grundwasser* 10 (3), S. 167–176.

Lakshmanan E, Kannan R, Senthil Kumar M. (2003) Major ion chemistry and identification of hydrogeochemical processes of groundwater in a part of Kancheepuram district Nadu, India. *Environmental Geoscince*, v. 10, no. 4, pp. 157-166

Leibundgut C, Maloszewski P, Külls C (2011) Tracers in hydrology: John Wiley & Sons.

Llamas MR, Custodio E (2002) Intensive Use of Groundwater: Challenges and Opportunities: CRC Press.

Małoszewski P, Zuber A (1982) Determining the turnover time of groundwater systems with the aid of environmental tracers: 1. Models and their applicability. *Journal of Hydrology*, 57(3), 207-231.

Mangin A (1975) Contribution à l'étude hydrodynamique des aquifères karstiques. 3ème partie. Constitution et fonctionnement des aquifères karstiques. Annales de Spéléologie. 30 (1): p. 21-124.

Margane A, Borgstedt A, Hamdan I, Subah A, Hajali Z (2009) Delineation of Surface Water Protection Zones for Wala Dam. Technical Report (12), S. 126. MWI, Amman, Jordan

Margane A, Hobler M, Almomani M, Subah A (2002) Contributions to the hydrogeology of northern and central Jordan. In: Geologisches Jahrbuch (Reihe C 68:52).

Margane A, Subah A, Hamdan I, Hajali Z, Almomani T (2010) Delineation of Groundwater Protection Zones for the Springs in Wadi Shuayb. In: Groundwater Resources Management-Technical Report (14), S. 98.

Margane A (2011) Site Selection for Wastewater Facilities in the Nahr el-Kalb-Catchment – General Recommendations from the Perspective of Groundwater Resources Protection. – Technical Cooperation Project 'Protection of Jeita Spring', Technical Report No.1, prepared by BGR, 155p.; Ballouneh, Libanon

Martin R (2013) Clogging issues associated with managed aquifer recharge methods. IAH Commission on Managing Aquifer Recharge.

Masciopinto C, La Mantia R, Pollice A, Laera G (2012) Managed aquifer recharge of a karstic aquifer in Nardó, Italy. Reclaim Water: Advances in Water Reclamation Technologies for Safe Managed Aquifer Recharge, 47.

Mays L (Ed.) (2009) Integrated Urban Water Management: Arid and Semi-Arid Regions: UNESCO-IHP (Vol. 3). CRC Press.

Meredith K (2009) Radiocarbon age dating groundwaters of the West Canning Basin, Western Australia.

MWI (2001) Standards, Regulations & Legislation for water reuse in Jordan. Ministry of Water and Irrigation. Water Resource Policy Support

MWI (2004) National Water Master Plan (NWMP). Ministry of Water and Irrigation, Amman, Jordan.

MWI (2006) Drinking water resources protection guidelines. Jordanian-German Technical Cooperation Project Groundwater Resources Management. unofficial translation.

MWI (2012) Ministry of Water and Irrigation. Amman, Jordan. Data base.

MWI (2013) Jordan Water Sector Facts and Figures 2013. Ministry of Water and Irrigation, Amman, Jordan.

MWI (2016) National Water Strategy of Jordan, 2016 - 2025. Ministry of Water and Irrigation, Amman, Jordan.

Nastev M, Rivera A, Lefebvre R, Martel R, Savard M (2005) Numerical simulation of groundwater flow in regional rock aquifers, southwestern Quebec, Canada. In: *Hydrogeology Journal* 13 (5-6), S. 835–848.

Nguyet VTM, Goldscheider N (2006) A simplified methodology for mapping groundwater vulnerability and contamination risk, and its first application in a tropical karst area, Vietnam. In: *Hydrogeology Journal* 14 (8), S. 1666–1675.

Ofterdinger US, Balderer W, Loew S, Renard P (2004) Environmental isotopes as indicators for ground water recharge to fractured granite. *Ground water*, 42(6), 868-879.

Page D, Dillon P, Vanderzalm J, Toze S, Sidhu J, Barry K, Levett K, Kerner S, Regel R (2010) Risk assessment of aquifer storage transfer and recovery with urban stormwater for producing water of a potable quality. *Journal of Environmental Quality*, 39(6), 2029-2039.

Pankow JF, Johnson RL, Hewetson JP, Cherry JA (1986) An evaluation of contaminant migration patterns at two waste disposal sites on fractured porous media in terms of the equivalent porous medium (EPM) model. *J. Contaminant Hydrol*., 1 (1986), pp. 65–76

Pavelic P, Dillon PJ, Barry KE, Gerges NZ (2006) Hydraulic evaluation of aquifer storage and recovery (ASR) with urban stormwater in a brackish limestone aquifer. *Hydrogeology Journal*, 14(8), 1544-1555.

Pearson FJ, Hanshaw BB (1970) Sources of dissolved carbonate species in groundwater and their effects on carbon-14 dating. Isotope hydrology, 1970, 271-286.

Pearson FJ, White DE (1967) Carbon 14 ages and flow rates of water in Carrizo Sand, Atascosa County, Texas. *Water Resources Research*, 3(1), 251-261.

Pedretti D, Fernàndez-Garcia D, Sanchez-Vila X, Barahona-Palomo M, Bolster D (2011) Combining physical-based models and satellite images for the spatio-temporal assessment of soil infiltration capacity. Stochastic environmental research and risk assessment, 25(8), 1065-1075.

Plummer LN (2005) Dating of young groundwater. In Isotopes in the Water Cycle (pp. 193-218). Springer Netherlands.

Plummer LN, Glynn PD (2013) Radiocarbon dating in groundwater systems. Chapter 4. In Isotopes methods for groundwater dating.

Powell JH, Moh'd, BK (2011) Evolution of Cretaceous to Eocene alluvial and carbonate platform sequences in central and south Jordan. *GeoArabia-Middle East Petroleum Geosciences*, 16(4), 29-82.

Qadir M, Sharma BR, Bruggeman A, Choukr-Allah R, Karajeh F (2007) Non-conventional water resources and opportunities for water augmentation to achieve food security in water scarce countries. *Agricultural water management*, 87(1), 2-22.

Rappl A, Wetzel KF, Buttner G, Scholz M (2010) Dye tracer investigations at the Partnach Spring (German Alps). *Hydrologie und Wasserbewirtschaftung*. 54 (4): 220-230

Ravbar N, Goldscheider N (2007) Proposed methodology of vulnerability and contamination risk mapping for the protection of karst aquifers in Slovenia. In: *Acta carsologica* 36 (6), S. 397–411.

Riepl D (2013) Knowledge-based decision support for integrated water resources management with an application for Wadi Shueib, Jordan. KIT Scientific Publishing.

Robert T, Caterina D, Deceuster J, Kaufmann O, Nguyen F (2012) A salt tracer test monitored with surface ERT to detect preferential flow and transport paths in fractured/karstified limestones. *Geophysics* 77(2):B55–B67

Romanov D, Gabrovsek F, Dreybrodt W (2007) Leakage below dam sites in limestone terrains by enhanced karstification: a modeling approach. *Environmental Geology*, 51(5), 775-779.

Rompré A, Servais P, Baudart J, de-Roubin MR, Laurent P (2002) Detection and enumeration of coliforms in drinking water: current methods and emerging approaches. *Journal of microbiological methods*, 49(1), 31-54.

Salem O, Visser JH, Dray M, Gonfiantini R (1980) Groundwater flow patterns in the western Lybian Arab Jamahiriaya. In Arid-Zone Hydrology: Investigations with Isotope Techniques. Vienna, IAEA: 165179.

Sauter M, Geyer T, Kovács A, Teutsch G (2006) Modellierung der hydraulik von karstgrundwasserleitern–eine übersicht. In: *Grundwasser* 11 (3), S. 143–156.

Scanlon BR, Reedy RC, Stonestrom DA, Prudic DE, Dennehy KF (2005) Impact of land use and land cover change on groundwater recharge and quality in the southwestern US. In: *Global Change Biology* 11 (10), S. 1577–1593.

Scanlon BR, Mace RE, Barrett ME, Smith B (2003) Can we simulate regional groundwater flow in a karst system using equivalent porous media models? Case study, Barton Springs Edwards aquifer, USA. In: *Journal of Hydrology* 276 (1), S. 137–158.

Schmidt S, Geyer T, Marei A, Guttman J, Sauter M (2013) Quantification of long-term wastewater impacts on karst groundwater resources in a semi-arid environment by chloride mass balance methods. *Journal of Hydrology*, 502, 177-190.

Schmoll O (2006) Protecting groundwater for health: managing the quality of drinking-water sources: World Health Organization.

Schudel B, Biaggi D, Dervey T, Kozel R, Müller I, Ross JH, Schindler U (2002) Einsatz künstlicher tracer in der Hydrogeologie: Praxishilfe [Use of artificial tracers in hydrogeology: a practical guide]. Bundesamt für Wasser und Geologie, Bern, Switzerland

Schwabe K, Albiac J, Connor JD, Hassan RM, González LM (2013) Drought in Arid and Semi-Arid Regions. Springer.

Seiler KP, Behrens H, Wolf M (1996) Use of artificial and environmental tracers to study storage and drainage of groundwater in the Franconian Alb, Germany, and the consequences for

groundwater protection. In: Proc. on Isotopes in Water Resources Management. IAEA, Vienna. pp. 135-145

Sowers J, Vengosh A, Weinthal E (2011) Climate change, water resources, and the politics of adaptation in the Middle East and North Africa. *Climatic Change*, 104(3-4), 599-627.

Steinel A, Schelkes K, Subah A, Himmelsbach T (2016) Spatial multi-criteria analysis for selecting potential sites for aquifer recharge via harvesting and infiltration of surface runoff in north Jordan. *Hydrogeology Journal*, 1-22.

Steinel A (2012). Guideline for Assessment and Implementation of Managed Aquifer Recharge (MAR) in (semi-) Arid Regions: Pre-feasibility Study for Infiltration of Floodwater in the Amman-Zarqa and Azraq Basins, Jordan. BGR.

Tamers MA (1967) Radiocarbon ages of groundwater in an arid zone unconfined aquifer. *Geophysical Monograph Series*, 11, 143-152.

Teutsch G, Sauter M (1991) Groundwater modeling in karst terranes: Scale effects, data acquisition and field validation. In Proc. Third Conf. Hydrogeology, Ecology, Monitoring, and Management of Ground Water in Karst Terranes, Nashville, TN (pp. 17-35).

Toride N, Leij FJ, van Genuchten MT (1999) The CXTFIT code for estimating transport parameters from laboratory or field tracer experiments. Research Report No. 137. Riverside, California: US Salinity Laboratory, USDA, ARS.

Trefry MG, Muffels C (2007) FEFLOW: A Finite-Element Ground Water Flow and Transport Modeling Tool. In: *Groundwater* 45 (5), S. 525–528.

United Nations Environment Programme (UNEP) (2012) The UN-water status report on the applicationof integrated approaches to water resources management. United Nations Environment Programme, Nairobi. ISBN 978-92-807-3264-1

van Beynen PE (2011) Karst Management. Netherlands: Springer. doi: 10.1007/978-94-007-1207-2

Vanderzalm JL, Page DW, Barry KE, Dillon PJ (2010) A comparison of the geochemical response to different managed aquifer recharge operations for injection of urban stormwater in a carbonate aquifer. *Applied Geochemistry*, 25(9), 1350-1360.

Vías JM, Andreo B, Perles MJ, Carrasco F, Vadillo I, Jiménez P (2006) Proposed method for groundwater vulnerability mapping in carbonate (karstic) aquifers: the COP method. In: *Hydrogeology Journal* 14 (6), S. 912–925.

Vidal M, Melgar J, Lopez A, Santoalla MC (2000) Spatial and temporal hydrochemical changes in groundwater under the contaminating effects of fertilizers and wastewater. In: *Journal of Environmental Management* 60 (3), S. 215–225.

Vogel JC (1968) Investigation of groundwater flow with radiocarbon. pp 355-69 of Isotopes in Hydrology. Vienna, International Atomic Energy Agency, 1967.

Voss KA, Famiglietti JS, Lo M, Linage C, Rodell M, Swenson SC (2013) Groundwater depletion in the Middle East from GRACE with implications for transboundary water management in the Tigris-Euphrates-Western Iran region. In: *Water resources research* 49 (2), S.914.

Wada Y, van Beek LPH, van Kempen CM, Reckman JWTM, Vasak S, Bierkens MFP (2010) Global depletion of groundwater resources. In: *Geophysical research letters* 37 (20).

Wang HF, Anderson MP (1995) Introduction to groundwater modeling: finite difference and finite element methods: Academic Press.

Wels C, Mackie D, Scibek J (2012) Guidelines for Groundwater Modelling to Assess Impacts of Proposed Natural Resource Development Activities. Ministry of Environment, Water Protection & Sustainability Branch.

Werz H, Hötzl H (2007) Groundwater risk intensity mapping in semi-arid regions using optical remote sensing data as an additional tool. In: *Hydrogeology Journal* 15 (6), S. 1031–1049.

Wolf L, Werz H, Hoetzl H, Ghanem M (2007) Exploring the potential of managed aquifer recharge to mitigate water scarcity in the Lower Jordan River Basin within an IWRM approach. Proceedings of the 6th international symposium on managed artificial recharge of groundwater, ISMAR6, Phoenix, Arizona USA October 28 – November 2, 2007.

Wolf L, Hötzl H (2011) SMART-IWRM: Integrated Water Resources Management in the Lower Jordan Rift Valley; Project Report Phase I: KIT Scientific Publishing.

World Health Organization (Ed.) (2004) Guidelines for drinking-water quality: recommendations (Vol. 1). World Health Organization.

Worthington SRH (2009) Diagnostic hydrogeologic characteristics of a karst aquifer (Kentucky, USA). In: *Hydrogeology Journal* 17 (7), S. 1665–1678.

WWAP (United Nations World Water Assessment Programme). 2015. The United Nations World Water Development Report 2015: Water for a Sustainable World. Paris, UNESCO.

Xanke J, Goeppert N, Sawarieh A, Liesch T, Kinger J, Ali W, Hötzl H, Hadidi K, Goldscheider N (2015) Impact of managed aquifer recharge on the chemical and isotopic composition of a

karst aquifer, Wala reservoir, Jordan. In: *Hydrogeology Journal* 23 (5), S. 1027–1040. 1–14. http://dx.doi.org/10.1007/s10040-015-1233-6.

Xanke J, Jourde H, Liesch T, Goldscheider N (2016) Numerical long-term assessment of managed aquifer recharge from a reservoir into a karst aquifer in Jordan. In: *Journal of hydrology*. http://dx.doi:10.1016/j.jhydrol.2016.06.058

Zinn BA, Konikow LF (2007) Potential effects of regional pumpage on groundwater age distribution. *Water resources research*, 43(6).

Zwahlen F (2004) Vulnerability and risk mapping for the protection of carbonate (karst) aquifers, final report (COST action 620). European Commission, Directorate-General XII Science. In: *Research and Development*, Brussels 297 pp.

Curriculum Vitae

Personal Information

Name	Julian Xanke
Date of birth	18.04.1982
Place of birth	Leimen
Nationality	German

Education

1992- 2001	A-level, Freie Waldorfschule Karlsruhe, Karlsruhe (Germany)

Civilian Service

Mar. 2002 – Dec. 2002	World Wide Fund for Nature (WWF) – Auen Institut, Rastatt (Germany)

Academic studies

Oct. 2003 – Jun. 2010	Karlsruher Institut für Technologie (KIT) – Karlsruhe (Germany) Dipl.-Geologist at the Institute for Applied Geology Karlsruhe Institute for Technology, KIT (former University of Karlsruhe) Major subject: regional and historical geology, hydrogeology, engineering geology, hydraulics Diploma thesis: "Geological, hydrogeological and geophysical investigations as a basis for groundwater protection zone concepts in the Al-Jiftlik area, Wadi Faria, West Bank, Palestine".
Sept. 2007 – Jun. 2008	Université de Lausanne (UNIL) – Lausanne (Switzerland) Major subject: Regional geology, structural geology, geomorphology, geochemistry

Professional experience

Mar. 2011 – Dec. 2016	Research fellow & PhD candidate at Institute of Applied Geoscience (AGW), Karlsruhe Institute of Technology (KIT) Topic: "Managed aquifer recharge into a karst groundwater system at the Wala reservoir, Jordan".
Dec. 2010 – Feb. 2011	Research fellow at Institute of Applied Geoscience (AGW), Karlsruhe Institute of Technology (KIT) Topic: Integrated water resources management (IWRM) in the frame of the SMART Project (Sustainable Management of Available Water Resources with Innovative Technologies)

Journal publications (peer-reviewed)

- Xanke J, Liesch T, Goeppert N, Klinger J, Gassen N, Goldscheider N (2017) Contamination risk and drinking water protection for a large-scale managed aquifer recharge site in a semi-arid karst region, Jordan. Hydrogeol. J. 1–15. http://dx.doi.org/10.1007/s10040-017-1586-0.
- Xanke, J., Jourde, H., Liesch, T., & Goldscheider, N. (2016). Numerical long-term assessment of managed aquifer recharge from a reservoir into a karst aquifer in Jordan. Journal of Hydrology, 540, 603-614. *http://dx.doi.org/10.1016/j.jhydrol.2016.06.058*
- Xanke, J., Goeppert, N., Sawarieh, A., Liesch, T., Kinger, J., Ali, W., Hötzl, H., Hadidi, K., Goldscheider, N., (2015). Impact of managed aquifer recharge on the chemical and isotopic composition of a karst aquifer, Wala reservoir, Jordan. Hydrogeol. J. 1–14. http://dx.doi.org/10.1007/s10040-015-1233-6

Reports

- Sawarieh A, Xanke J (2013) Impacts of Wala Reservoir stored storm waters on Wala-Haidan Well Field, Jordan. SMARTII - Project Deliverable D312, SMART project
- Gassen N, Stoeckl L, Xanke J (2013) Conceptual Model for a Tracer Test in Wadi Hidan - Technical Cooperation Project 'Water Aspects in Land-Use Planning', technical report no. 1. prepared by BGR
- Gassen N, Al Hyari M, Hanbali B, Obaiat A, Kirsch H, Toll M, Xanke J (2013) Delineation of Groundwater Protection Zones for Hidan Well Field. Fachbericht Nr. 3 des TZ-Projekts 'Wasseraspekte in der Landnutzungsplanung', verfasst von BGR und MWI; 98 S., Amman.

Conference contributions

- Xanke J, Jourde H, Liesch T, Goldscheider N (2016) Numerical simulation of managed aquifer recharge into a karst groundwater system at the Wala reservoir, Jordan. IAH – Conference Montpellier, September 2016 – Presentation
- Klinger J, Xanke J, Alfaro P, Grimmeisen F, Salameh E, Salman A (2016) Integrating Managed Aquifer Recharge into regional water management in Jordan IAH – Conference Montpellier, September 2016 – Presentation
- Xanke J, Jourde H, Liesch T, Goldscheider N (2016) Numerical simulation of Managed Aquifer Recharge into a karst aquifer using an Equivalent Porous Medium approach. EUROKARST Conference, Neuchatel, Switzerland - Poster
- Klinger J, Alfaro P, Grimmeisen F, Xanke J, Riepl D, Subah A, Goldscheider N (2016) From research to implementation: IWRM for an urbanized area in Jordan. Tagungsband, 25. Tagung der Fachsektion Hydrogeologie in der DGGV 2016, Grundwasser - Mensch – Ökosysteme, 13.-17.04.2016, Karlsruhe
- Stoeckl L, Gassen N, Xanke J, Subah A, Königer P, Himmelsbach T (2014)Jahrestagung der Arbeitsgemeinschaft Stabile Isotope e.V. Oktober 2014, München – Poster
- Xanke J, Klinger J, Liesch T, Goeppert N, Sawarieh A, Goldscheider N (2026) Hydrogeological assessment of a managed aquifer recharge site at the Wala reservoir, Jordan. In: Grundwasser - Mensch - Ökosysteme : 25. Tagung der Fachsektion Hydrogeologie in der DGGV 2016, Karlsruher Institut für Technologie (KIT), 13.-17. April 2016
- Stoeckl L, Gassen N, Xanke J, Subah A, Königer P, Himmelsbach T (2014) Jahrestagung der Arbeitsgemeinschaft Stabile Isotope e.V. Oktober 2014, München – Poster
- Xanke J, Sawarieh A, Seder N, Ali W, Goldscheider N, Hötzl H (2012) Conference "Hydrogeology of Arid Environments", March 14 - 17, 2012, Hannover - Germany, Poster

Supplementary Information

Supplementary Material - Chapter 2

- Table S1 Hydrochemical data of Hidan and Wala wells from 2001 to 2011.

Sample ID	Sample Date	pH	Temp °C	EC µS/cm	TDS mg/L	Na mgL1	K mg/L	Mg mg/L	Ca mg/L	Cl mg/L	SO_4 mg/L	HCO_3 mg/L	NO_3 mg/L	SI Calcite	SI Aragonite	SI Dolomite	SI Gypsum	SI Anhydrite	pCO2 in Vol% of [atm]
Reservoir	12.11.2003	7.9	-	618	473	40.3	10	22	55.9	56.8		249	3.5	0.6	0.4	1.1	-2	-2.2	0.3
	01.06.2004	7.5	23	633	560	29.2	16	27	68.3	28.4	14.9	372	4.4	0.4	0.3	0.8	-2.3	-2.5	1.1
	28.11.2004	8.1	-	231	192	18.4	12	4.1	23.7	16	13	99.4	5.9	0.1	-0	-0	-2.7	-2.9	0.1
	24.08.2005	8.3	-	443	876	95.2	5.9	53	84	148	147	333	9.5	1.2	1.1	2.5	-1.3	-1.5	0.2
	13.12.2005	8	-	528	391	27.4	7.4	16	48.9	27.3	20.2	243	0.8	0.7	0.5	1.2	-2.3	-2.5	0.2
	29.01.2006	8.3	-	528	375	32	9	11	50.9	31.6	25.4	214	2	0.8	0.7	1.3	-2.2	-2.4	0.1
	26.04.2006	8.1	-	254	197	18.2	7	5	26.3	23.1	13.4	101	3.7	0.1	0	-0	-2.7	-2.9	0.1
Wala 1	01.06.2004	7.3	28	1501	1028	104	9.8	61	101	170	167	377	38	0.4	0.2	0.9	-1.2	-1.4	2
	28.11.2004	7.4	-	1419	1046	124	10	52	110	183	164	361	42	0.5	0.3	1	-1.1	-1.4	1.6
	24.08.2005	7.3	-	1361	938	95.9	8.2	49	106	172	74.9	411	23	0.5	0.4	1	-1.5	-1.7	1.9
	13.12.2005	7.2	-	1448	989	106	12	55	102	148	186	352	27	0.2	0.1	0.6	-1.1	-1.3	2.5
	05.04.2006	7.5	-	1388	986	98.2	11	43	107	160	173	364	30	0.6	0.5	1.3	-1.1	-1.3	1.1
	07.11.2006	7.4	-	1388	902	98.2	11	43	107	160	173	364	30	0.5	0.3	0.9	-1.1	-1.3	1.6
	16.07.2007	7.3	-	1128	733	75.7	4.7	38	108	141	176	321	16	0.3	0.2	0.6	-1.1	-1.3	1.7
	11.01.2009	7.2	-	1092	710	82.8	3.1	34	95.2	104	117	309	14	0.2	0.1	0.4	-1.3	-1.5	2
Wala 14	17.03.2003	7.3	31	1313	971	89.7	7	47	118	150	149	395	16	0.5	0.4	1.1	-1.1	-1.3	2.1
	09.07.2003	6.6	30	1312	1024	84	6.7	53	124	139	186	425	7.2	-0	-0	-0	-1	-1.2	12.3
	12.11.2003	7.6	-	1361	955	86.3	5.1	49	117	156	166	366	9.1	0.8	0.7	1.6	-1.1	-1.3	1
	01.06.2004	7.9	32	1430	1019	92	6.3	63	105	142	181	414	14	1.1	1	2.4	-1.1	-1.3	0.6
	24.08.2005	7.1	-	1324	953	89.9	5.5	50	109	170	174	343	11	0.3	0.1	0.6	-1.1	-1.3	2.7
	13.12.2005	7.3	-	1350	924	87.2	5.5	48	107	131	139	400	6.8	0.5	0.3	1	-1.2	-1.4	2.2
	05.04.2006	7.5	-	1342	967	92.2	5.5	51	100	136	192	377	14	0.7	0.5	1.4	-1.1	-1.3	1.2
	06.11.2006	7.3	-	1278	941	85.1	4.3	46	102	137	172	383	12	0.5	0.4	1	-1.1	-1.3	1.9
	16.07.2007	7.5	-	1278	831	85.1	4.3	46	102	137	172	383	12	0.7	0.5	1.4	-1.1	-1.3	1.2
	11.01.2009	7.6	-	1281	833	97.8	3.9	49	120	140	165	383	11	0.8	0.6	1.6	-1.1	-1.3	1.1
Hidan 9	10.10.2001	7.8	-	767	603	36.8	3.1	32	81	59.3	65.3	303	23	0.8	0.6	1.5	-1.6	-1.8	0.5
	18.03.2003	7.9	24	942	690	54.5	5.9	36	87	107	88.3	290	22	0.8	0.7	1.6	-1.5	-1.7	0.3
	10.07.2003	7.1	28	936	688	51.1	5.5	35	89.6	92	72.5	321	22	0.1	-0	0.1	-1.5	-1.7	2.9
	11.04.2004	7.7	-	1240	772	70.4	5.5	47	89.2	128	102	305	25	0.7	0.6	1.6	-1.4	-1.6	0.7
	01.06.2004	7.9	27	1009	722	57.5	5.5	47	81	103	86.9	314	27	0.9	0.7	1.8	-1.5	-1.7	0.4

	28.11.2004	8	-	928	711	59.8	5.1	40	86.8	99.1	86.4	300	34	0.9	0.8	1.9	-1.5	-1.7	0.3
	24.08.2005	8.1	-	929	661	54.1	4.7	32	82.2	89.1	74.9	304	21	1	0.9	2	-1.6	-1.8	0.2
	26.09.2007	7.4	-	924	601	61.4	4.3	35	91.8	95.1	75.4	324	25	0.4	0.3	0.8	-1.5	-1.7	1.2
	02.04.2008	7.9	-	840	546	60	3.1	32	88.6	87.3	71.5	307	24	0.9	0.7	1.7	-1.5	-1.8	0.4
	08.04.2009	8.2	-	859	558	51.1	3.9	32	84.8	83.1	68.2	265	23	1.1	1	2.1	-1.6	-1.8	0.2
	27.06.2009	7.8	-	925	601	61.4	4.7	32	85.8	100	77.8	320	23	0.7	0.6	1.4	-1.5	-1.7	0.5
	07.02.2011	7.7	-	906	589	56.1	3.1	27	78.8	85.6	76.8	266	18	0.6	0.4	1.1	-1.5	-1.8	0.5
	09.02.2011	7.7	-	900	585	56.8	3.5	29	83.4	90.2	82.6	282	19	0.6	0.4	1.1	-1.5	-1.7	0.6
Hidan 13	10.10.2001	7.5	-	983	741	62.8	4.7	34	94.8	107	80.2	334	24	0.6	0.4	1.1	-1.5	-1.7	1
	18.03.2003	7.9	26	1090	765	64.9	6.3	37	95	116	91.7	333	21	0.9	0.8	1.8	-1.4	-1.6	0.4
	10.07.2003	7	29	1102	804	66	5.5	38	101	122	104	350	17	0.1	0	0.2	-1.3	-1.5	3.5
	12.11.2003	7.9	-	1113	802	69.9	5.1	39	93.4	117	95	359	23	0.9	0.8	1.9	-1.4	-1.6	0.5
	11.04.2004	7.9	-	1271	826	75.9	5.5	34	110	126	106	345	23	1	0.8	1.8	-1.3	-1.5	0.5
	01.06.2004	7.3	27	1192	829	74.8	5.9	43	97.2	128	107	346	28	0.4	0.2	0.7	-1.4	-1.6	1.7
	28.11.2004	7.4	-	1087	784	79.6	5.5	35	97.8	121	116	305	25	0.4	0.3	0.8	-1.3	-1.5	1.1
	24.08.2005	7.9	-	1129	799	71.5	5.5	48	88	122	104	341	19	0.9	0.7	1.9	-1.4	-1.6	0.5
	06.11.2006	7.5	-	1099	830	69.5	6.7	38	99	147	135	315	18	0.5	0.4	0.9	-1.2	-1.5	1.1
	26.09.2007	7.3	-	1102	716	80.5	4.3	41	107	127	107	362	19	0.4	0.3	0.8	-1.3	-1.5	1.7
	02.04.2008	7.5	-	977	635	80	3.1	36	100	120	95.5	333	21	0.5	0.4	1	-1.4	-1.6	1.1
	01.07.2008	8.1	-	928	603	76.1	4.7	33	94.8	117	84.5	320	26	1.1	0.9	2.1	-1.5	-1.7	0.3
	27.06.2009	7.4	-	1102	716	79.4	5.1	37	101	130	108	343	20	0.4	0.3	0.8	-1.3	-1.5	1.5

Table S2 Electrical conductivity (EC) data of Hidan and Wala wells from 1984 to 2011.

Sample ID	Collection Date	EC [µS/cm]
Hidan 01	09.05.2000	1013
	15.05.2000	967
	08.06.2000	1051
Hidan 02	11.08.1989	749
	27.05.2000	971
	10.10.2001	986
	09.03.2004	1235
	18.05.2004	1030
	11.01.2009	1094
	08.04.2009	1080
	27.06.2009	1108
	07.03.2011	1115
	09.03.2011	1115
Hidan 03	24.01.1988	614
Hidan 04	05.02.1989	570
	13.07.1999	994
Hidan 05	13.05.1989	595
	19.04.1999	933
	21.11.1999	910
	03.04.2001	836
	03.04.2003	1071
	09.03.2004	1177
	18.05.2004	941
	02.06.2004	1070
	27.04.2005	1049
	23.08.2005	982
	25.10.2005	982
	19.01.2006	1003
	03.05.2006	1013
	28.03.2007	930
	26.09.2007	946
	01.07.2008	787
	18.02.2009	865
	08.04.2009	891
	27.06.2009	918
	30.03.2010	940
	07.02.2011	895
	09.02.2011	886
Hidan 06	23.08.1989	653
Hidan 07	17.08.1989	563
	10.10.2001	821
	03.12.2002	874
	08.01.2003	868
	09.03.2004	1074
	08.04.2009	874
	27.06.2009	980
	09.02.2011	930
	14.02.2011	937
Hidan 08	23.08.1989	582
	11.01.1999	1138
	13.01.1999	1068
	11.05.2003	1215
Hidan 09	10.10.2001	768
	02.12.2002	777
	18.03.2003	942
	10.07.2003	936
	12.11.2003	934
	27.01.2004	1393
	09.03.2004	1129
	11.04.2004	1240
	01.06.2004	1009
	21.09.2004	967
	28.11.2004	928
	17.01.2005	1023
	07.03.2005	1063
	31.05.2005	1001
	24.08.2005	929
	13.12.2005	969
	19.01.2006	992
	05.04.2006	906
	13.06.2006	1067
	26.09.2007	924
	02.04.2008	840
	08.04.2009	859
	27.06.2009	925
	07.02.2011	906
	09.02.2011	900
Hidan 10	15.06.1989	621
	03.09.1996	919
	18.05.2004	1036
Hidan 11	23.11.1989	672
	21.11.1999	925
	18.04.2000	973
Hidan 12	02.08.1999	981

	09.08.1999	975
	21.11.1999	956
	10.10.2001	965
	03.12.2002	1035
	08.01.2003	975
	18.05.2004	1006
	17.10.2005	1102
	08.04.2009	1055
	05.08.2009	1095
	09.02.2011	1083
Hidan 12b	12.02.2005	1243
	13.02.2005	1228
	08.04.2009	1043
	27.06.2009	1092
	07.02.2011	1048
	09.02.2011	1020
Hidan 13	20.07.1999	988
	21.11.1999	984
	18.04.2000	1003
	03.04.2001	1024
	10.10.2001	984
	02.12.2002	1047
	03.12.2002	1058
	08.01.2003	999
	18.03.2003	1090
	03.04.2003	1110
	08.07.2003	1102
	10.07.2003	1102
	12.11.2003	1113
	04.03.2004	1273
	09.03.2004	1198
	11.04.2004	1271
	01.06.2004	1192
	21.09.2004	1137
	28.11.2004	1087
	17.01.2005	1102
	07.03.2005	1172
	31.05.2005	1172
	24.08.2005	1129
	17.10.2005	1141
	13.12.2005	1146
	27.04.2006	1077
	13.06.2006	1160
	06.11.2006	1099
	08.11.2006	1099
	26.09.2007	1102
	02.04.2008	977
	01.07.2008	928
	27.06.2009	1102
Hidan 15	19.09.1992	672
	03.04.2001	1023
	10.10.2001	985
	24.06.2002	1011
	03.12.2002	1059
	08.01.2003	1000
	03.04.2003	1071
	01.10.2003	875
	09.03.2004	1232
	18.05.2004	1011
	17.10.2005	1138
	19.01.2006	1170
	08.04.2009	1013
	27.06.2009	1088
	14.02.2011	1029
Hidan 16	30.07.1999	972
	07.08.1999	980
	10.10.2001	961
	03.12.2002	1028
	08.01.2003	980
	09.03.2004	1135
	18.05.2004	1001
	17.10.2005	1099
Hidan 16a	31.12.2004	1112
	01.01.2005	1106
	01.02.2009	1046
	29.04.2010	1069
	07.03.2011	1030
	09.03.2011	1040
Hidan 16b	19.01.2006	1128
	27.06.2009	1064
	29.04.2010	1040
	09.02.2011	961
	14.02.2011	1006
Wala 01	19.11.1984	930
	19.02.1985	900
	28.04.1985	970
	03.12.1985	748
	14.01.1986	930

	03.02.1986	970
	12.03.1986	920
	05.04.1986	950
	30.08.1986	990
	14.10.2002	1270
	01.06.2004	1501
	12.07.2004	1568
	20.09.2004	1450
	21.09.2004	1450
	28.11.2004	1419
	17.01.2005	1401
	07.03.2005	1497
	31.05.2005	1442
	24.08.2005	1361
	13.12.2005	1448
	03.04.2006	1388
	05.04.2006	1388
	13.06.2006	1412
	07.11.2006	1128
	16.07.2007	1092
	11.01.2009	1239
Wala 02	09.10.1995	975
	03.09.1996	1034
	27.05.2000	971
	10.10.2001	986
	13.12.2005	1238
Wala 03	05.03.1980	657
Wala 04	30.03.1985	1107
	03.09.1996	925
	13.10.1998	1276
	24.10.2007	1136
	25.10.2007	1139
	26.10.2007	1132
	17.12.2010	1119
	18.12.2010	1126
	22.12.2010	1126
	27.02.2011	1360
	28.02.2011	1378
	01.03.2011	1379
Wala 05	10.02.1984	860
	02.10.2007	1331
	04.10.2007	1321
	14.12.2010	1422
	15.12.2010	1425
	16.12.2010	1419
	09.03.2011	1073
Wala 06	15.10.1984	921
	01.05.1995	888
	09.10.1995	893
	03.09.1996	846
	02.01.1997	903
	27.05.1997	904
	18.08.1997	1416
	21.08.1997	1250
	23.12.1997	881
	24.11.1999	1370
	18.04.2000	1189
	24.06.2007	1247
Wala 07	01.05.1995	888
	09.10.1995	893
	03.09.1996	846
	02.01.1997	903
	27.05.1997	904
	23.12.1997	881
	05.07.1998	1196
	05.07.1998	1196
	10.10.2001	820
Wala 09	15.09.1985	569
	31.08.1992	538
	01.05.1995	888
	09.10.1995	893
	03.09.1996	846
	02.01.1997	903
	27.05.1997	904
	23.12.1997	881
	10.10.2001	768
	08.07.2003	936
	12.11.2003	934
	27.01.2004	1393
	11.04.2004	1240
	01.06.2004	1009
	06.07.2004	903
	07.03.2005	1063
	24.08.2005	929
	13.12.2005	969
	04.04.2006	906
	13.06.2006	1067
	01.05.1995	888

	09.10.1995	893
	03.09.1996	846
	02.01.1997	903
	27.05.1997	904
	23.12.1997	881
	22.07.1999	1183
	02.08.2000	1201
	14.10.2002	1230
	02.12.2002	1220
	17.03.2003	1180
	03.04.2003	1260
	08.07.2003	1270
	09.07.2003	1270
	12.11.2003	1284
	04.03.2004	1440
	11.04.2004	1428
	01.06.2004	1280
	06.07.2004	1046
	12.07.2004	1359
	20.09.2004	1263
	28.11.2004	1197
	17.01.2005	1228
	07.03.2005	1224
	27.04.2005	1174
	31.05.2005	1208
	24.08.2005	1166
	25.10.2005	1197
	13.12.2005	1217
	05.04.2006	1145
	03.05.2006	1133
	12.06.2006	1142
	08.11.2006	1089
	28.03.2007	1037
	16.07.2007	1031
	02.04.2008	963
	10.06.2008	980
Wala 14	29.06.1985	864
	29.10.1995	1235
	03.09.1996	1260
	30.12.1996	1219
	08.04.1999	1262
	19.04.1999	1281
	20.07.1999	1366
	21.11.1999	1251
	18.04.2000	1272
	14.10.2002	1507
	02.12.2002	1332
	17.03.2003	1313
	08.07.2003	1312
	09.07.2003	1312
	12.11.2003	1361
	27.01.2004	1068
	04.03.2004	1350
	01.06.2004	1430
	06.07.2004	1270
	20.09.2004	1377
	28.11.2004	1308
	16.01.2005	1325
	17.01.2005	1325
	07.03.2005	1406
	31.05.2005	1375
	24.08.2005	1324
	13.12.2005	1350
	03.04.2006	1342
	05.04.2006	1342
	12.06.2006	1389
	06.11.2006	1278
	08.11.2006	1278
	16.07.2007	1281
	02.04.2008	1190
	11.01.2009	1109
Wala 15	01.05.1995	888
	09.10.1995	893
	03.09.1996	846
	02.01.1997	903
	27.05.1997	904
	23.12.1997	881
	18.04.2000	986
	03.04.2001	1023
Wala 15	24.06.2002	1011
Wala 17	27.12.2006	833
	28.12.2006	846

Table S3 Tritium data of Hidan wells, Wala wells, Wala rainfall and Wala reservoir from 1987 to 2010.

Location	Date	Tritium (TU) ± 1
Hidan 12	10.10.2001	0.8
Hidan 13	10.10.2001	0.9
	02.12.2002	0.0
	18.03.2003	0.5
	10.07.2003	1.0
	27.01.2004	1.4
	20.09.2004	0.3
	16.01.2005	2.0
	31.05.2005	0.2
	13.12.2005	1.8
	27.04.2006	2.7
	13.06.2006	2.0
	06.11.2006	1.4
Hidan 15	10.10.2001	0.8
Hidan 16	10.10.2001	1.2
Hidan 2	13.12.2005	1.0
	29.01.2006	1.0
	26.04.2006	2.5
	06.11.2006	1.0
Hidan 3	23.10.1990	1.0
Hidan 4	23.10.1990	1.0
Hidan 5	23.10.1990	1.0
Hidan 6	23.10.1990	1.6
Hidan 7	10.10.2001	0.9
Hidan 9	10.10.2001	1.1
	02.12.2002	0.7
	18.03.2003	0.6
	27.01.2004	1.4
	20.09.2004	0.5
	17.01.2005	1.7
	31.05.2005	0.8
	13.12.2005	1.4
	05.04.2006	1.0
	13.06.2006	1.0
	26.04.2008	2.6
	15.03.2010	2.7
Reservoir	01.12.2002	3.7
	17.03.2003	5.2
	09.07.2003	5.4
	12.11.2003	8.0
	27.01.2004	3.6
	20.09.2004	4.4
	16.01.2005	3.6
	31.05.2005	3.1
	24.08.2005	4.2
	13.12.2005	5.2
	29.01.2006	4.9
	26.04.2006	6.2
	13.06.2006	8.7
	13.07.2006	7.1
	06.11.2006	6.5
	15.03.2010	3.6
RW 6	20.03.2002	0.3
RW 7	27.03.2002	1.1
RW 8	04.10.2002	0.6
Wala 1	01.12.2002	1.6
	27.01.2004	1.3
	20.09.2004	1.7
	16.01.2005	1.7
	31.05.2005	2.0
	13.12.2005	2.7
	13.12.2005	3.8
	29.01.2006	2.2
	05.04.2006	1.0
	13.06.2006	1.3
	06.11.2006	2.6
	14.10.2002	0.8
Wala 13	02.12.2002	0.0
	09.07.2003	1.9
	12.11.2003	3.2
	27.01.2004	1.5
	20.09.2004	1.4
	16.01.2005	1.4
	31.05.2005	0.9
	13.12.2005	2.5
	05.04.2006	2.5
	12.06.2006	1.8
	08.11.2006	1.7
	14.10.2002	0.8
	17.03.2003	0.7
Wala 14	14.10.2002	1.1
	02.12.2002	0.6
	16.12.2002	1.5
	27.01.2004	0.6
	20.09.2004	0.1
	16.01.2005	1.0
	31.05.2005	0.6
	24.08.2005	4.2
	13.12.2005	1.0
	29.01.2006	1.0
	05.04.2006	1.0
	12.06.2006	2.3
	06.11.2006	1.1
Wala climate station	01.01.1987	11.8
	01.02.1987	29.0
	01.10.1987	15.0

01.01.1988	12.5
01.02.1988	16.1
01.03.1988	12.4
01.04.1988	23.9
01.12.1988	9.1
01.01.1989	10.2
01.02.1989	11.4
01.03.1989	12.5
01.01.1990	7.4
03.01.1990	10.3
01.02.1990	17.2
01.01.1991	6.4
03.01.1991	9.2
01.02.1991	10.3
01.12.1991	9.1
01.01.1992	8.5
01.02.1992	5.2
01.11.1992	8.2
01.12.1992	17.5
01.01.1993	16.6
01.02.1993	10.2
01.12.1993	3.3
01.01.1994	8.7
01.02.1994	7.9
01.03.1994	12.0
01.11.1994	5.7
01.12.1994	4.6
01.02.1995	11.2
01.01.1996	12.7
01.03.1996	8.3
04.01.1997	12.3
01.03.1997	6.9
02.04.1997	10.9
01.02.1998	5.9
01.03.1998	8.4
01.02.1999	7.9
01.01.2000	7.2

Table S4 Data for oxygen-18 and deuterium of Hidan wells, Wala wells, recharge wells, Wala reservoir and Wala climate station from 1987 to 2010.

Location	Date	Oxygen-18 [‰] (± 0.15)	Deuterium [‰] (± 1)
Wala 14	14.10.2002	-5.48	-25.90
	02.12.2002	-5.09	-25.81
	16.12.2002	-5.16	-25.90
	17.03.2003	-5.16	-25.60
	09.07.2003	-5.19	-25.73
	12.11.2003	-5.15	-26.50
	27.01.2004	-4.96	-26.50
	04.03.2004	-5.28	-25.70
	11.04.2004	-5.38	-26.00
	01.06.2004	-5.21	-25.93
	06.07.2004	-5.36	-25.10
	20.09.2004	-5.34	-28.10
	28.11.2004	-5.16	-25.43
	16.01.2005	-5.15	-25.30
	07.03.2005	-5.14	-25.78
	24.08.2005	-1.64	-19.31
	13.12.2005	5.31	-25.71
	29.01.2006	-5.54	-25.72
	05.04.2006	-6.40	-25.48
	12.06.2006	-5.42	-25.84
	06.11.2006	-5.30	-23.90
	02.04.2008	-5.54	-26.51
Wala 1	14.10.2002	-5.36	-26.35
	01.12.2002	-5.27	-26.89
	27.01.2004	-5.40	-24.40
	04.03.2004	-5.39	-25.80
	11.04.2004	-5.48	-26.60
	01.06.2004	-5.44	-25.60
	12.07.2004	-5.47	-26.70
	20.09.2004	-5.36	-27.50
	28.11.2004	-5.27	-26.40
	16.01.2005	-5.35	-26.50
	07.03.2005	-5.30	-26.30
	24.08.2005	-6.10	-24.77
	13.12.2005	-6.68	-26.51
	29.01.2006	-5.05	-24.76
	05.04.2006	-5.95	-25.42
	13.06.2006	-5.84	-26.04
	12.01.2009	-5.73	-25.71
Wala 13	14.10.2002	-5.59	-26.67
	02.12.2002	-5.43	-26.80
	17.03.2003	-5.48	-26.78
	09.07.2003	-5.35	-25.70
	12.11.2003	-5.28	-26.50
	27.01.2004	-5.38	-26.50
	04.03.2004	-5.60	-26.40
	11.04.2004	-5.55	-27.40
	01.06.2004	-5.30	-26.50
	12.07.2004	-5.42	-27.20
	20.09.2004	-5.58	-25.90
	28.11.2004	-5.45	-28.40
	16.01.2005	-5.45	-26.69
	07.03.2005	-5.49	-27.40
	24.08.2005	-6.06	-24.40
	13.12.2005	-6.50	-25.85
	05.04.2006	-6.47	-26.81
	12.06.2006	-6.62	-26.42
	08.11.2006	-5.72	25.31
	12.01.2009	-5.79	-27.17
Hidan 9	10.10.2001	-5.51	-24.60
	02.12.2002	-5.25	-25.20
	18.03.2003	-5.30	-24.80
	12.11.2003	-5.06	-26.10
	27.01.2004	-5.19	-24.60
	11.04.2004	-5.22	-24.90
	01.06.2004	-5.20	-25.90
	06.07.2004	-5.30	-26.40
	20.09.2004	-5.39	-26.50
	28.11.2004	-5.29	-22.90
	17.01.2005	-5.35	-27.10
	24.08.2005	-5.78	-24.53
	13.12.2005	-6.28	-25.93
	29.01.2006	-5.57	-24.87
	05.04.2006	-5.68	-27.46
	13.06.2006	-5.17	-25.34
	26.04.2008	-5.37	-23.43
	15.03.2010	-5.85	-30.80
Hidan 12	10.10.2001	-5.30	-25.40
Hidan 13	10.10.2001	-5.29	-24.30
	02.12.2002	-5.02	-23.97
	18.03.2003	-5.06	-24.14
	10.07.2003	-4.95	-24.70
	12.11.2003	-5.12	-25.40
	27.01.2004	-5.19	-24.70
	04.03.2004	-5.31	-24.90
	11.04.2004	-5.27	-25.90
	01.06.2004	-5.15	-24.70
	06.07.2004	-5.04	-25.40
	20.09.2004	-5.21	-27.20
	28.11.2004	-5.13	-24.40
	16.01.2005	-5.22	-24.24
	07.03.2005	-4.26	-24.20
	24.08.2005	-5.56	-23.83
	13.12.2005	-6.62	-26.23
	29.01.2006	-6.56	-27.72

	27.04.2006	-5.95	-26.61
	13.06.2006	-4.91	-25.38
	06.11.2006	-5.22	-23.76
Hidan 15	10.10.2001	-5.24	-24.90
Hidan 16	10.10.2001	-5.22	-23.80
RW 1	12.02.2002	-5.55	-27.79
	28.02.2002	-5.79	-27.66
	03.01.2002	-5.68	-27.28
RW 3	12.02.2002	-5.46	-27.06
RW 5	14.03.2002	-5.58	-27.77
RW 6	20.03.2002	-5.41	-27.53
RW 7	27.03.2002	-5.54	-28.02
	12.02.2002	-5.41	-27.09
RW 8	04.10.2002	-5.91	-29.68
Hidan 3	23.10.1990	-5.17	-23.50
Hidan 4	23.10.1990	-5.43	-24.00
Hidan 5	23.10.1990	-5.33	-23.70
Hidan 6	23.10.1990	-5.27	-24.20
Hidan 2	13.12.2005	-7.18	-28.43
	29.01.2006	-5.77	-25.53
	26.04.2006	-6.68	-26.66
	12.06.2006	-6.52	-27.75
	06.11.2006	-6.17	-29.36
Wala 1	06.11.2006	-5.51	-23.52
	03.04.2006	-5.71	-26.21
	13.07.2006	-5.30	-26.06
	06.11.2006	-5.30	-24.64
Hidan 16 A	12.01.2009	-5.36	-24.30
Reservoir	01.12.2002	-0.68	-15.77
	17.03.2003	-7.25	-32.45
	20.04.2003	-6.72	-29.71
	09.07.2003	-3.50	-16.30
	12.11.2003	-5.23	21.60
	27.01.2004	-5.01	-24.50
	04.03.2004	-5.14	-23.20
	11.04.2004	-4.45	-21.90
	01.06.2004	-3.66	-18.80
	06.07.2004	-3.72	-19.30
	12.07.2004	-3.44	-17.50
	20.09.2004	-0.36	-4.90
	28.11.2004	-6.71	-22.20
	16.01.2005	-7.00	-27.10
	07.03.2005	-5.25	-24.20
	24.08.2005	-1.64	-19.31
	13.12.2005	-6.74	-8.56
	29.01.2006	-6.39	-7.75
	26.04.2006	-8.46	-34.87
	13.06.2006	-6.59	-31.71
	13.07.2006	-5.44	-28.43
	06.11.2006	-5.43	-25.35
	15.03.2010	-7.46	-40.70

Wala climate station	01.10.1987	-2.51	-4.44
	01.01.1988	-6.31	-19.76
	01.02.1988	-8.33	-42.50
	01.03.1988	-3.91	-12.60
	01.04.1988	-0.05	-4.30
	01.12.1988	-3.06	-0.90
	01.01.1989	-6.63	-29.90
	01.02.1989	-5.03	-14.50
	01.03.1989	-4.97	-23.70
	01.11.1989	-4.08	-22.00
	01.12.1989	-6.83	-39.40
	01.01.1990	-6.79	-37.40
	01.02.1990	-2.19	-6.32
	03.01.1990	-4.42	-15.50
	01.01.1991	-5.69	-20.30
	01.02.1991	-4.18	-13.80
	03.01.1991	-7.10	-41.60

Table S5 Water balance of Wala reservoir and aquifer from 2002 to 2012.

Year	2002	2003	2004	2005	2006	2007	2008	2009	2010	2011	2012	Sum
Inflow (m^3)	11,174,417	11,564,958	24,454,589	1,489,690	20,590,585	6,491,840	1,089,272	15,380,636	35,922,755	3,152,800	4,622,241	135,933,783
Stored Inflow (m^3)	11,174,417	11,564,958	11,062,589	1,489,690	11,590,585	6,491,840	1,089,272	10,787,634	10,919,087	3,152,800	4,622,241	83,945,113
Spillway (m^3)	0	0	13,392,000	0	9,000,000	0	0	4,593,002	25,003,668	0	0	51,988,670
Recharge (m^3)	4,003,800	12,749,851	11,207,912	5,242,663	8,200,682	7,574,764	999,408	8,542,625	9,406,803	2,833,440	3,366,820	74,128,768
Evaporation (m^3)	43,386	331,249	583,307	579,367	866,752	797,411	392,735	958,891	1,225,842	969,050	1,036,125	7,784,115
Abstraction (m^3)	9,958,118	11,701,686	12,371,760	11,348,874	11,933,586	11,403,074	13,728,237	12,374,865	11,892,825	11,633,717	10,728,651	129,075,393

Supplementary Material - Chapter 4

Concept of vulnerability and risk mapping

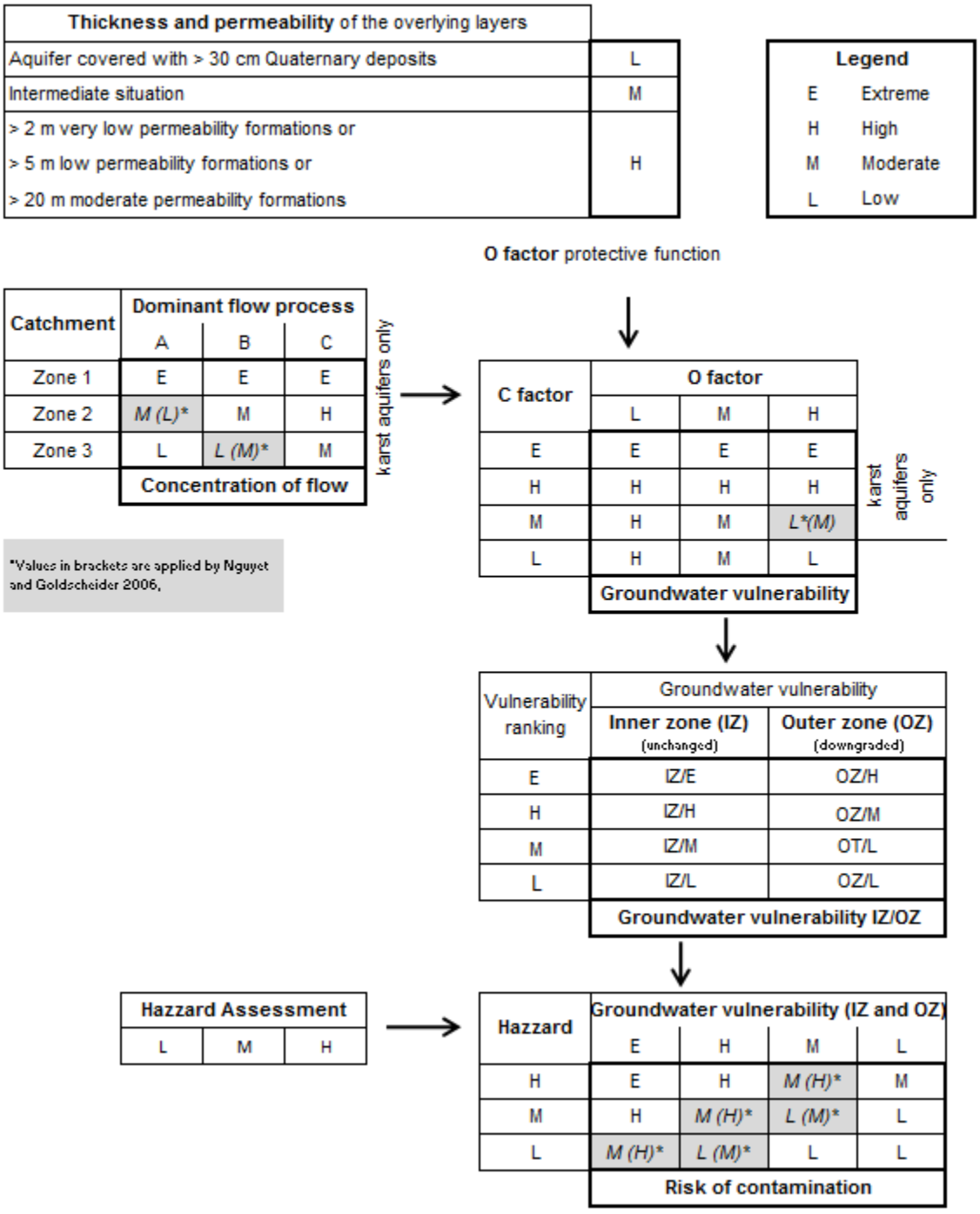

Fig. S1 concept of vulnerability and risk mapping after Nguyet and Goldscheider (2006) adapted on the regional characteristics of Wadi Hidan and Wadi Wala catchment.

Protective function and flow maps

The results show (Fig. S2a) that high protection is afforded by almost 84 % of the land surface in the Wala catchment (mainly on the plateau). About 14 % of the area provides moderate protection (mainly in the central catchment). The low-protection Wadi As Sir outcrops in the northern part of the study area, which is partly covered by the city of Amman, accounts for about 2 % of the total catchment area. In the Hidan catchment, almost 49 % of the land surface provides high protection (mainly on the plateau in the south). Moderate protection is assigned to about 50 % of the catchment (mainly in the northern part). The Wadi As Sir outcrops along Wadi Wala, providing low protection, but covering less than 1 % of the total area.

Dominant flow process type A was assigned to the outcrops of the Wadi As Sir formation, type B to the Amman and Al Hisa formations, and type C to the Wadi Ghudran and Muwaqqar chalk formations. Catchment Zone 1 required an adaption, and was delineated along the wadi (a losing stream) between the wellfield and the reservoir with a 100 m buffer zone on both sides to match the whole dry wadi bed. This is a modification relative to 20 m buffer, as proposed by Nguyet and Goldscheider (2006). Zone 2 comprises the surface catchment of the wadi up to an elevation of 700 m asl. This limit was set according to changes in the landscape since the area below 700 m asl is characterized by steep flanks along wadis, whereas the terrain above 700 m asl forms a dissected plateau. Consequently, a stronger and faster surface runoff generation is assigned to the steep slopes. Zone 3 simply comprises the rest of the Hidan surface catchment. Catchment Zone 4 is not present in the study area.

For the Wala catchment, “low” values of flow concentration account for about 77 % of the outcrops, “moderate” for about 21 % and “high” for 2 %, whereas “extreme” values are absent. For the Hidan catchment, flow concentration is low in about 38 %, moderate in 55 %, high in 6 % and extreme in 1.5 % of the area. High and extreme values are valid for the slopes of Wadi Wala and within the wadi itself (Fig. S2b).

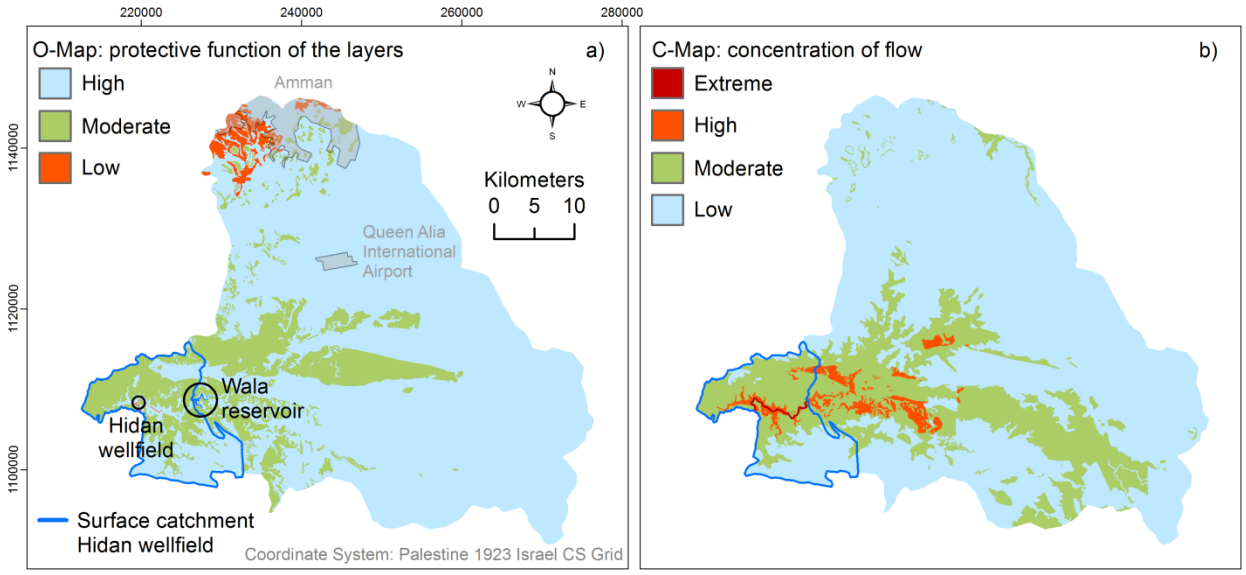

Fig. S2 a Protective function (O factor) of geological layers at Wala reservoir and Hidan wellfield catchment. b C map shows the concentration of flow

Vulnerability and land use

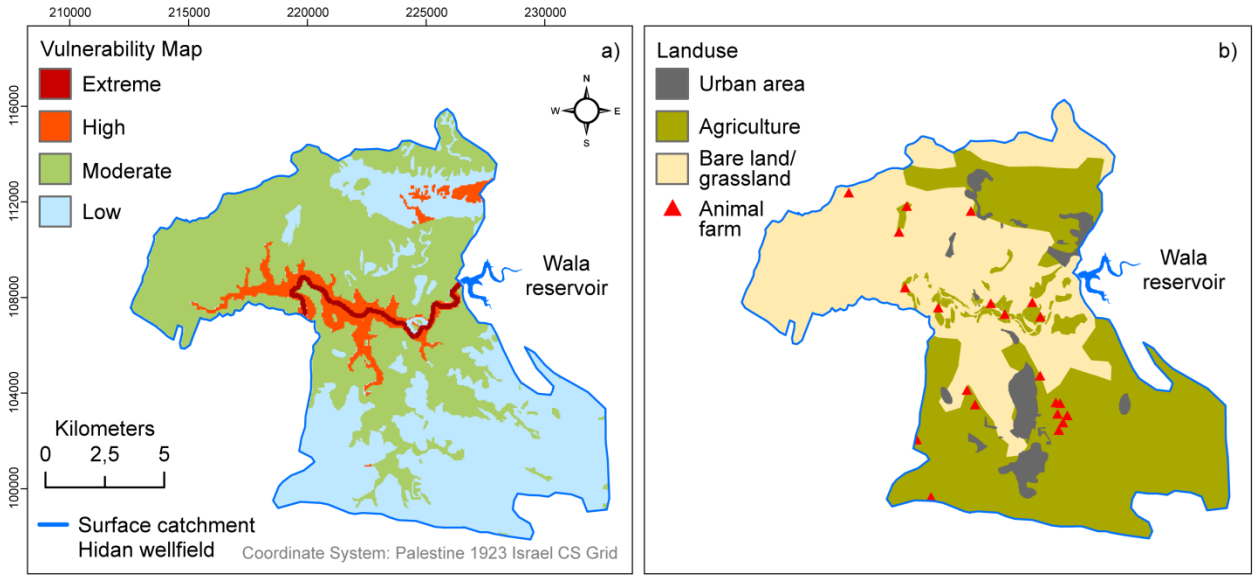

Fig. S3 a Vulnerability of Hidan catchment, b distribution of land use